UILU-ENG-96-2005

CIVIL ENGINEERING STUDIES
Hydraulic Engineering Series No. 50

ISSN: 0442-1744

HYDRAULIC MODEL STUDY FOR THE DROWN PROOFING OF YORKVILLE DAM, ILLINOIS

By

Jeffrey W. Freeman[1] and Marcelo H. García[2]

[1] Research Assistant
[2] Project Supervisor

Sponsored by:

**Illinois Department of Natural Resources
Office of Water Resources (SRA 95-165)**

**HYDROSYSTEMS LABORATORY
DEPARTMENT OF CIVIL ENGINEERING
UNIVERSITY OF ILLINOIS AT URBANA-CHAMPAIGN
URBANA, ILLINOIS**

May 1996

ABSTRACT

Yorkville Dam is located on the Fox River in Yorkville, Illinois. It is a low overflow structure (approximately 6 feet high) with a 530 ft wide modified ogee crest. Completion of the dam in 1961 did not include any riverbed protection below the dam. As time went on, the flow plunging down the face of the spillway, as well as the turbulent forces generated by a hydraulic jump, eroded away the original bed material and created a large scour hole. The advent of this scour hole caused the hydraulic jump to become submerged for all tailwater depths and changed the hydraulic behavior of the structure because the submerged hydraulic jump was not able to dissipate the excess energy in the same manner as a normal hydraulic jump would. The mechanism by which a submerged hydraulic jump dissipates excess energy is through the formation of a roller. The unrelenting forces of this roller have captured many unwilling victims, and caused many drowning deaths at Yorkville Dam.

In 1977, the Division of Water Resources of the Illinois Department of Transportation (IDOT) attempted to remedy the situation. They placed large riprap inside the scour hole having equivalent diameters of up to 2 ft. After sometime, it appeared that the riprap remediation had not eliminated this deadly flow pattern. Once again, many people were drowning at the structure. In 1991, a survey of the spillway clearly showed that the riprap had since been scoured out by the plunging waters and a new scour hole had developed. Thus, creating the same roller problem.

The objectives of this study were to construct a sectional physical model, using Froude similarity and sediment transport characteristics. The model calibration consisted of reproducing the scour holes observed for both the original river bed and the existing (riprapped) bed conditions. Next, the flow structures inside the scour hole were observed and characterized. Lastly, several alternatives were considered and modeled with the aim of eliminating the so called "drowning machine". The scour holes were reproduced with fairly good results, while the flow structures inside the scour holes showed their devastating power. Five alternatives were explored, including: 1) a conventional stilling basin, 2) a 10:1 boulder slope, 3) a 10:1 sloping smooth face, 4) a four-step spillway and 5) a six-step spillway. Of the five alternatives, the four-step spillway seemed the most feasible and cost effective because it dissipates the excess energy in a safe fashion while offering an aesthetically pleasing appearance.

The findings of this study should be applicable to most of the low overflow structures experiencing similar drowning accidents in the State of Illinois.

ACKNOWLEDGMENTS

We would like to thank the Illinois Department of Natural Resources, Office of Water Resources, for providing the funding for this very interesting study.

We would also like to thank Paul Moyano and Cary Troy for their participation in the project as undergraduate research assistants.

The Civil Engineering Department Shop constructed all the structures needed for the study. Their help is gratefully acknowledged.

This report was submitted by Jeffrey W. Freeman in partial fulfillment of the requirements for the degree of Master of Science in Environmental Engineering in Civil Engineering in the Graduate College of the University of Illinois at Urbana-Champaign in May 1996.

Table of Contents

List of Tables

List of Figures

1. Introduction

1.1 Generalities

Hydraulic jumps, in general, have been studied for nearly a century due to their well known importance in all kinds of engineering applications. The hydraulic jump takes on different forms depending on the surrounding flow characteristics. One of these forms, the submerged hydraulic jump, which may occur downstream of an open channel control structure when the tailwater is high, has not been studied to a great extent. Perhaps the limited amount of research on the submerged hydraulic jump can be attributed to the quiescent and seemingly safe nature of its surface. The surface is misleading though, and upon further investigation one can see that the internal characteristics of this complex flow structure render it quite dangerous. For this reason it is rightfully dubbed the "drowning machine" (Leutheusser, 1988).

A hydraulic jump often occurs at the toe of an overflow structure such as a spillway. The jump, through its ability to dissipate energy, completes the transition from a supercritical plunging flow to the subcritical open channel flow of the tailwater (see figure 1.1). The tailwater depth determines the hydraulic jump's primary mechanism of energy dissipation.

Figure 1.2 depicts the four tailwater conditions that could develop below a low overflow structure with a flat bed, as well as the condition that develops for a scoured-out bed. Condition A occurs for low tailwater, which causes the jump to be swept away from the toe of the spillway. As the tailwater rises, the jump starts to move closer to the spillway. It continues to move closer until the tailwater has reached an optimal depth where the toe of the jump is right at the toe of the spillway (Condition B). A further increase in tailwater depth drowns the hydraulic jump and it becomes submerged (Condition C). The plunging flow generates a roller as its mechanism for energy dissipation. The roller axis is in the spanwise direction to the flow. This roller is commonly called the "hydraulic" by canoeists and water safety experts who understand its power to capture unwilling victims (Leutheusser, 1988).

The jump will become submerged to various degrees depending on the height of the tailwater. Eventually, the tailwater rises to such a high level that the submerged hydraulic jump disappears and the flow barely notices the presence of the spillway (Condition D). The surface will become undular, and then eventually flat at extreme tailwater levels.

Conditions A - D have been described before (Leutheusser and Birk, 1991; Leutheusser, 1988), but it is interesting to observe the effects of tailwater depth on the hydraulic jump when there is a scour hole at the toe of the spillway. The presence of a scour hole, whether it is the shape

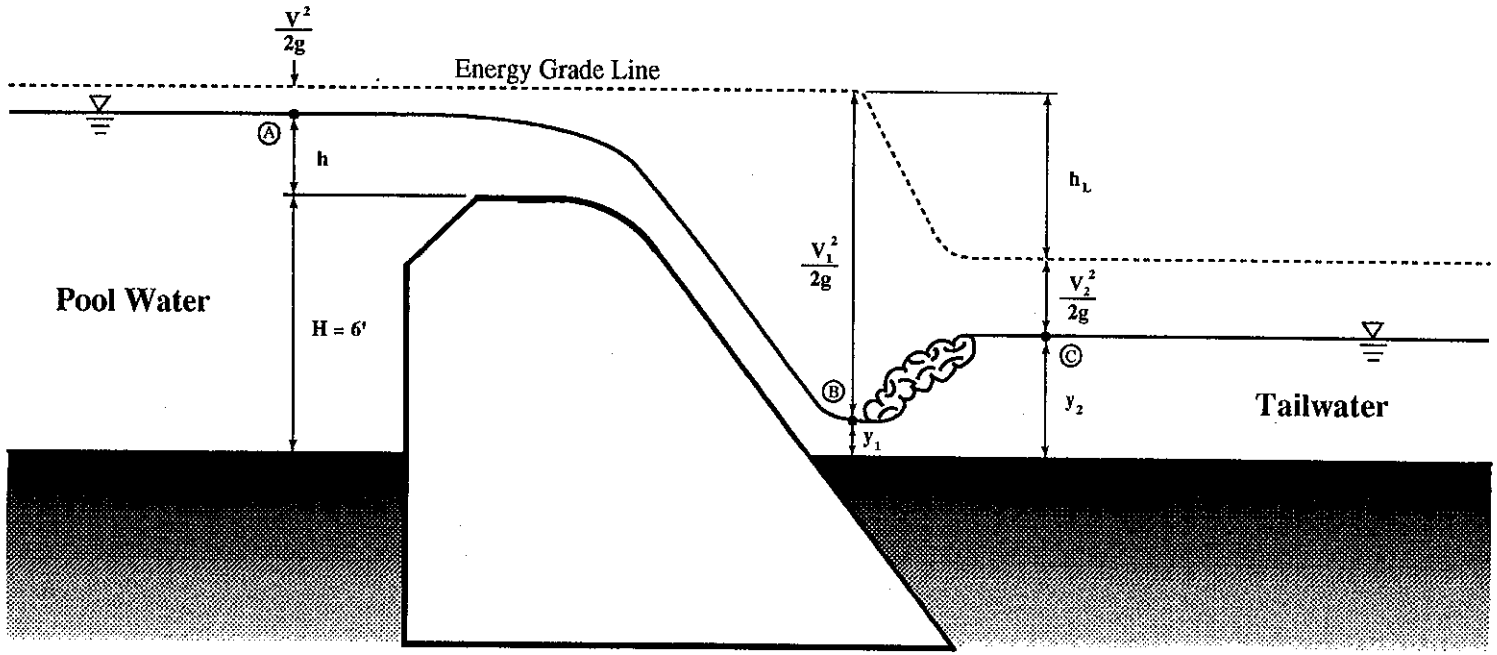

Figure 1.1 Energy distribution at a low overflow structure.

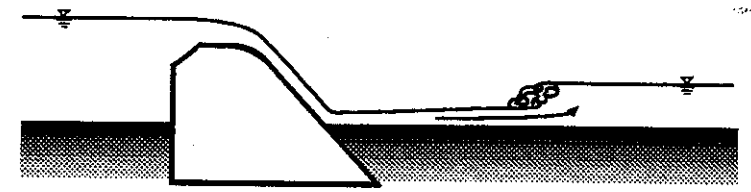

Case A
Swept-Out
Hydraulic Jump

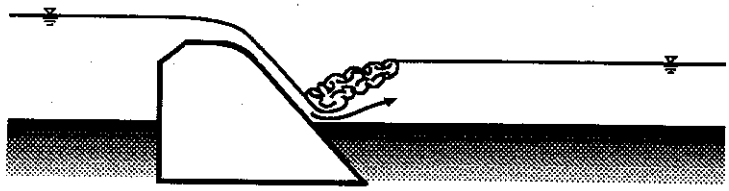

Case B
Optimum
Hydraulic Jump

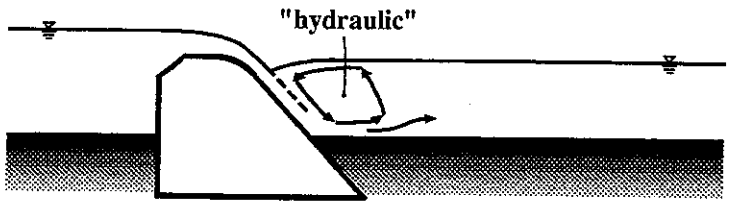

Case C
Submerged
Hydraulic Jump

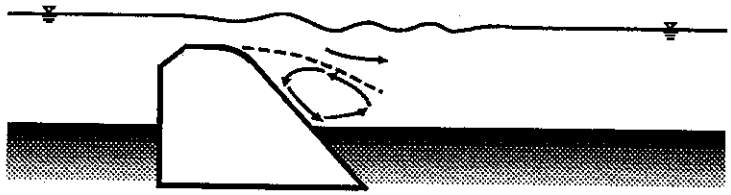

Case D
Surface
Nappe

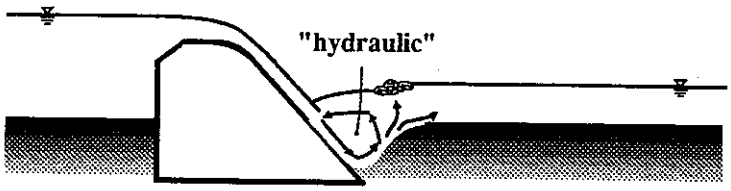

Case E
Submerged Hydraulic
Jump with Scour Hole

Figure 1.2 States of spillway flow as a function of tailwater depth.

that causes the flow to assume or merely the increased depth of the water inside the hole (or a combination of the two) causes the jump to become submerged at all tailwater levels. The flow dissipates its energy in the same fashion as the submerged hydraulic jump over a flat bed (i.e. by generating a roller). One can see from inspection of Case E in Figure 1.2 that the water surface just below the spillway has an upstream direction. Therefore, anything that is on the surface will be pushed back towards the plunging nappe, and anything that is caught in another portion of the roller will be circulated around and eventually thrust towards the plunging nappe. This circulation pattern could continue infinitely because swimmers of all skill levels cannot generate the amount of force necessary to counter act the large forces that the roller generates (Leutheusser, 1988). For this reason, there have been many deaths at low overflow structures that create such a situation.

1.2 Motivation

Yorkville Dam is located on the Fox River approximately 35.9 miles upstream of the confluence with the Illinois River. The dam is 940 feet upstream from the Route 47 bridge (see figure 1.3). The drainage area to this point in the watershed is 1804 square miles. The dam was constructed by the State Division of Waterways in 1960-1961. It was named the Glen D. Palmer Dam after a former Director of Conservation. The dam has a modified ogee crest, the length of the spillway is 530 feet, the height of the dam is approximately 6 feet, and the crest elevation is 575.0 feet above M.S.L. Figure 1.4 shows a schematic of the dam.

Completion of the dam in 1961 did not include any scour protection below the spillway. The original sediment was highly susceptible to erosion and hence a large scour hole was created. In 1976 Yorkville officials noted that many individuals had lost their lives at the dam by drowning. The officials asked the state for a site review. The state officials noticed the large scour hole (see the boundaries of the 1976 scour hole in figure 1.5a) below the spillway and decided this was presumably causing the problem. In an attempt to remedy the situation, the Division of Water Resources decided to eliminate the scour hole by filling the hole with riprap (see figure 1.5a). This work was completed from October 11, 1977 to July 7, 1978 at a cost of approximately $100,000 (IDOT, 1995).

Fifteen years after the riprap addition, the Chief of Yorkville contacted IDOT to request assistance. At that time, 12 people had lost their lives at the dam in the last 26 years. Table 1.1 shows the dates and the flow rates at which the accidents occurred. In fact, a survey conducted by IDOT in 1991 clearly showed that the riprap put in place to reduce the scour hole had since scoured out and a new scour hole had formed (see figure 1.5b). The magnitude of the scour hole was not nearly as large as the 1977 scour hole, but it was large enough to generate the same conditions.

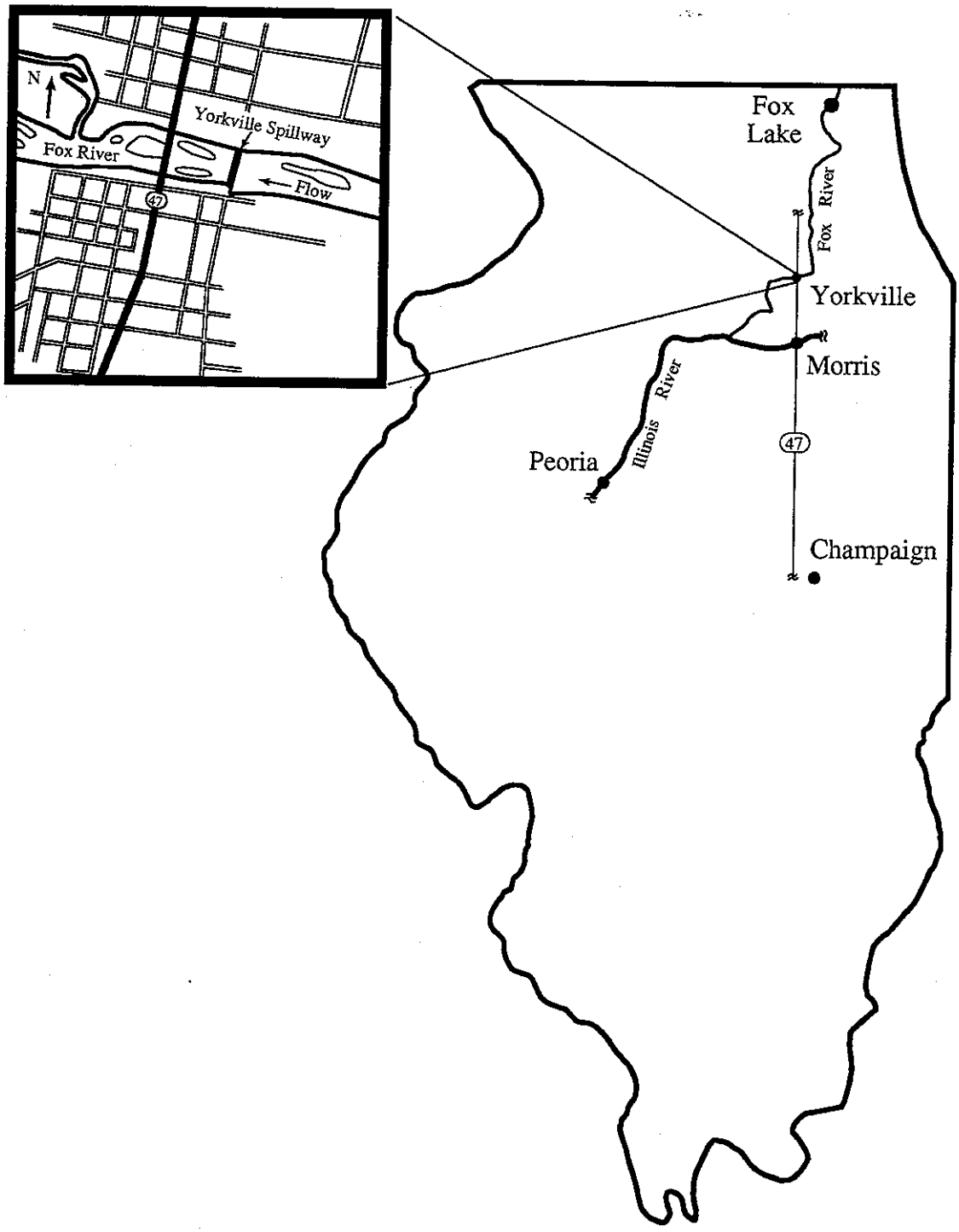

Figure 1.3 Location of Yorkville Dam on the Fox River at Yorkville, Illinois.

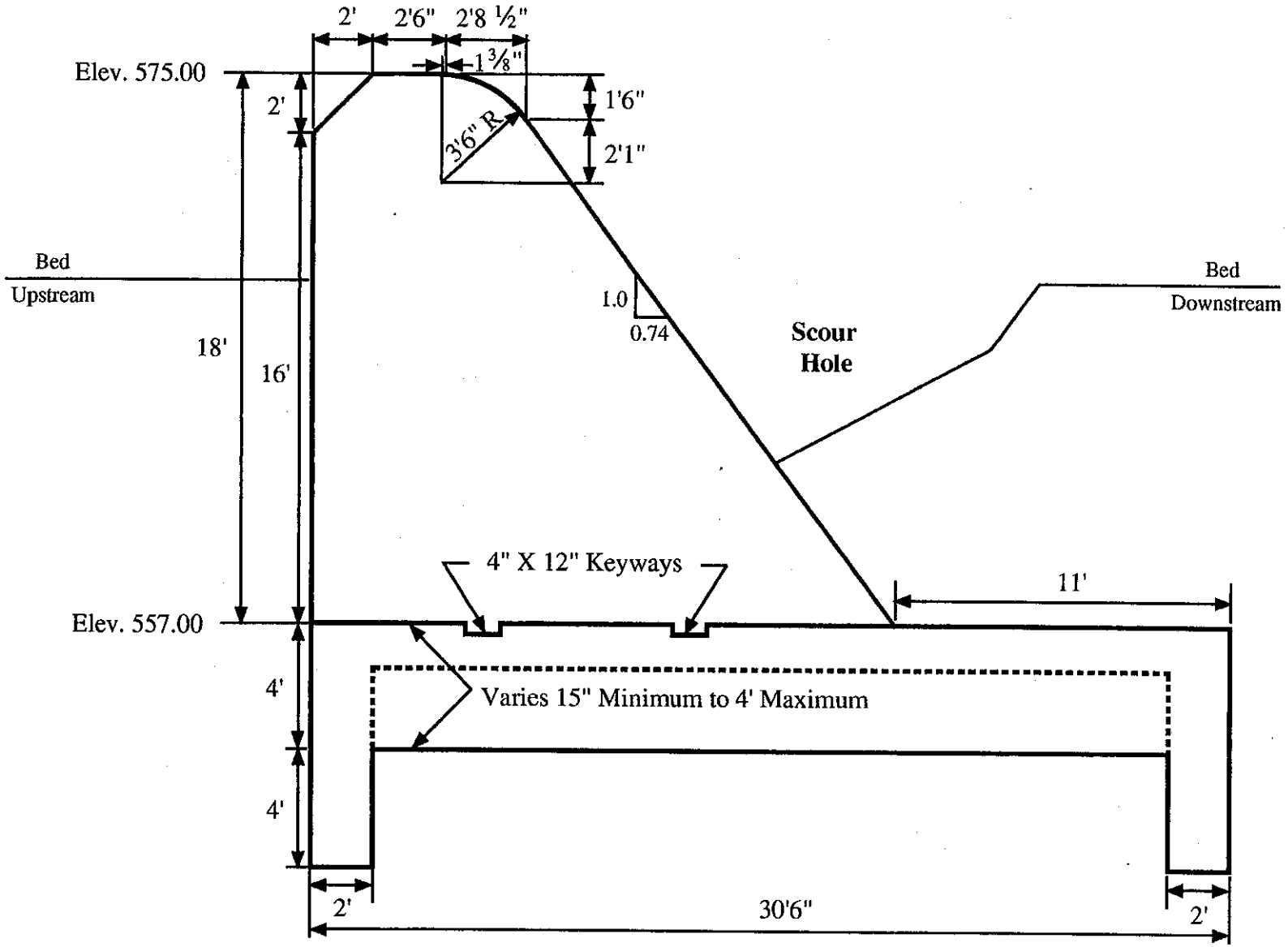

Figure 1.4 Cross section of the Glen D. Palmer Dam - Yorkville, IL.

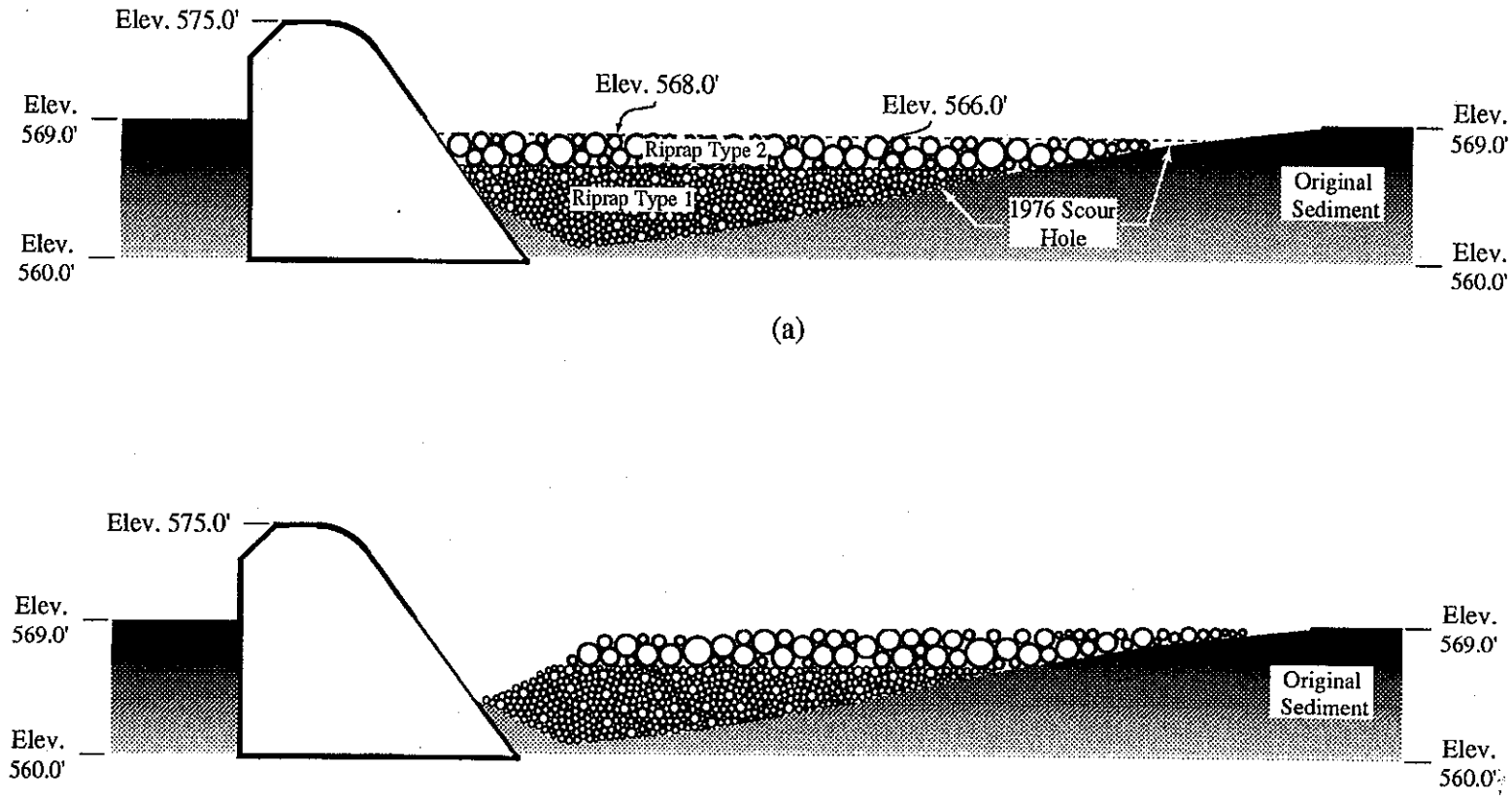

Figure 1.5 Schematic of spillway conditions for: (a) the 1976 DWR riprap design, and (b) the scour hole that was generated by 1991.

Date	Water Depth on Spillway (feet)	Flow Rate (cfs)
July 11, 1968	0.96	1740
June 13, 1971	0.56	784
July 17, 1972	1.31	2870
July 23, 1972	0.99	1880
May 1, 1976	1.66	4150
June 24, 1984	0.90	1620
July 4, 1990	1.08	2140
July 5, 1992	0.50	655
July 10, 1993	0.57	806

Table 1.1: Dates and flow rates when drowning incidents occurred (Source: IDOT, 1995).

The presence of the scour holes created a submerged hydraulic jump as described in section 1.1 and illustrated in figure 1.2. Many victims have entered the "hydraulic" from upstream. These "brave" souls often come over the spillway in boats. It is unclear why a boater would disregard the clearly marked signs on the reach explaining the danger of proceeding over the spillway, but it has occurred. Once the boat impacts the tailwater and subsequently enters the "hydraulic" it often capsizes leaving the individuals fighting for their lives.

The other way that people have entered the hydraulic is from the downstream side. The low tailwater conditions, that often occur in the summer months, are quite popular for fishermen, or even people who are just exploring the river. These people have waded out into seemingly safe tailwater depths that do not even go past their knees. Often times the observer gets too close to the scour hole and is swept into the "hydraulic". Once they are inside the roller they can only hope to be rescued before they drown.

1.3 Objectives

Due to the amount of danger this flow structure puts on public safety, the Illinois Department of Natural Resources funded the Civil Engineering Department at the University of Illinois to conduct a physical model study.

The laboratory study for the drown proofing of the Yorkville Dam consisted of four main objectives. The first objective was to scale and construct the model of the spillway. The second objective was to calibrate the model. This included matching the flow characteristics of the prototype to the flow characteristics of the model and checking if the 1976 scour hole and the 1991

riprap lined scour hole could be reproduced. After proper calibration of the model, the third objective of the research was to study the flow characteristics of the roller. The fourth and final objective was to explore possible alternatives that would eliminate the dangers of the submerged hydraulic jump or any other unsafe flow characteristics. The optimal alternative would render the structure practically drown proof by eliminating the formation of the roller while dissipating the energy of the flow without causing erosion problems further downstream over the range of flow conditions historically experienced by the hydraulic structure.

2. Literature Review

2.1 Introduction

Research on the submerged hydraulic jump started as early as the 1940's. The research then, and for many years after, focused primarily on characterizing the flow parameters of the submerged jump and then comparing those characteristics to the free jump. Of major interest to the hydraulic engineer was the comparisons of energy dissipation, scour characteristics, and pressure fluctuations. The early research noticed the presence of a roller and consequently a backward flow region, but did not tend to consider the dangers that this type of flow could exert on safety at low overflow structures.

More recently, a few publications have called attention to the strain a submerged hydraulic jump can put on public safety. It is obvious, as it will be shown in this study, that this flow structure promotes drowning. For this reason, research objectives on the submerged jump have moved towards its removal all together. There has been a fair amount of work defining possible modifications for low overflow structures to achieve this goal.

The objective of this section is to outline the research that has been done on the submerged jump and summarize the measures people have suggested to eradicate the dangerous phenomenon. This includes the definition of the submerged jump along with a description of its flow parameters. It also includes the summary of experimental observations and theoretical derivations that have lead to equations describing the submerged jump. Finally, this section summarizes some of the suggested modifications and presents the studies which have been conducted to eliminate the existence of the submerged jump.

2.2 Submerged Hydraulic Jump

Before 1963, there was a limited amount of observations and measurements published on the submerged hydraulic jump. The first known observations were published in 1943 by Walter Moore, and also Boris A. Bakhmeteff and Nicholas V. Feodoroff. These researchers described observations of retarded bed velocities for a submerged hydraulic jump (Rao and Rajaratnam, 1963). Next, Harold H. Henry published measurements, along with observations by Liu describing discharge coefficients for the submerged jump (Rao and Rajaratnam, 1963). From 1955 to 1956, Smetana and Woycicki separately presented their observations of the submerged hydraulic jump. Smetana presented a schematic representation of the submerged jump, and

developed some empirical equations describing its energy dissipation (Rao and Rajaratnam, 1963)). He suggested that the submerged jump offered greater dissipation than the free jump, and that the dissipation increased with greater submergence (Rao and Rajaratnam, 1963). Woyciki, on the other hand, developed an empirical equation describing the length of the jump (Rao and Rajaratnam, 1963).

A submerged hydraulic jump may occur at an underflow or an overflow structure. Figure 2.1 depicts the experimental setup used by Rao and Rajaratnam (1963), Rajaratnam (1965), Narasimhan and Bhargava (1976), and Long et. al. (1990) to study the submerged jump. It consisted of a supercritical flow entering a subcritical open channel flow through an underflow structure thus, creating a hydraulic jump at the intersection of the two flow regimes. The researchers used a tailgate to adjust the submergence of the jump. They all noticed that the flow divided into two regions. These are the forward flow region and the backward flow region (roller). Figure 2.1 also includes a typical velocity distribution that will occur at a given cross section.

Rao and Rajaratnam (1963) made the first main contribution to a better understanding of the submerged jump. By considering Smetana's work and the experimental work they conducted, Rao and Rajaratnam presented a definition diagram for a submerged jump. In order to quantify the amount of submergence, they defined the submergence factor S, as:

$$S = \frac{y_4 - y_2}{y_2} \tag{2.1}$$

where y_4 is the tailwater depth, and y_2 is the subcritical sequent depth of a free jump as given by the hydraulic jump (Belanger's) equation. The experimental measurements were used to verify theoretically developed equations. Equations were proposed for the backed-up water depth (or the water depth at the beginning of the subcritical flow) and the energy loss for the submerged jump. The experimental measurements compared quite favorably with the theoretical equations.

These researchers, through extensive analysis of the energy loss of the submerged hydraulic jump, showed results contrary to the observations of Smetana. Rao and Rajaratnam (1963) concluded that the energy loss for the submerged jump is greater than the free jump only under certain flow conditions. They developed a theoretical equation to find the optimal submergence that achieves the maximum energy loss. This was a function of the supercritical Froude number (they also verified the equation with experimental measurements). For conditions greater than the optimal submergence they found that the energy loss was less than that for the free jump (Rao and Rajaratnam, 1963).

Lastly, Rao and Rajaratnam investigated the flow velocity close to the bed. This allowed for the assessment of the scour potential presented by the submerged jump. The researchers found

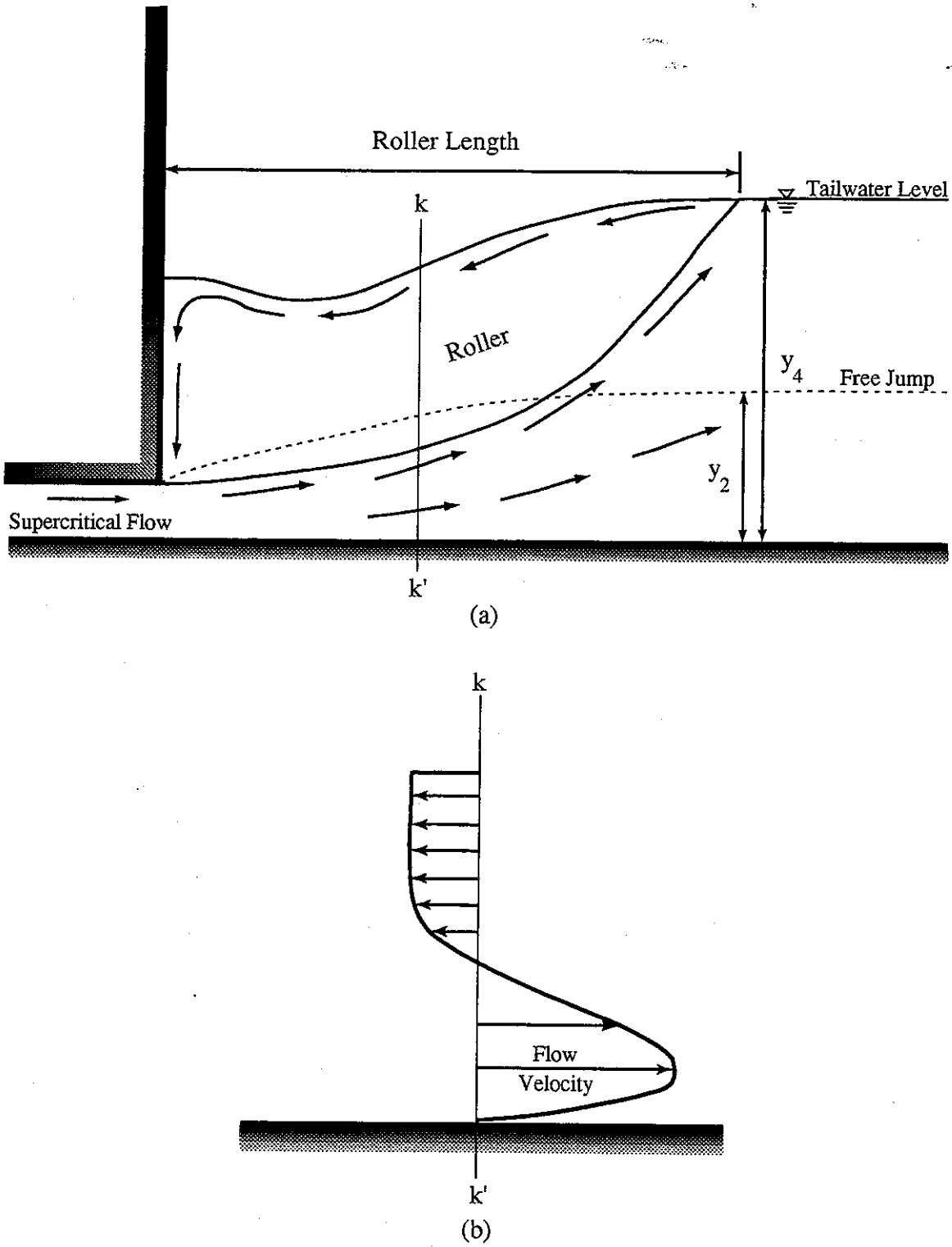

Figure 2.1 Submerged hydraulic jump (a) general characteristics and (b) vertical velocity distribution.

that as the submergence of the jump increased, high velocities continued along the bed for long distances (Rao and Rajaratnam, 1963). This, of course, is undesirable. With this, and the observations on energy dissipation in mind, the researchers concluded that the submerged hydraulic jump "is not to be preferred over the free jump".

In 1965, Rajaratnam presented a paper that continued the analysis of the experimental work first published in 1963. He analyzed the submerged jump as a plane turbulent wall jet under an adverse pressure gradient over which a backward flow was placed. Rajaratnam found that the velocity distribution in the experimental work (forward flow only) was similar to the velocity distribution of the plane wall jet under the previously described conditions. The surface profiles for a submerged jump and a plane wall jet under an adverse pressure gradient over which a backward flow was placed compared favorably, also (Rajaratnam, 1965).

The analysis of the backward flow showed a useful observation. Rajaratnam found that the discharge per unit width of the backward flow increases with an increase in submergence while keeping the incoming supercritical Froude number fixed, and that it also increases with an increase in the supercritical Froude number while keeping the submergence fixed (Rajaratnam, 1965). It should be noted that Rajaratnam did not have complete closure between the two flows though. He had some trouble collating the forward flow discharge and the backward flow discharge into one discharge. It seems that even though the overall magnitude of the backward flow could have been erroneous, the supercritical Froude number and submergence relationships would still apply. Finally, Rajaratnam was able to quantify the boundary shear stress as a function of the coefficient of skin friction and the maximum velocity (as defined by the plane wall jet). He used previously developed turbulent wall jet equations for the skin friction coefficient.

Narasimhan and Bhargava (1976) presented more observations on the submerged jump. They pointed out that there are larger magnitudes of pressure fluctuations for the free jump than the submerged jump. This suggested to them that a submerged jump under low submergence may be a safer energy dissipator than the free jump when considering the structural design of a stilling basin. They also noted that these pressure fluctuations promote scour, and for that reason, one might consider designing for a slightly submerged jump under certain conditions.

Long et. al. (1990) continued to add to the data describing the submerged jump by presenting Laser Doppler Anemometry (LDA) measurements. They measured the time averaged components of velocity (u and v), kinematic turbulence shear stress, and the turbulence intensities. By applying a characteristic length scale, they were able to group all the major flow characteristics (i.e. velocities, turbulence shear stresses and turbulence intensities) together. Interestingly, they found that the decay of the maximum velocity, normalized with the average streamwise velocity, behaved the same for free jumps, submerged jumps, and wall jets when it was plotted against the streamwise coordinate normalized with the characteristic length (Long et. al., 1990). When

considering the fully developed region of the submerged jump in comparison to wall jets, Long et. al. (1990) demonstrated that the behavior of the streamwise velocity and turbulent shear stress was similar in both cases. The most significant observations that the researchers contributed were those of the three dimensional nature of the submerged jump.

As discussed previously, the submerged jump could also occur at an overflow structure. Figure 2.2 depicts a submerged jump below a weir. The flow is divided into five regions as described by Fan (1993). These regions include the nappe, deceleration, aeration, counter-current, and recovered regions. A submerged jump at a ogee shaped spillway would contain all of these regions except for the aeration region. Observations by Leutheusser (1988, 1991) and Fan (1993) focus on the submerged jump at overflow structures. It should be noted that the flow characteristics and velocities of submerged jumps at overflow and underflow structures are similar, but not identical. However, the major characteristics of the two structures are assumed equivalent for this analysis.

Leutheusser (1988) presented a paper discussing the dangers of the submerged hydraulic jump. He pointed out that the design of safe hydraulic structures often overlooks some of the environmental dangers the structure might present (Leutheusser, 1988). Leutheusser went on to discuss the states of weir flow for a flat bed in a way similar to that described in figure 1.2, and pointed out that the submerged jump is by far the most dangerous. He continued by presenting some approximate values for flow velocities and forces that may occur at a low overflow structure under submerged flow conditions. These velocities are of the same magnitude as the velocities an average swimmer can generate, suggesting that a person would have a difficult time swimming out of the "drowning machine" (Leutheusser, 1988). Next, Leutheusser presented a graphic chronology of events that may occur to a drowning victim. Finally, Leutheusser concluded that hydraulic engineers need to be aware of the environmental dangers that develop below these structures and promulgate designs that maximize dam safety (Leutheusser, 1988).

Leutheusser (1991) published another paper that discusses the dangerous conditions that can occur at a low overflow structure. He suggested that the dangerous submerged jump may often occur because the design of many overflow structures are too low. This does not allow the flow to go through the proper, free hydraulic jump. Leutheusser also pointed out the difficulty of designing these structures for such a wide range of flows. He then presented a graph depicting the proper weir heights, or proper heads for drop structures, to allow the free jump to occur.

Fan (1993), under the direction of Leutheusser, focused his attention on the backward flow region of a submerged jump below a weir. Fan (1993) found the dimensionless length of the countercurrent region (countercurrent region length normalized with the tailwater depth) to vary linearly with submergence. A surface Froude number was defined and used to describe the flow in the counter current region. The backward surface velocity that was used in the surface Froude

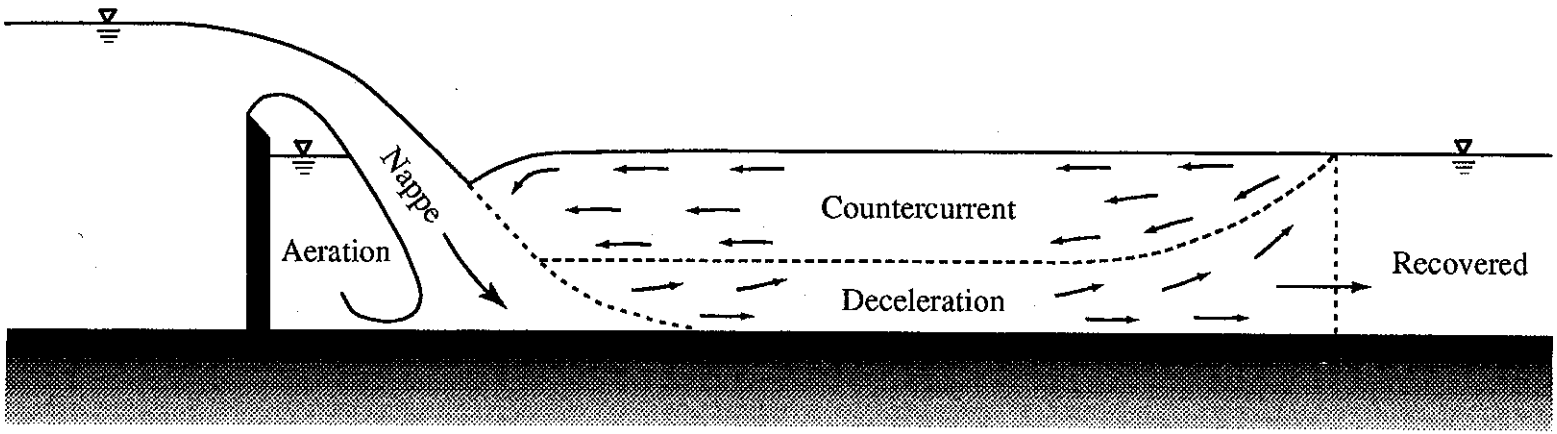

Figure 2.2 Regions of flow for a submerged hydraulic jump at an overflow structure.

number was found to decrease with submergence (Fan, 1993). When considering the critical submergence, which is defined at the transition between the submerged jump and the undular surface nappe, he found that it exhibits hysterisis. The transition from the submerged jump to the undular surface nappe, which was denoted the "flip jump", occurred at a higher submergence than the transition from the undular surface to the submerged jump, which was denoted the "flop drop" (Fan, 1993).

2.3 Eliminating the Submerged Jump

There has been many instances in which people have lost their lives due to drowning at a hydraulic structure. This, of course, includes the Yorkville Dam. The understanding of the dangerous flow structure that the submerged jump creates has lead to designs or modifications that eliminate it. Possible modifications have included: increased spillway elevations, baffled chutes, labyrinth weirs, raised grouted stilling basins, and step spillways.

2.3.1 Increased Spillway Elevations & Baffled Chutes

Leutheusser's (1991) suggestion to pay close attention to the design head at an overflow structure was discussed in section 2.2. He also realized that this design head has practical limitations, though. When the design head is too high, he advises the use of a baffled chute as denoted Basin IX by the Bureau of Reclamation. The baffles will dissipate the energy by cascading action and do not allow the formation of a roller (Leutheusser, 1991).

Hotchkiss and Comstock (1992) attempted to validate Leutheusser's (1991) remarks. They easily reproduced the "hydraulic" in the laboratory and profoundly agreed with Leutheusser's conclusions regarding dam safety for this flow pattern. They did, however, disagree with Leutheusser's baffled chute suggestion as an alternative to eliminate the dangerous roller. Hotchkiss and Comstock (1992) tested a 1:6 scale model representing a Bureau of Reclamation Basin IX design. While they agreed the baffled chute dissipated the energy head as the flow cascaded through the baffles, they felt this structure would add another safety concern. The researchers tested flows similar to the flows that developed the "hydraulic" (under unbaffled conditions) as well as flows that would develop Case B and Case A from figure 1.2. For such a flow range, Hotchkiss and Comstock (1992) found that the introduction of a representative float (either a recreational boat or person) over the spillway showed the possibility for injury while negotiating the baffles. The float often became wedged in-between the baffles because the baffles were not completely submerged. The boat was only able to pass unobstructed for discharges well over the design discharge (Hotchkiss and Comstock, 1992). For this reason Hotchkiss and

Comstock (1992) suggested designs presented by Hauser et. al. (1991) to eliminate this safety concern.

Leutheusser (1992) elaborated on the observations of Hotchkiss and Comstock (1992). He understood Hotchkiss and Comstock's (1992) remarks, but wanted to establish that there are no "safe" hydraulic structures. He suggested that the excessive amount of turbulence and agitation the baffles will promote would presumably keep most people away. This is contrary to the quiescent nature of the "hydraulic", which attracts many unknowing victims.

2.3.2 Labyrinth Weir

Hauser et. al. (1991) investigated the use of labyrinth weirs below hydropower dams. The objective of the design was to increase minimum flows between generating periods and increase tailwater dissolved oxygen (DO). The proper design of the labyrinth weir regarding safety would limit the discharge per unit width. Hauser (1991) pointed out that a high discharge per unit width could develop the aforementioned roller. An increase in the crest length would decrease the discharge per unit width below the suggested 2 cfs/ft maximum. Any flow above 2 cfs/ft would promote dam safety problems (Hauser et. al., 1991). A clear advantage to the labyrinth weir is its aerating characteristics. Any extra amount of oxygen mass transfer would, of course, improve the health of the river. Hauser et. al. (1991) did point out the disadvantages of the labyrinth weir, though. These include: the increased crest length for aeration and dam safety over other alternatives, and the fact that the labyrinth weir is non-navigable (Hauser et. al., 1991).

2.3.3 Raised Grouted Stilling Basins

Pugh (1989) presented a proposed modification for boater safety on the Tieton Diversion Dam. The scouring action of the drop structure created a 6 to 7 foot deep hole just below the crest. There was a roller, similar to the flow structure already discussed, below the dam that retained boats. Pugh (1989) physically modeled the drop structure and then designed the proposed modification. He originally attempted to place riprap inside the hole and minimize the head differential between upstream and downstream. The riprap was placed flat for about 10 feet and then dropped off with a 3 to 1 slope until it reached the bed elevation. The scaled two-foot riprap was easily eroded and a large scour hole developed again below the crest. Pugh (1989) found that a four-foot diameter riprap was necessary to withstand scour. The large riprap did cause additional problems since fins formed in the gaps between the rocks. This, he felt, could be hazardous to boaters. The hazards and economics associated with the four-foot riprap suggested that another

alternative was warranted. Pugh (1989) found that the two-foot riprap with a grouted cover would withstand the flow and eliminate the roller.

2.3.4 Stepped Spillways

Recently, there has been a lot of attention directed toward the use of stepped overflow structures. Problems that promote the use of stepped structures are the excessive cost of bed protection below the structure and the existence of the aforementioned "hydraulic". The dissipation of the energy head along the face of the structure limits the amount of residual energy remaining at the bottom, and therefore, limits the energy available for the formation of both a roller or an exorbitant amount of bed scour.

In order to get a better understanding of the use of stepped structures, the hydraulics of such structures must first be discussed. Next, equations that have been developed to compute dissipation over a stepped structure will be presented. Then, some examples will be cited in which stepped structures have been used.

2.3.4.1 Fluid Mechanics of Stepped Spillways

Sorenson (1985) noticed a distinct difference between high and low flows over his stepped spillway model. At very low discharges, Sorenson (1985) observed the flow cascading from step to step in a "thin choppy layer that clings to the face of each step". At higher flows, he observed rotating vortices of flow behind the sheet of flow. Rajaratnam (1990), along with the observations of Essery and Horner, divided these two flow regimes into the nappe flow regime (figure 2.3) and the skimming flow regime (figure 2.4). In the nappe flow regime, the flow falls from one step to the other as a falling jet. The energy dissipation is achieved by jet breakup in the air, jet mixing on the step, and the possible occurrence of a hydraulic jump (Rajaratnam, 1990). Chanson (1994a) further divided the nappe flow regime into three subcategories, which include: 1) nappe flow with a fully developed hydraulic jump (which occurs for low flows and small flow depths) (figure 2.3a), 2) nappe flow with a partially developed hydraulic jump (figure 2.3b), and 3) nappe flow without a hydraulic jump (figure 2.3c). For the skimming flow regime, the water moves along the face of the steps as a coherent stream. The flow is cushioned by the recirculating fluid that is trapped between the steps. The momentum transfer from the skimming flow to the rotating fluid, which intern causes a shear stress, appears to cause the energy dissipation (Rajaratnam. 1990).

The two flow regimes also entrain air in different manners. Air entrainment, for the nappe flow regime, occurs at the intersection of the falling nappe with the receiving pool by jet breakup. Entrainment also occurs in the hydraulic jump downstream of the impact of the nappe (Chanson,

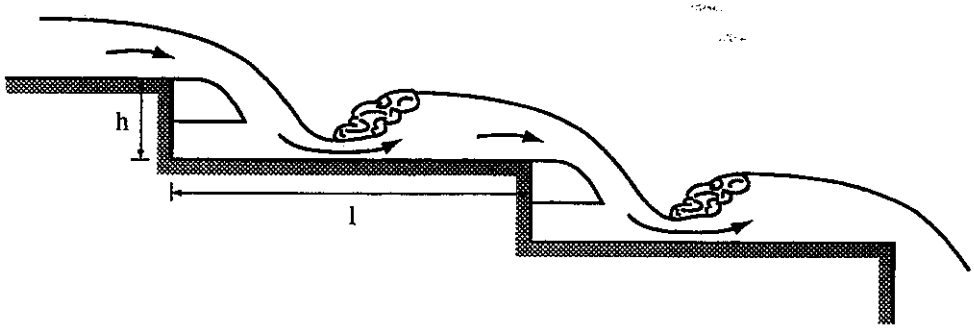

(a) Nappe Flow with a fully developed hydraulic jump.

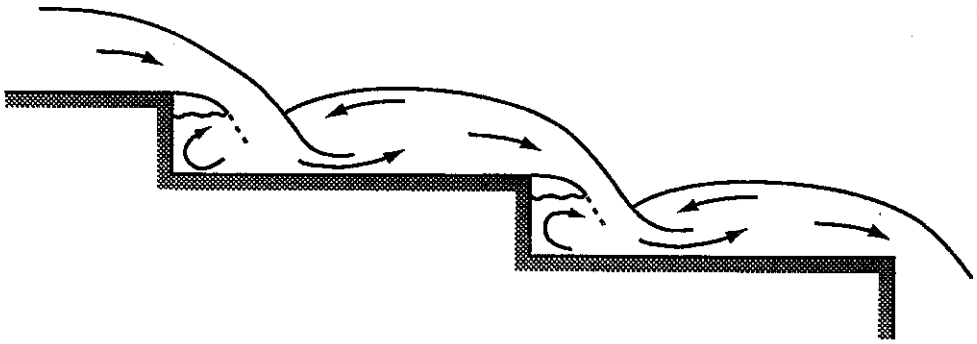

(b) Nappe Flow with a partially developed hydraulic jump.

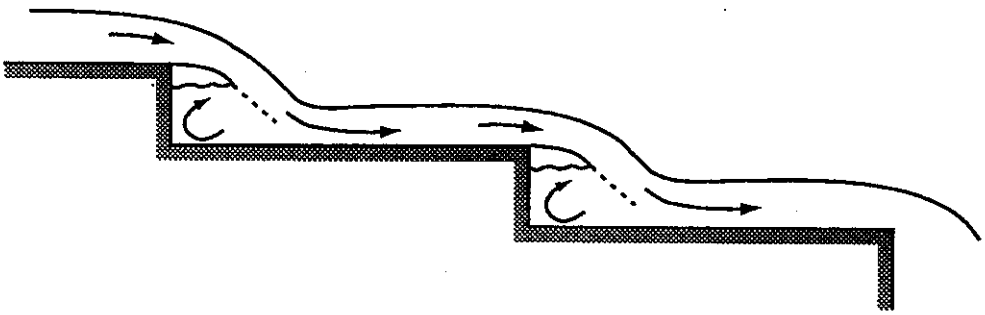

(c) Nappe Flow without a hydraulic jump.

Figure 2.3 Three states of nappe flow regime.

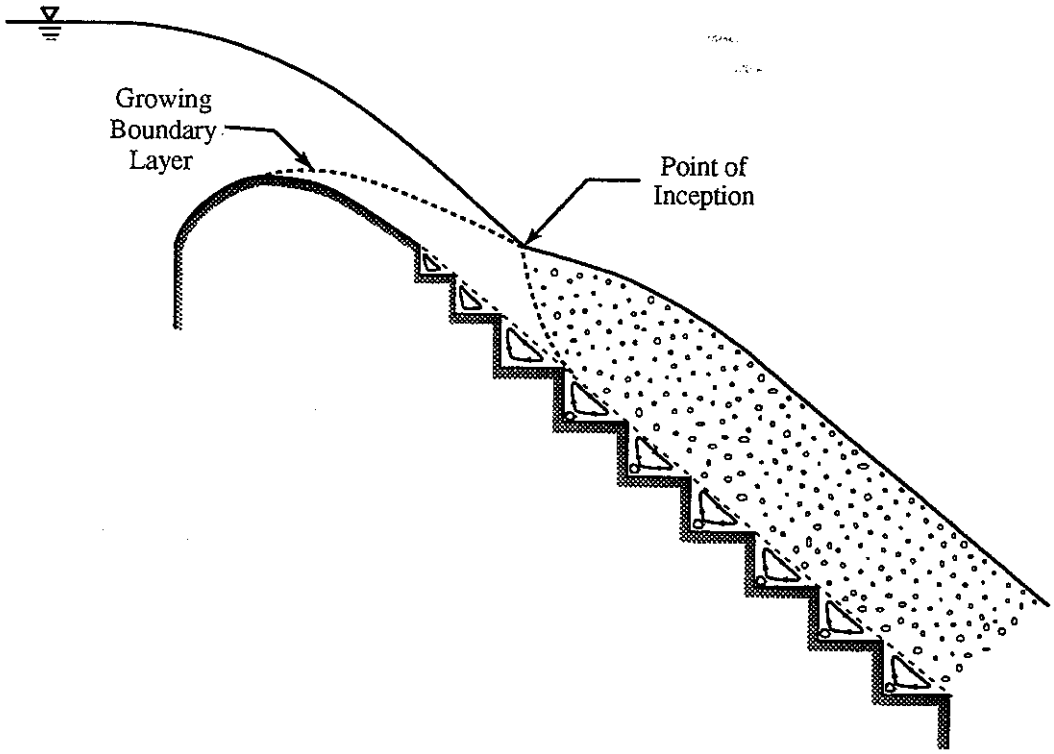

(a) Boundary layer growth for a stepped spillway.

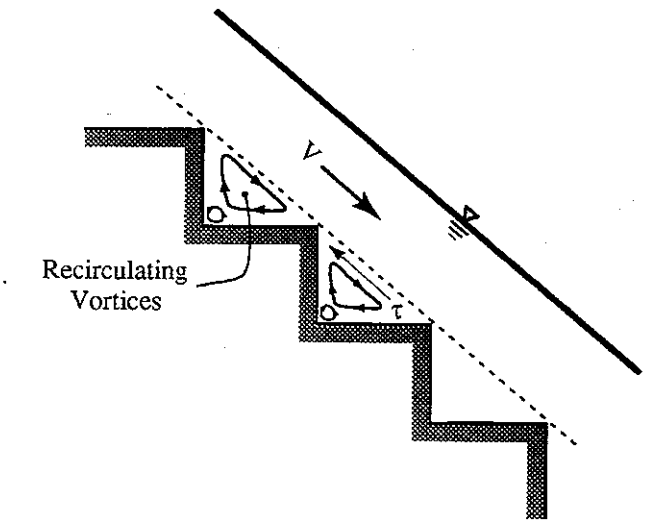

(b) Recirculating vortices that cause flow resistance.

Figure 2.4 Skimming flow regime over a stepped chute.

1994a). Chanson (1994a) states that there is a limited amount of entrainment on the surfaces of the nappe because of the small surficial area. The skimming flow regime, on the other hand, entrains air through another process. The skimming sheet of water is highly turbulent. This promotes the conditions of free-surface aeration. For a long chute, the flow begins to proceed over the steps as a smooth, glassy stream, until the growth of the turbulent boundary layer intersects the water surface. At this point, the point of inception (see figure 2.4), air entrainment begins. The mixture of air and water will reach an equilibrium after a short distance and remain the same for the remainder of the chute (Chanson, 1994a).

Since there is a difference in the flow characteristics for the two regimes, it is necessary to know the transition between them. Rajaratnam (1990) used a limited amount of experimental measurements to define that transition. He concluded that the onset of skimming flow occurs when the ratio of y_c/h, where y_c is the critical depth and h is the step height, is approximately equal to 0.8. For flows with y_c/h greater than approximately 0.8, the flow will be in the skimming flow regime, and for flows with y_c/h less than approximately 0.8, the nappe flow regime will prevail.

Chanson (1994a,b) took the analysis for the transition one step further. He suggests that the "onset of skimming flow" occurs when the cavity beneath the falling nappe disappears. This, he states, is a function of discharge, step height (h), and step length (l). Analysis of stepped structure data for h/l between 0.2 and 1.25 resulted in the following empirical equation:

$$\frac{(d_c)_{onset}}{h} = 1.057 - 0.465\frac{h}{l} \qquad (2.2)$$

where $(d_c)_{onset}$ is the characteristic critical depth. The skimming flow regime occurs for $d_c > (d_c)_{onset}$, where d_c is the critical flow depth (Chanson, 1994a,b).

Mondardo and Fabiani (1995) question the validity of Chanson's equation describing the transition from the nappe to the skimming flow regime. They pointed out the low regression coefficient (r = 0.79) that Chanson's equation achieved. They attributed the error to the heterogeneous data Chanson used to develop the equation. Some of the data points correspond to stepped gabion weirs. These, they argue, will have different flow characteristics than an impermeable concrete cap. For that reason, Mondardo and Fabiani (1995) gave separate equations describing the transition. For concrete or smooth steps they proposed:

$$\frac{d_c}{h} = 1.19474 - 0.59501\frac{h}{l} \qquad (2.3)$$

with r = 0.92, and for gabion chutes they suggested:

$$\frac{d_c}{h} = 0.78145 - 0.17725\frac{h}{l} \qquad (2.4)$$

with r = 0.95.

Chanson (1995) warns that care should be taken using any of the proposed equations, because they provide only estimates. There was a limited amount of data to regress all of the above equations and more data would be necessary to validate a representative equation (Chanson, 1995).

2.3.4.2 Energy Dissipation for Stepped Structures

Relationships describing the energy dissipation for stepped structures are necessary to formulate stepped spillway designs. There has been some equations proposed in an attempt to satisfy that need (i.e. Rajaratnam, 1990; Peyras et. al., 1992; Chamani and Rajaratnam, 1994; Chanson, 1994a,b). Unfortunately, for every equation developed there seems to be some contradicting data (e.g. Christodoulou, 1993). This, in general, has to do with the two different flow regimes, and therefore, the two different dissipative phenomena that occur in stepped structures. Some of the main observations concerning energy dissipation and a description of the equation developments, will be presented herein. Then the dissipative characteristics that are accepted by the majority will be summarized.

Sorenson (1985) observed excellent energy dissipation over his stepped spillway model. The majority of the flows that he analyzed were in the skimming flow regime. His model, which consisted of 58 steps at an approximately 38° slope, showed significant velocity reductions at the toe of the spillway when compared to a smooth spillway. This included a 2.8 to 3.0 reduction in velocity for the larger discharges and a 4 fold decrease at the lower discharges.

Rajaratnam (1990) developed an equation describing energy dissipation for the skimming flow regime. He achieved this by assuming that the flow becomes fully developed after it has proceeded over the first few steps. By quantifying the shear stress, and therefore, frictional loss, the energy dissipation was calculated. Rajaratnam (1990) used Sorenson's (1985) measurements to calculate a representative coefficient of fluid friction.

Christodoulou (1993) found the energy dissipation in the skimming flow regime, for a much smaller amount of steps, to be significantly less than Sorenson's (1985) data. This also disagrees with Rajaratnam's (1990) equation. Christodoulou's (1993) experiments were conducted at a similar slope, and therefore, similar h/l ratio as Sorenson (1985), but for 10-13 steps instead of 58. This would seem to demonstrate that the relative head loss is a function of the number of steps (Christodoulou, 1993).

Peyras et. al. (1992) found 3, 4, and 5 stepped porous gabion weirs aided in dissipation by up to 10% over an impermeable stepped face. This was attributed to the flow resistance generated by

flow through the porous media. Peyras et. al (1992) also observed a much higher dissipation for the nappe flow regime over the skimming flow regime.

Stephenson (1991) gave some pertinent observations for the design of a stepped spillway under nappe flow conditions. He suggests that the greater the l/h ratio is, and consequently the smaller the slope of the step tips, the greater the dissipation. Where it is feasible and cost effective, Stephenson (1991) suggests a stepped slope of 1 on 5 to achieve excellent dissipation under the nappe flow regime.

Chamani and Rajaratnam (1994) developed an equation describing energy dissipation for the nappe flow regime. By introducing an average relative energy loss per step, they were able to obtain the total energy loss by summing the individual losses. Chamani and Rajaratnam's (1994) equations compared favorably with early experimental measurements.

Chanson (1994a,b) presented energy dissipation equations for the nappe flow regime as well as the skimming flow regime. The nappe flow equation was developed assuming fully developed hydraulic jumps (see figure 2.4), while the skimming flow equation was developed assuming fully developed normal flow. Chanson's (1994a,b) equations compared favorably with the previously discussed data and other data sources. Comparison of the two equations lead Chanson (1994a,b) to conclude that greater energy dissipation is achieved for the nappe flow regime over the skimming flow regime at small dams, while on the other hand, there is greater energy dissipation for the skimming flow regime for large dams ($H_{dam}/d_c > 35$). Some researchers question the validity of the latter part of the previous statement (e.g. Chanson, 1995), but for the design at Yorkville dam (i.e. a low head structure) the greatest dissipation will be achieved for the nappe flow regime. Thus, it is not important for this analysis to justify maximum energy dissipation for large dams.

Chanson (1995) states that although there are some discrepancies among researches on some issues related to stepped structures (i.e. the equations describing the energy dissipation and the transition for nappe to skimming flow, and the flow regime which renders the maximum dissipation), there are some conclusions that are widely accepted. It seems all researchers agree that there are larger rates of energy dissipation for stepped spillways than smooth chutes. They also agree that if the height of the spillway is kept constant, the energy dissipation decreases with an increase in discharge, and alternatively, the energy dissipation increases with an increase in dam height if the discharge is kept constant. Lastly, most researchers find that it is appropriate to consider the residual head (i.e. the energy remaining at the toe of the structure), when analyzing energy dissipation.

2.3.4.3 Previous Experience with Stepped Structures

Using stepped structures for hydraulic release is not a new concept. The first known stepped structures were built in 694 BC on the Khosr River in Iraq (Chanson, 1994a). A little later in history, it seems that the Romans used stepped overflow structures (Chanson, 1994a; Frizell, 1992). In the early 1900's, there were stepped masonry dams in the US. The most recent rejuvenation of stepped structures for hydraulic release seems to be attributed to the roller-compacted concrete (RCC) method of construction (Frizell, 1992). In this section of the report, some of the most recent stepped structure experimental observations and model studies will be presented. Energy dissipation is the primary objective for the stepped designs. This, consequently, either cuts down on the stilling basin design and/or eliminates the existence of a roller at the toe of stepped structures.

Sorenson (1985) developed a stepped spillway for the Monksville Dam in New Jersey. He conducted a Froude scale model study at a 1:10 and a 1:25 scale. The 120 foot Monksville Dam model was designed with 58 steps imposed into the standard WES profile. Sorenson (1985) was especially interested in designing a smooth flow transition when the falling nappe encountered the first few steps. He noticed that a thin sheet of flow deflected off the first step and reattached to the structure several steps down the slope for low discharges. Since this was unacceptable, he solved the problem by adding a few smaller steps up the face of the profile. Stephenson (1991) found the same problem and corrected it in the same manner. Sorenson (1985) concluded that the stepped spillway dissipative characteristics are comparable to those of a smooth spillway with a hydraulic jump stilling basin. Sorenson (1985) observed flows mostly in the skimming flow regime, as discussed previously.

Frizell (1992) discussed the use of RCC to fabricate stepped structures. Frizell (1992) presented a table that lists 15 dams which utilize steps for energy dissipation. This list includes dams in the U.S., Africa, Australia, and France. Frizell (1992) also highlighted some of the research the Bureau of Reclamation, was and still is, conducting to aid in the design of these stepped structures. Laboratory observations were conducted for stepped overlays that are used on the face of embankment dams. These observations aid in the design of new embankment dams, as well as the maintenance of old dams which are no longer able to store the probable maximum flood (PMF).

Frizell et. al. (1994) continued observations for the step overlays. After completion of the laboratory experiments, the researchers conducted field observations on a stepped overlay. They found the overlay to be a stable and an efficient energy dissipator, just as the laboratory experiments suggested. The extra dissipation that the steps achieved significantly reduced the stilling basin design (Frizell et. al., 1994).

As discussed in Section 2.3.4.2, Peyras et. al. (1992), conducted model tests for the design of stepped gabion structures. This was primarily motivated by the use of gabion structures in the Saheliam area of Africa. He conducted observations on a 1:5 scale model with step slopes of 1 on 1, 1 on 2, and 1 on 3. Three, four, and five step arrangements were tested. Peyras et. al. (1992) found that proper construction of the stepped structures could withstand flows up to 3 $m^3/s/m$ without damage. This is clearly safer than a smooth gabion slope which will not accept flows greater than 1 $m^3/s/m$. Peyras et. al. (1992) suggests that the steps give extra dissipation that will decrease the necessary stilling basin length by 10 - 30%. This, he states, will reduce the project cost by 5 - 10%.

Davis and George (1985) conducted a 1:30 Froude scale sectional model of the Little Falls Dam. The Little Falls Dam is a low overflow structure with a 12.4 ft elevation difference between the top of the spillway and the downstream bed. The original dam contained an end sill which aided in energy dissipation. The existence of the end sill coupled with the hydraulics of the spillway (i.e. water elevations) caused a strong roller. From 1975 to 1983, seventeen people drowned at the dam. In order to eliminate the dangerous roller, Davis and George (1985) tested three modifications. One of the modifications was a deflector plate at approximately 2 ft below the top of the dam. Davis and George (1985) hoped the plate would direct the flow along the downstream surface and eliminate the existence of a roller. This arrangement created good results for some of the tailwater elevations, but not for others. Of the three modifications, the deflector plate was the most sensitive to tailwater conditions. For this reason Davis and George (1985) concluded that the deflector plate should not be considered as an alternative. The next modification was a 4H:1V sloping boulder surface. This modification eliminated the existence of the roller, but it was unsure how feasible it was. To insure the rock stability at large discharges, the diameter of the boulders were found to be 5 ft. Davis and George reasoned that this large diameter, and therefore, weight of each rock would be difficult to work with (if they were even available). The last, and recommended, modification that the researchers tried was a stepped spillway. The steps were fabricated with numerous grout-filled bags (that were sized large enough to insure stability). The step tips formed a 4H:1V slope down the face. This modification also eliminated the roller, and seemed more feasible to the researchers than the rock slope because the bags could be placed and then filled in situ.

Dodge (1989) conducted a 1:35 Froude scale model study of the Roosevelt Diversion weir. The low overflow dam, which drops from a spillway top elevation of 2180.25 ft MSL to a downstream elevation at approximately 2173.00 ft MSL, contains a hydraulic jump stilling basin with an end sill. While the as-built structure performed well hydraulically, it did not perform safely. The Roosevelt Diversion weir had the same problem as the Little Falls Dam. The end sill promoted a keeper roller which tended to capture swimmers and boaters.

The Froude scale model of the existing spillway demonstrated the power of the keeper roller. This was accomplished by introducing a scaled kayak and observing the severity of the existing flow structure. Dodge (1989), with the objective of removing the roller, then tested numerous step configurations. To check for the safety of each alternative, the kayak was also introduced. The final suggested design consisted of one 3.25 ft high step followed by four 1 ft high steps. The lengths of the steps decreased down the spillway with h/l ratios of 0.31, 0.16, 0.21 and 0.33, respectively.

2.4 Conclusions

The preceding literature review described the work that has been presented on submerged hydraulic jumps and the designs to eliminate them. The primary objective of this study is to design a structure that eliminates the submerged jump at the Yorkville Dam (a low overflow structure). It is clear from the literature that there is no set design criteria for this task. Some of the aforementioned studies discuss designs for stepped chutes, riprapped slopes, labyrinth weirs, and grouted stilling basins, but it would be difficult to promulgate a design from the limited amount of data without a design validation. When considering the use of a stepped structure, there is more data and equations available, but most of them are not applicable to low overflow structures. For these reasons it was necessary to conduct a physical model study for the Yorkville Dam to find an alternative that offers the most appropriate solution.

3. Model Design

3.1 Froude Similarity

Both geometric and dynamic similitude must exist between model and prototype to obtain accurate flow characteristics and measurements in a hydraulic model study. When gravitational forces clearly predominate, which is the case with most-open channel hydraulic structures, similarity can be established by equating the ratio of inertial forces to gravitational forces in the model to the same ratio in the prototype. The Froude number (F_r) is the dimensionless parameter that gives the ratio between inertial forces and gravitational forces. It is written as:

$$F_r = \frac{V}{\sqrt{Hg}} = \frac{\text{inertial}}{\text{gravitational}} \tag{3.1}$$

where V is the mean flow velocity, H is the mean flow depth, and g is the gravitational acceleration. Similarity is then achieved when the Froude number in the model is the same as the Froude number in the prototype.

A geometric length scale of 1 to 9 was chosen to satisfy all the facility constraints in Hydrosystems Laboratory. This relatively large scale also allowed all flow patterns to be visible over a wide range of conditions. The 3 ft wide sectional model therefore, corresponds to a 27 ft wide section of the spillway. The homogenous flow characteristics in the prototype, along the whole spillway crest, justify the use of a sectional model. Using the Froude number and the selected length scale, the model and prototype parameters were quantified with the following similitude relationships:

$$L_r = \frac{L_p}{L_m} = 9 \tag{3.2}$$

$$A_r = L_r^2 = 81 \tag{3.3}$$

$$V_{lr} = L_r^3 = 729 \tag{3.4}$$

$$T_r = L_r^{1/2} = 3 \tag{3.5}$$

$$V_r = L_r^{1/2} = 3 \tag{3.6}$$

$$q_r = L_r^{3/2} = 27 \tag{3.7}$$

where,

L_r = length ratio
A_r = area ratio
V_{lr} = volume ratio
T_r = time ratio
V_r = velocity ratio
q_r = specific discharge ratio

From this point forward, the subscripts m and p refer to model and prototype respectively, and the subscript r denotes the ratio between model and prototype.

3.2 Movable-Bed Similarity

A movable-bed was employed to study the scouring characteristics of the flow. Sediment was scaled to match the sediment transport characteristics of the existing bed material. This included the present day riprap as well as the existing bed sediment before the riprap was put in place.

Physical movable-bed modeling is as much an art as it is a science, and different criteria have been developed over the years by different schools. Herein, a criterion previously used with some apparent success for solving sedimentation problems in midwest streams with the help of movable-bed models, is used (Parker et al., 1988). It involves the so called bed shear velocity u_*, a surrogate for quantifying flow-induced bed shear stress, and the sediment fall velocity V_s in a quiescent fluid, which is indicative of the hydraulic behavior of the sediment material making up the river bed. Then the criterion used in this study to scale the sediment is given by:

$$\left(\frac{u_*}{V_s}\right)_m = \left(\frac{u_*}{V_s}\right)_p \tag{3.8}$$

Prototype sediment samples (beyond the riprapped area) were collected by the Urbana office of the USGS and they were analyzed to determine particle size distributions. From the sediment samples, an average sediment gradation was developed and the corresponding fall velocity of each gradation increment was computed with the aid of figure 3.1. An average prototype friction velocity was determined using USGS discharge measurements on the Fox River and open channel flow relationships. Then the model friction velocity was computed using Froude similarity (a detailed discussion for the friction velocity computations is included in Appendix A). Finally, the corresponding model terminal fall velocity was calculated using equation 3.8. From that value,

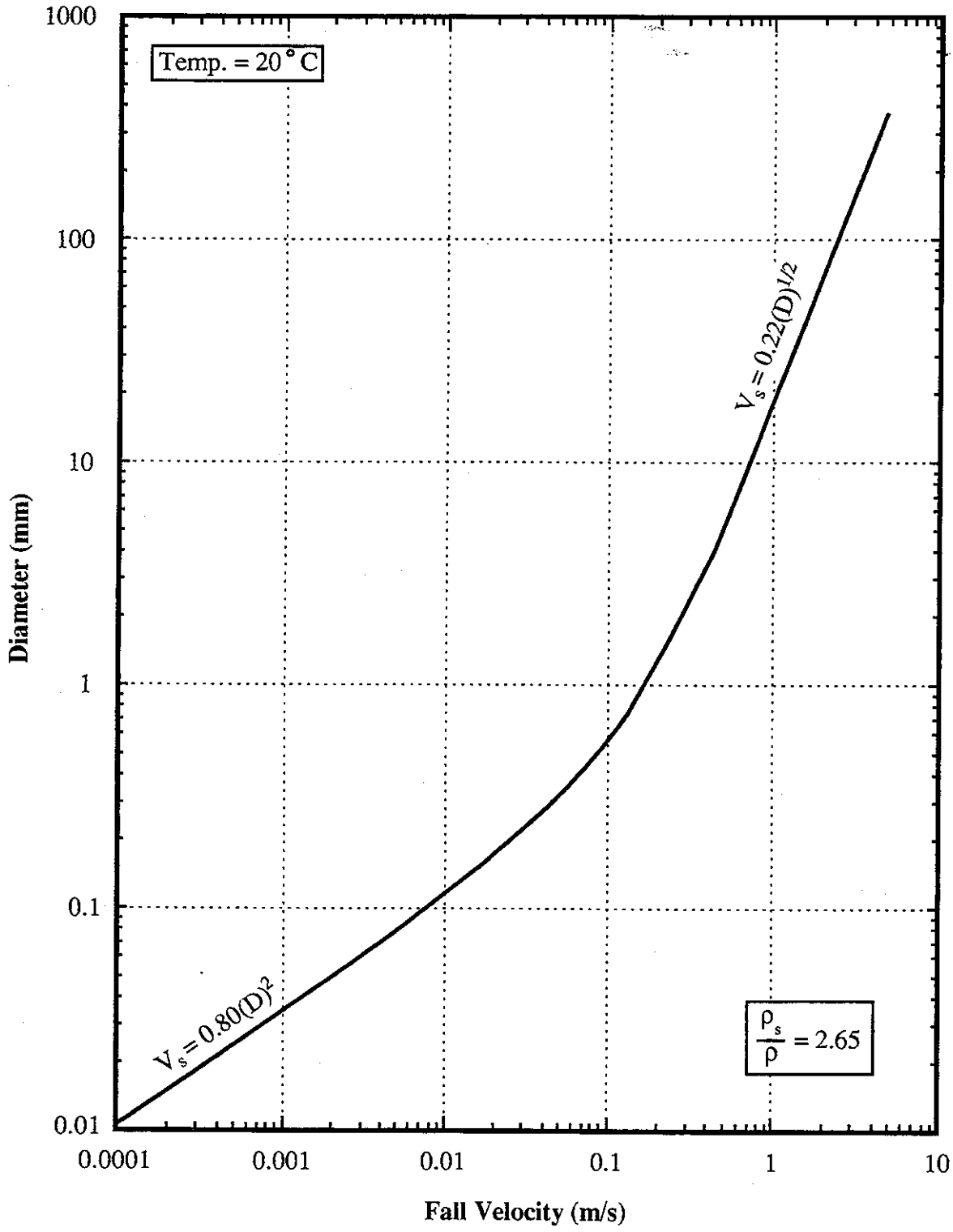

Figure 3.1 Particle diameter submerged sediment fall velocities.

figure 3.1 was used to determine the model particle diameter corresponding to the computed terminal fall velocity.

A local construction material distributor supplied the necessary sand and gravel which was used to develop the model sediment. After laborious sediment sieving and mixing, the final model sediment gradation was developed. Figure 3.2 contains the average prototype sediment gradation, the corresponding scaled gradation, and the model sediment gradation that was used. The model gradation used agrees favorably with the scaled gradation. The scaled gradation and the model gradation corresponded to a D_{50} (diameter for which 50 % of the sediment is smaller by weight) of 2.07 mm and a 2.31 mm, respectively, while the prototype had a D_{50} of 13.43 mm.

The original designs for the riprap were attained along with the design gradations. Since, the riprap is so coarse, it was scaled geometrically. The geometric scaling of the riprap can be justified by once again referring to figure 3.1. For the coarser material, the particle fall velocity scales with $D^{1/2}$. Since the friction velocity was scaled with Froude similarity, also (see appendix A) the scaling relationship (equation 3.8) agrees with Froude similarity. Therefore, the riprap can be scaled geometrically (i.e. scaling by equation 3.8 would compute the same diameters as geometric scaling, so either one could be used). Notice that the fall velocity of particles coarser than approximately 1 mm follows Froude similarity, but for particles with mean sizes smaller than approximately 1 mm geometric scaling would not give the correct sediment size for a movable-bed model. This is precisely why the original sediment was scaled using equation 3.8 and not by geometric scaling (i.e. some of the particle diameters were less than 1 mm).

Figure 3.3 contains the design riprap gradations (recall there were two riprap types, figure 1.5), the scaled riprap gradation, and the modeled riprap. Table 3.1 contains the D_{90}, D_{50}, and D_{10} for the two types of riprap. The modeled riprap type 1 compares quite favorably to the scaled

	Riprap Type 1			Riprap Type 2		
Diameter	Prototype (cm)	Scaled (mm)	Modeled (mm)	Prototype (cm)	Scaled (mm)	Modeled (mm)
D(90)	25.52	28.36	29.09	59.27	65.86	44.24
D(50)	13.18	14.64	16.20	43.40	48.22	33.00
D(10)	6.89	7.65	10.34	14.84	16.49	26.74

Table 3.1: D_{90}, D_{50} and D_{10} for riprap type 1 and riprap type 2.

gradation. On the other hand, the modeled riprap type 2 showed some variability from its corresponding scaled gradation. The rock used to model riprap type 2 was the only one commercially available that was close to that size. Nevertheless, the main objective, which was to

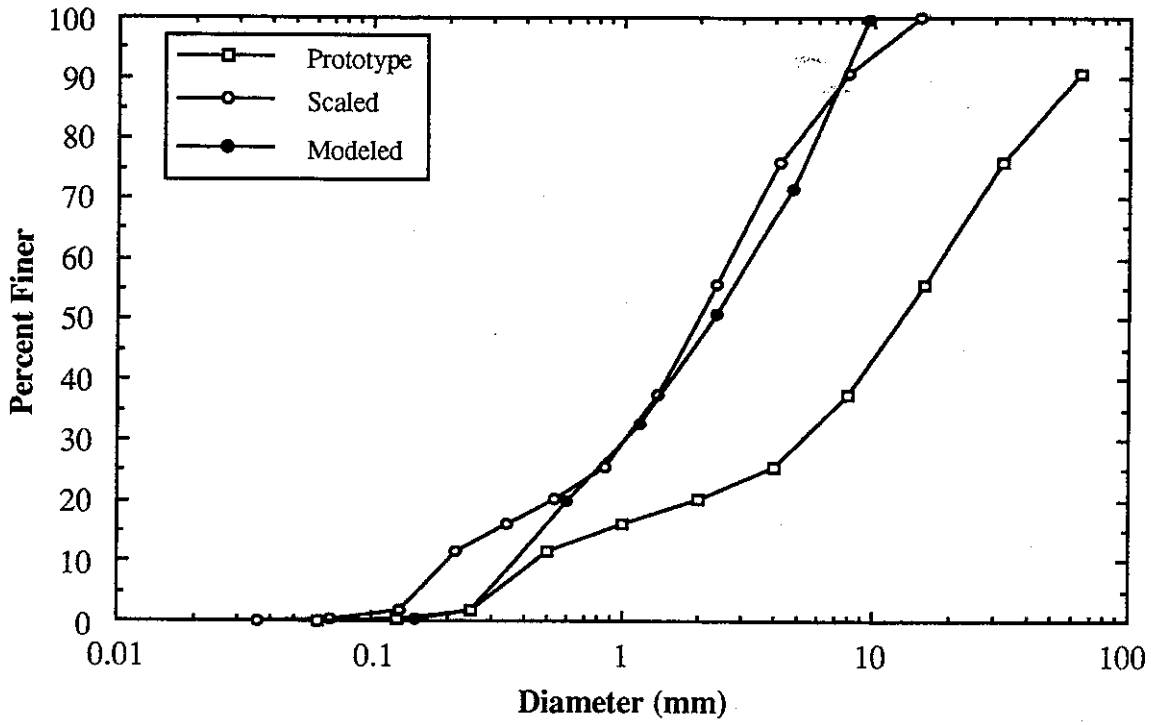

Figure 3.2: Existing sediment, the corresponding scaled sediment and the modeled sediment gradations.

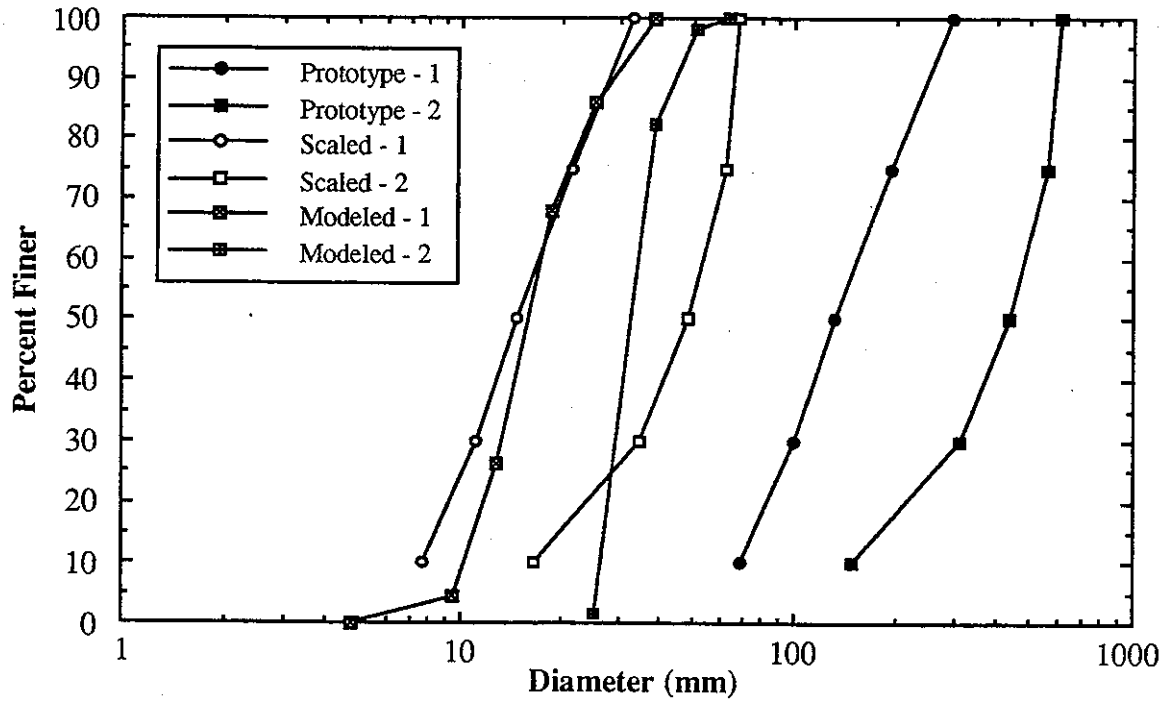

Figure 3.3: Type 1 & 2 design riprap, the corresponding scaled riprap and the modeled riprap gradations.

develop a scour hole in the model that was geometrically similar to the existing prototype scour hole, was accomplished (as it will be shown later).

3.3 Laboratory Setup

The hydraulic model was constructed in a 64 feet (19.5 meter) long by 3 feet (0.9 meter) wide tilting flume at the Hydrosystems Laboratory of the Civil Engineering Department on the campus of the University of Illinois at Urbana-Champaign. For the first 16.4 feet (5 meters) of the channel the Plexiglas sidewalls are 4 feet (1.22 meters) tall, while the remaining 47.6 feet (14.5 meters) of the channel have 2 feet (0.61 meter) Plexiglas sidewalls. A schematic of the laboratory setup is shown in figure 3.4. Water was supplied to the channel from a constant head tank. After entering the channel, it passed through a series of honeycomb grids which straightened the flow so that it was uniformly distributed across the channel width. The flow passed over the experimental section, the spillway and movable bed, and exited the channel over a hydraulically operated tailgate which helped in controlling tailwater elevations. The flow leaving the flume entered a large sump below the laboratory floor, where it could be recirculated to the constant head tank with a set of pumps.

An angled manometer and an upright manometer each filled with fluid having a specific gravity of 1.75, were utilized to measure flow rates. The measured pressure differentials from an elbow in the flow line were calibrated with a set of weighing tanks. The two manometer setups were necessary because of the range of flows studied. The angled manometer was utilized for the lower flows, while the upright manometer was utilized during higher flows (the angled manometer was disengaged with a valve at the higher flows to prevent fluid from blowing out of the tubes).

The channel bed was set horizontal. The slope of the channel would not play a large role in the scouring process of the spillway, so a slope adjustment was not considered necessary. The sectional model was placed 12.4 feet (3.78 meter) from the honeycomb grids. The model placement in this portion of the channel allowed a larger model scale, because the pool water elevations were higher than the tailwater elevations for all flows tested. The higher pool water could utilize the extra height given by the 4 feet (1.22 meter) sidewalls. It also allowed for the flow structure and scouring process just below the spillway to be more visible than would have been possible with the 2 feet (0.61 meter) sidewalls.

The 1:9 scaled model was constructed from the dimensions given in figure 1.4. Prototype surveys suggested that neither of the scour holes had reached an elevation below 561.00 feet MSL. For this reason, the model was constructed down to a prototype elevation of 560 feet MSL. The prototype surveys also demonstrated that the bed beyond the scour hole is at an average prototype elevation of 569.00 feet MSL. For the 1:9 scale, this meant that the bed surface was 1 foot above

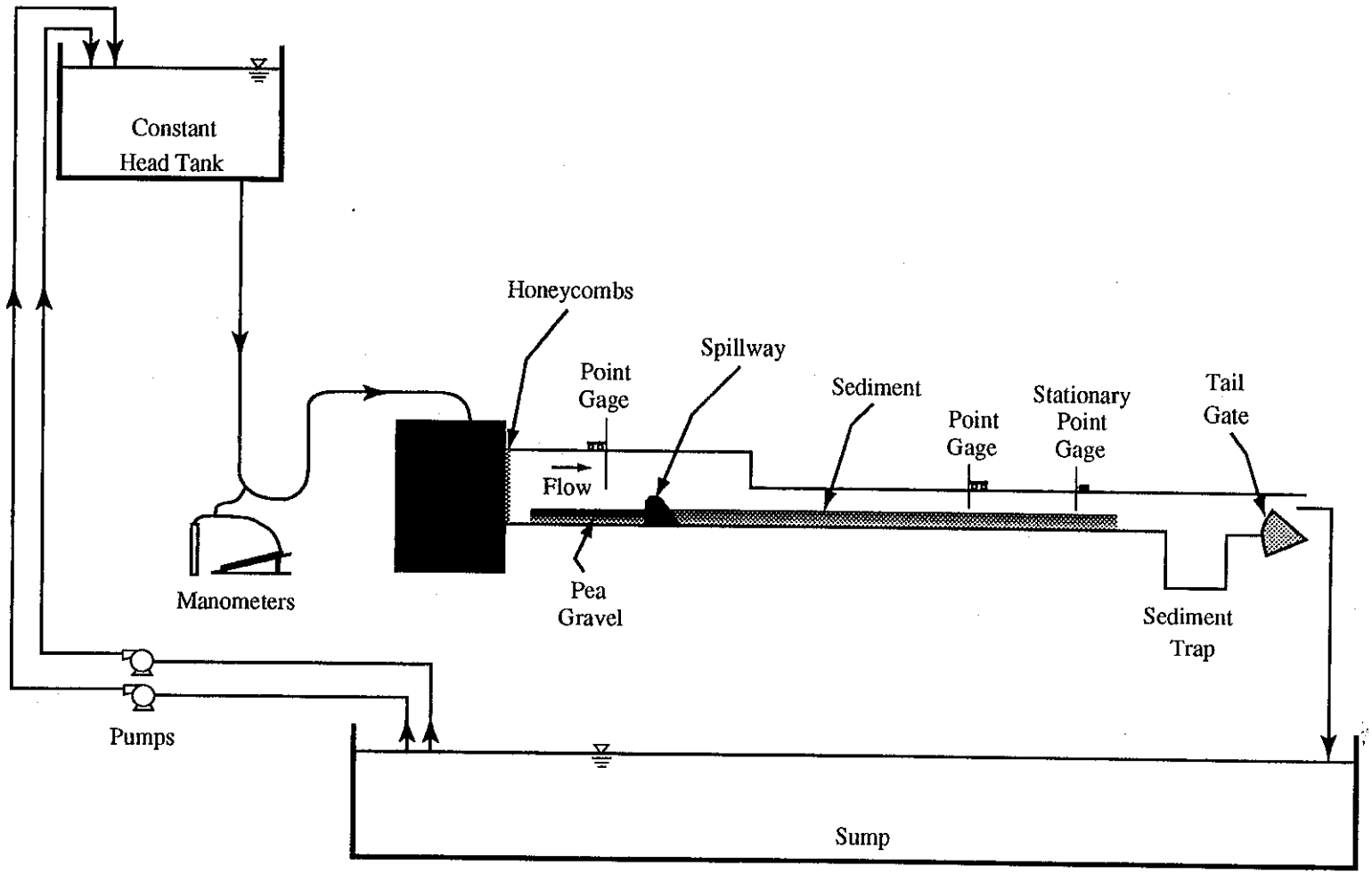

Figure 3.4: Laboratory setup.

the channel bottom. The modeled sediment was originally placed downstream of the spillway at this level for the first calibration run, as well as the first experimental runs, for each alternative. For the riprap calibration, the rock was placed as described by the original designs in 1977 (IDOT). Upstream from the model section, a coarse pea gravel was placed to a prototype elevation of 569 feet MSL. This simulated the upstream river bed.

To aid with the model measurements, two moveable point gages were employed along the channel. One was placed upstream and one downstream of the spillway. A stationary point gage was placed well downstream to measure tailwater elevations. Prototype pool water and tailwater elevations were obtained from HEC-2 simulations provided by the Illinois DNR. These simulations were verified with actual discharge measurements taken by the IDOT Division of Water Resources at Yorkville Dam. Figure 3.5 contains the pool water (figure 3.5a) and the tailwater (figure 3.5b) rating curves. These relationships were scaled down and used in the model. All measurements in the model were referred to the top of the spillway. Since, this elevation is known (575 ft MSL), and would not change, it seemed to be the easiest benchmark to use during the experiments.

The setup for each experiment was first started by filling up the channel from downstream with a hose to a level well above the expected tailwater elevation. This was necessary because if the unprotected downstream bed was subjected to a direct flow discharge, there would have been a large amount of scour. This would not have been representative of the scour that would occur when the nappe was plunging into the tailwater. Next, the stationary point gage was set to the scaled down tailwater elevation. Then, the flow from the constant head tank was turned on and adjusted until it had reached the target discharge. Lastly, the tailgate was lowered until the tailwater elevation matched the stationary point gage reading. If the model is operated correctly, the tailwater (at reasonable distance downstream from the hydraulic jump) would attain normal flow conditions.

To get an idea of the magnitudes of the flows that the Yorkville Dam encounters, flood frequency calculations were obtained. Table 3.2 lists computed return periods for the Yorkville reach. Included in the table are the Corps of Engineers simulated discharges, return periods calculated by the DNR, and the return periods computed assuming a Gumbel distribution. The Corps used a HEC-2 model for the Fox River Watershed along with 24-hour rainfall amounts from the U.S. Weather Bureau Technical Paper No. 40 to develop the flood insurance analysis (IDOT, 1995). The DNR used the HEC Flood Frequency Analysis computer program to obtain their values. The values were computed using a skew coefficient of -0.40 for the Log-Pearson Type III Distribution. The Gumbel Distribution return periods were obtained by using a graphical procedure and Gumbel probability paper. The Corps of Engineers estimations are the most conservative of the three.

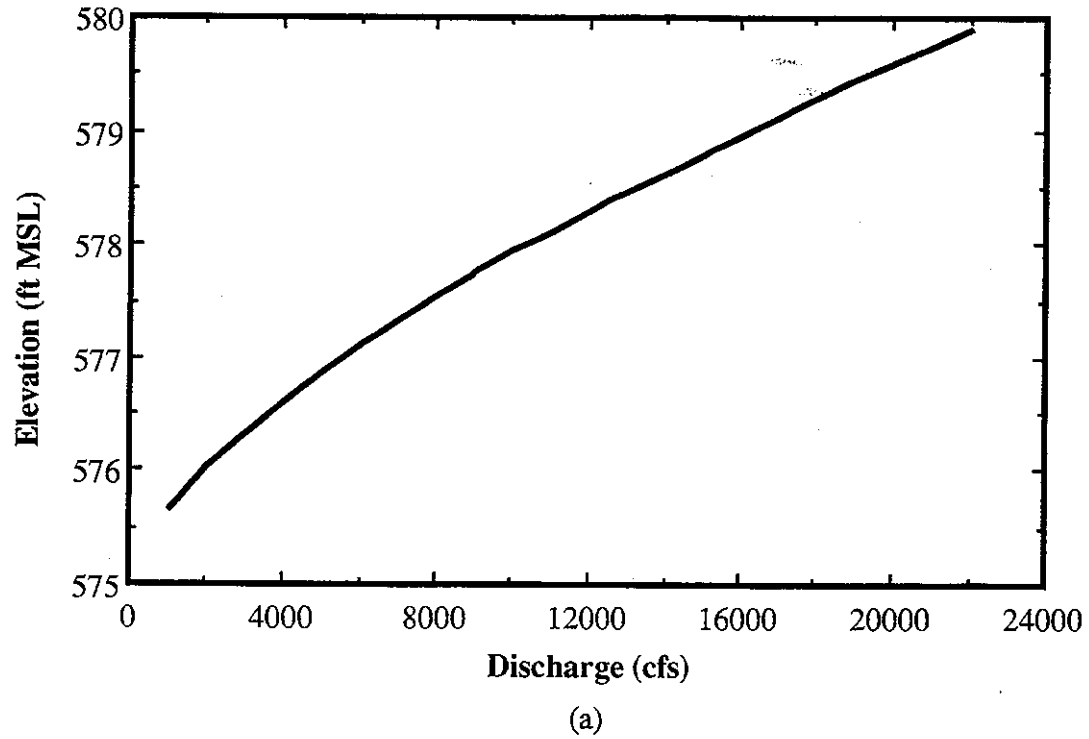

(a)

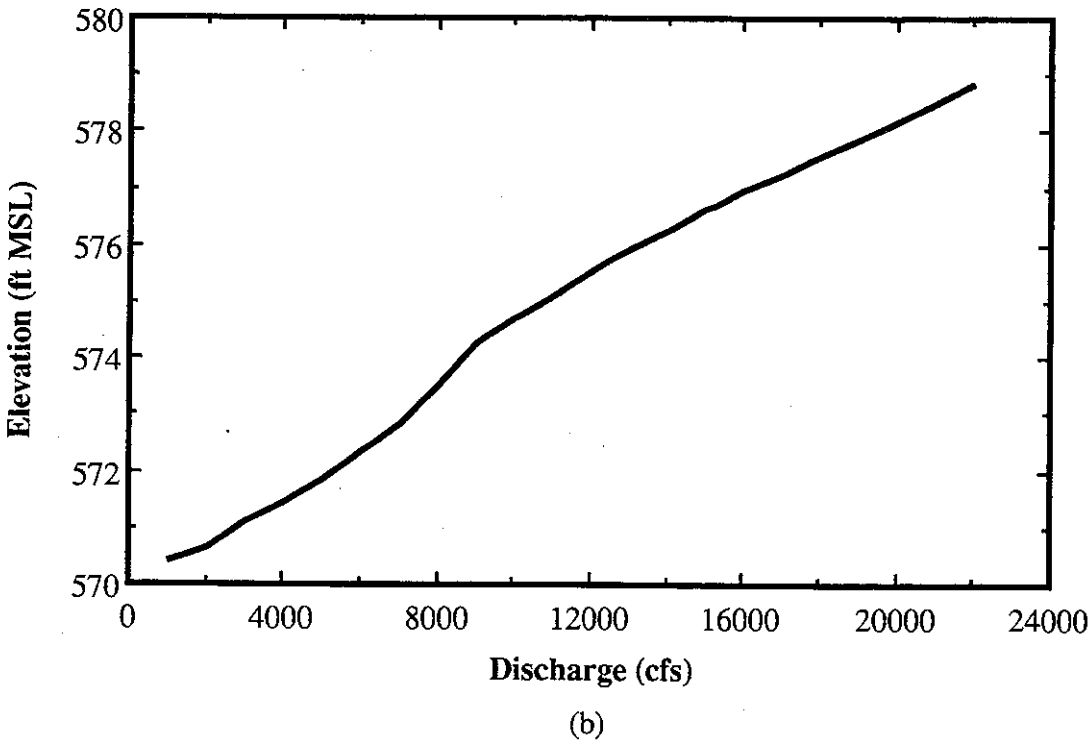

(b)

Figure 3.5: Prototype rating curves for (a) the upper pool, and (b) the tailwater.

Return Period (years)	Corps of Engineers (cfs)	FFA Program (cfs)	Gumbel Dist. (cfs)
1	5000	3640	-
2	7000	6360	6300
5	8900	8410	8200
10	10580	9530	9300
25	12500	-	10800
50	15220	11500	11900
100	17697	12200	13000
500	22615	13600	15600

Table 3.2: Computed return periods for the Fox River at Yorkville, IL.

3.4 Model Construction

The model spillway was constructed in the shop of the Civil Engineering Department. The model cross section was cut into numerous plywood sheets. The plywood sheets were then fastened together to a width of 3 feet (0.9 meter). Concrete was then poured into the form until the spillway section took the scaled Yorkville Dam shape.

4. Model Calibration and Verification

4.1 Original Scour Hole Development

Once the model was constructed, the calibration process first started. Proper calibration of the model was necessary to verify that any experimentally tested model modifications would produce the same characteristics in the prototype. During model calibration and verification of the Yorkville Dam, an attempt was made to reproduce the original scour hole (1976 survey, see figure 1.5). Tailwater measurements were made along the channel to ensure the flow was at, or near, normal flow conditions. Flow depth measurements in the upper pool were also made, and the scour holes were surveyed so that both could be compared with the corresponding prototype values. Table 4.1 lists the experimental conditions for the original scour hole calibration analysis. Appendix B contains a list of all the experiments done during the study. From this point onward, any values given correspond to the prototype, unless otherwise specified.

Experiment	Discharge (cfs)	Tailwater Elev. (ft MSL)	Tailwater Depth (ft)
A	2021	570.68	1.68
B	7000	572.84	3.84
1	1000	570.40	1.40
2	6000	572.36	3.36
3	10000	574.70	5.70
4	15000	576.64	7.64

Table 4.1: Experimental conditions for the original scour hole calibration.

The scaled sediment (see figure 3.2 and section 3.2) was placed in the channel to an elevation of 569.00 ft MSL. The first two experiments, experiment A and experiment B, were primarily test runs. After those two experiments, the final methodology for model operation was set (see section 3.3 for the discussion of model operation). The model setup for experiment A and B was similar, but not identical to all the other experiments. The model was started in the same manner as all the other experiments, but the tailwater was not adjusted to a fixed elevation. It was instead adjusted until the flow had approximately reached normal depth (it should be noted that perfect model construction would ensure both methods would give the same results). Nevertheless, the measurements taken from these two experiments are useful and will still be summarized.

Due to sediment sorting during the scouring process, it was originally thought that it would be necessary to replace the sediment after each run with the original gradation. It eventually became obvious that complete replacement of the sediment in the channel was very time consuming. For this reason, the remainder of the experiments were run in a consecutive sequence. The bed was set at an elevation of 569.00 ft MSL, and the lowest discharge was studied first (1000 cfs). For this series of experiments the water was turned off after the scour hole had reached an equilibrium shape, and then the scour hole was surveyed. With the scour hole still present in the channel, a higher flow was then discharged over the spillway (6000 cfs). That scour hole was surveyed, and then the next discharge was studied (10000 cfs and then 15000 cfs). The above stepwise development was justified because it was known that the scour hole for the sediment would get larger for a larger discharge. Since the scouring rate was not as important as the final scour hole dimensions, it did not matter what size the hole began, but rather that it became larger and reached the equilibrium for that flow condition.

During each experiment, pictures were taken from the side of the experimental section at approximately half-hour increments. Each subsequent picture was taken from the same distance, and therefore, contained the same dimensions as the preceeding pictures. The pictures were then analyzed to make sure the experiments were run long enough to achieve equilibrium. It was discovered that operating the model for 3 hours was sufficient enough time to develop, within reason, equilibrium conditions. This corresponds to a prototype elapsed time of about 9 hours (from equation 3.5).

4.1.1 Scour Hole Description and Measurements

Even for the lowest flow there was a considerable amount of scour below the spillway (i.e. 1000 cfs). It was clear that all the plunging flows down the face of the spillway conveyed a shear stress above the critical shear stress, and that sediment transport was initiated. For all the flows, the scouring process began as soon as the water was discharged over the spillway. Lowering of the tailwater to the final position only increased the amount of scour. Initially, it appears that all sediment sizes were scoured out. As the scour hole became deeper, the larger sediment was not able to escape and consequently began to circulate in the rolling motion of the flow. Therefore, the sediment was sorted and the coarsest material remained inside the hole, resulting in the armoring of the scour hole. The sediment that was able to escape the scour hole moved down stream in the form of a delta. As more sediment was eroded from the hole, it moved along the surface of the delta and eventually deposited in front of it. As the supply of sediment continued, the delta moved father downstream. Most of the fine material left the scour hole leaving behind only the coarsest

material. Since, the flow did not have enough energy to move this material outside of the scour hole it eventually reached an equilibrium.

The higher the amount of energy the flow possessed, the larger the scour hole it could develop. Even though the tailwater was rising with an increase in discharge, it was not enough to cushion the scouring action of the plunging nappe. Figure 4.1 depicts the scouring action for a 6000 cfs discharge. If one looks closely at the face of the scour hole, it is clear that only the coarser gravel remains. It is also possible to see that this flow generated a good amount of air entrainment. If one looks at the photo, with a little imagination, it is possible to distinguish the circular motion inside the scour hole. Figure 4.2 depicts the scouring action for a 15000 cfs discharge. For this flow, the scour hole has increased a good amount. The jump is so submerged that there is not a lot action inside of the hole. At this flow depth the discharge over the spillway is such, that the situation is similar to that of Case D in figure 1.2.

As discussed previously, the flow for each experiment was turned off after the scour had reached an equilibrium. The scour hole was then surveyed using a Kenek, model WH-201c, bed profiler. The profiler had a mechanical head that measured from a set elevation to the bed elevation. The profiler was calibrated with the top of the spillway. Figure 4.3 contains the surface profiles for the six experiments run in this portion of the study. All length scales where made dimensionless with the height of the spillway (upstream height, which equals 6 ft in prototype and 0.667 ft in the model), and all elevations are referenced to the top of the spillway. This places the top of the spillway at a dimensionless elevation of 1.0, and the original bed at a dimensionless elevation of 0.0.

Figure 4.4 compares the experimentally generated scour holes to the dimensionless plots for both the original scour hole (1976) and the riprapped scour hole (1991). One might notice from figure 4.4 that the surface of even the largest discharge (15000 cfs), which corresponds to the 50 year flood by the Corps of Engineers calculations, does not compare that favorably to the 1976 scour hole. It should be noted, that the maximum discharge the Yorkville Dam has experienced was 9820 cfs in 1973. One might also notice that the surveys for the 7000 cfs, 10000 cfs, and 15000 cfs discharges show that the scour hole had reached the bottom of the channel, whereas the prototype scour hole had not scoured to that elevation.

It would seem that there are two reasons why the scour holes do not match up. It is possible that the present day sediment is not representative of the sediment that was originally present at the spillway (i.e. from 1960 to 1976). The original material might have consisted of a finer sediment that has since completely washed downstream, leaving behind only the coarsest material. The other reason why the scour hole in the prototype is larger, is because the modeling is being done for normal flow conditions. The tailwater did not instantaneously reach an increased elevation when the discharge over the spillway increased at Yorkville Dam. It took time for the tailwater to

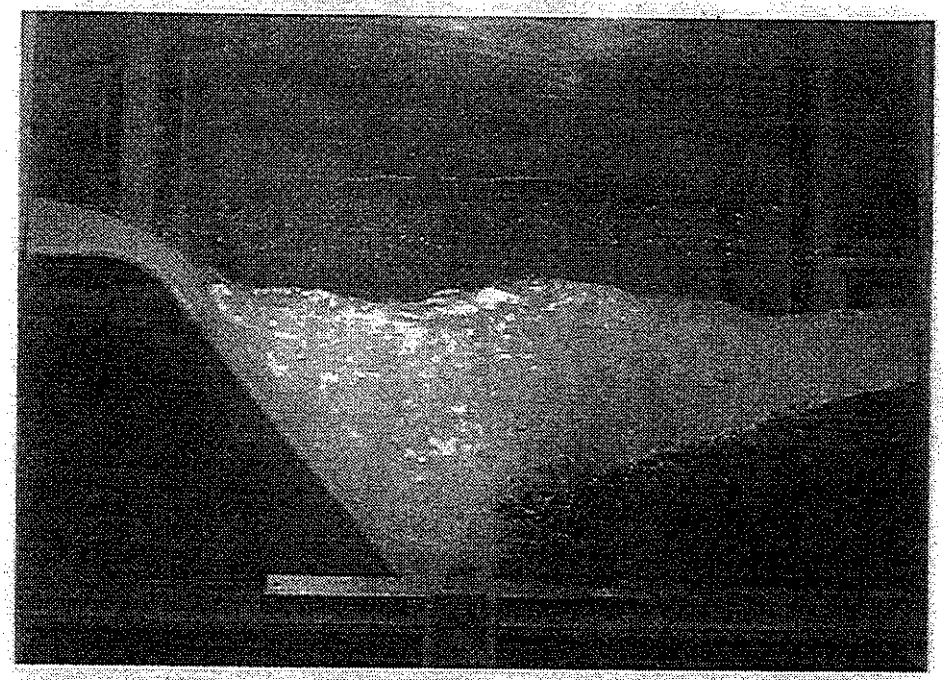

Figure 4.1: Sediment scour at Q = 6,000 cfs.

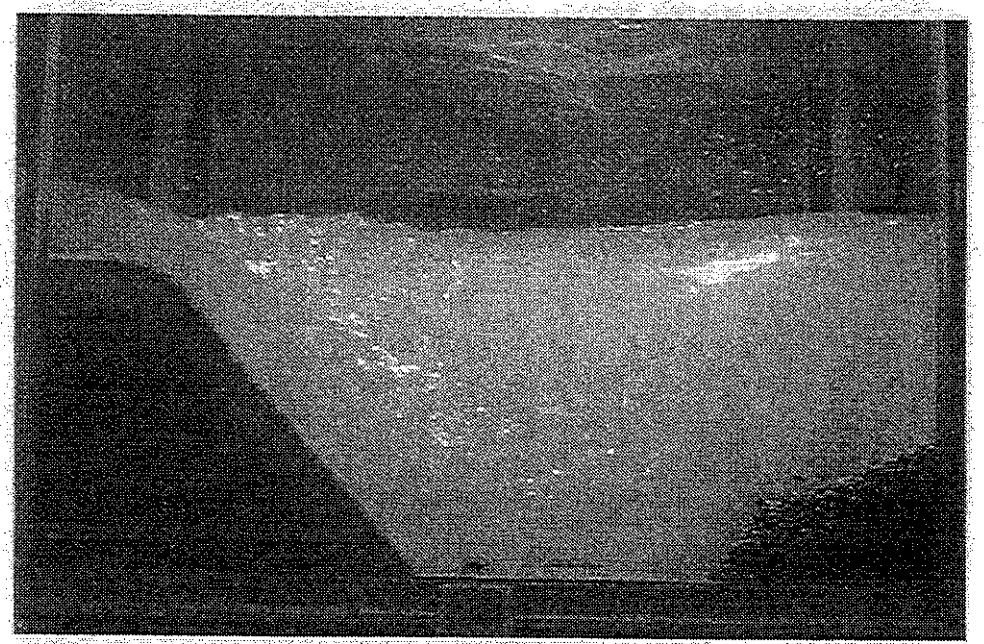

Figure 4.2: Sediment scour at Q = 15,000 cfs.

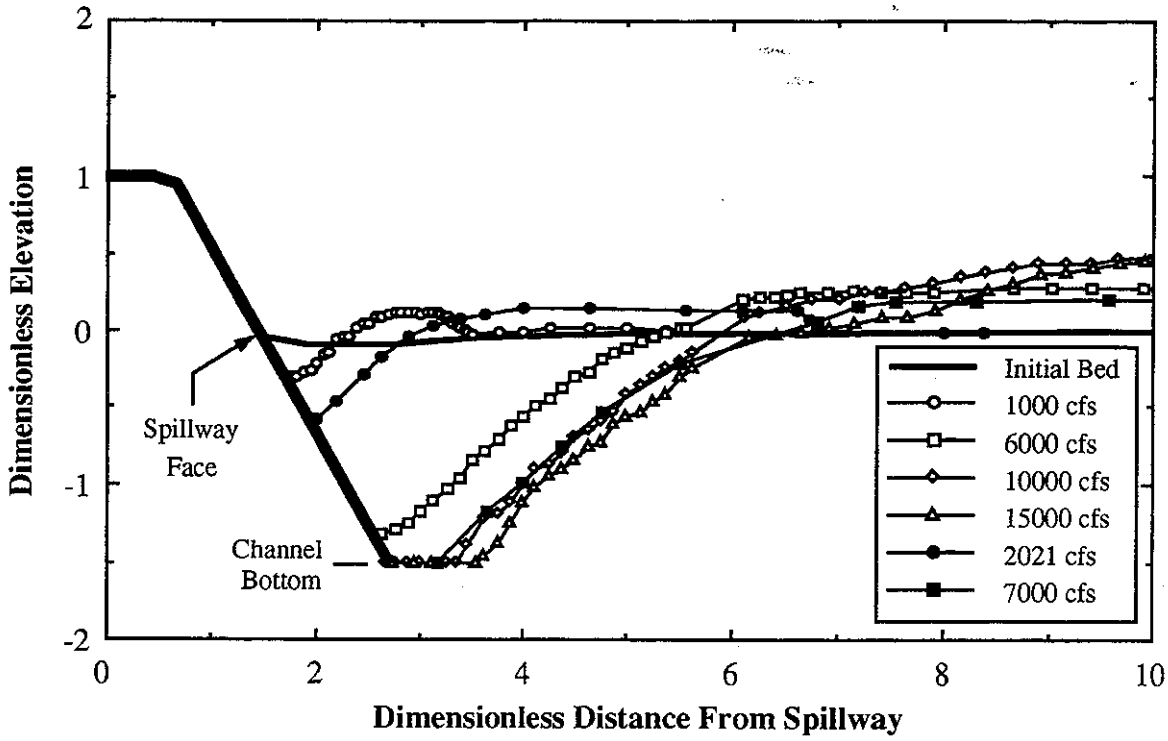

Figure 4.3: Sediment scour hole surveys.

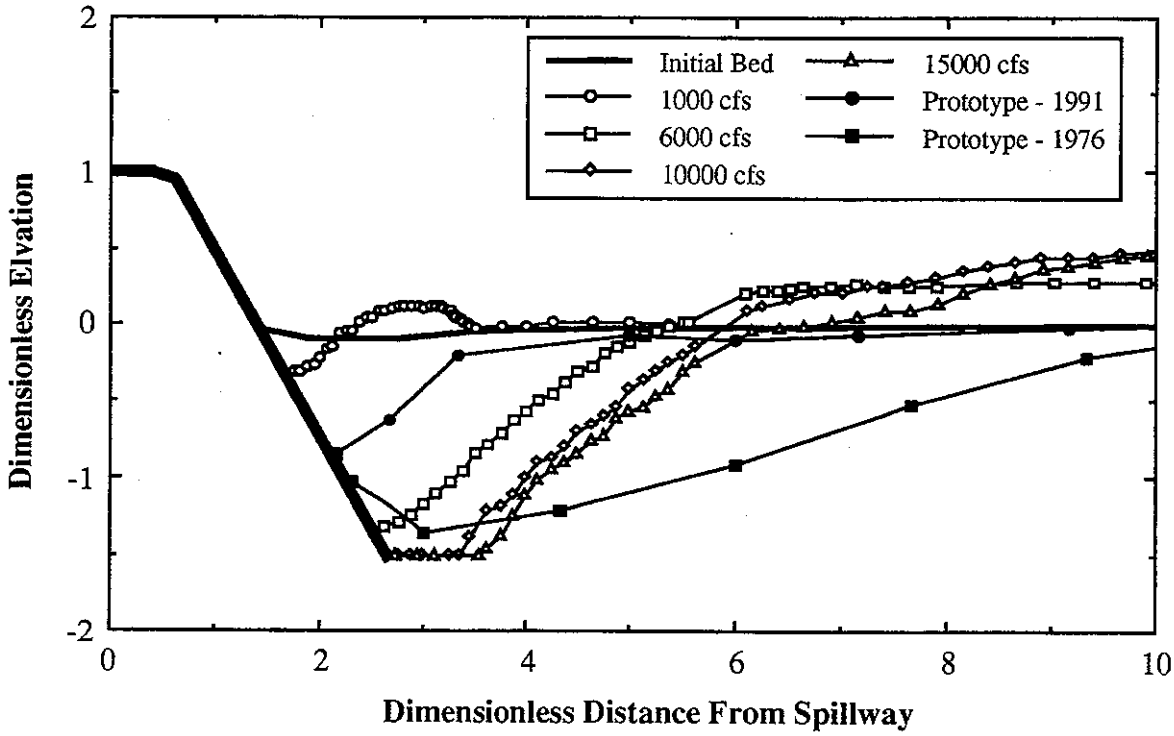

Figure 4.4: Prototype and experimental scour holes.

adjust. While the tailwater was adjusting to its new elevation, the flow was scouring to an increased amount, as compared to the scour that occurs for the higher tailwater. There is no reasonable way to model the hydrograph of the prototype, and therefore, the variation in tailwater. Overall, though, the scour holes did show a shape similar to that of the prototype, and developed the same conditions that are present today (i.e. the "hydraulic"). Observations of the "hydraulic" for the sediment scour hole will be discussed in the next chapter.

4.1.2 Tailwater and Pool Water Measurements

After the model was started, and the tailwater elevation was set, tailwater elevation measurements were made with the moveable point gage. Figure 4.5 contains a plot of the measured dimensionless tailwater elevations for each experiment compared to the HEC-2 simulated prototype elevations. The elevations were measured downstream of the hydraulic jump and then made dimensionless with the spillway height. The streamwise length was made dimensionless with the spillway height, also (6 ft in the prototype). The plot clearly shows that no backwater effects were noticed over the first 171 feet (52 meters) of the reach. This is a good indicator that the model was operated properly.

Table 4.2 contains the spillway head values (made dimensionless with the spillway height) as well as those estimated with HEC-2 in a tabular form. Figure 4.6 contains a plot of the measured dimensionless heads on the spillway for the range of discharges studied. The measured head is compared to the simulated heads obtained from HEC-2. In the model, the pool water elevations seem to be a little higher than the corresponding elevations in the prototype. The difference between the two, seems to be larger at lower flows than higher flows.

Experiment	Discharge (cfs)	Measured Head (ft)	Prototype Head (ft)
A	2021	1.224	1.035
B	7000	2.619	2.355
1	1000	0.864	0.660
2	6000	2.349	2.125
3	10000	3.123	2.965
4	15000	3.906	3.815

Table 4.2: Measured pool water heads and the corresponding prototype values.

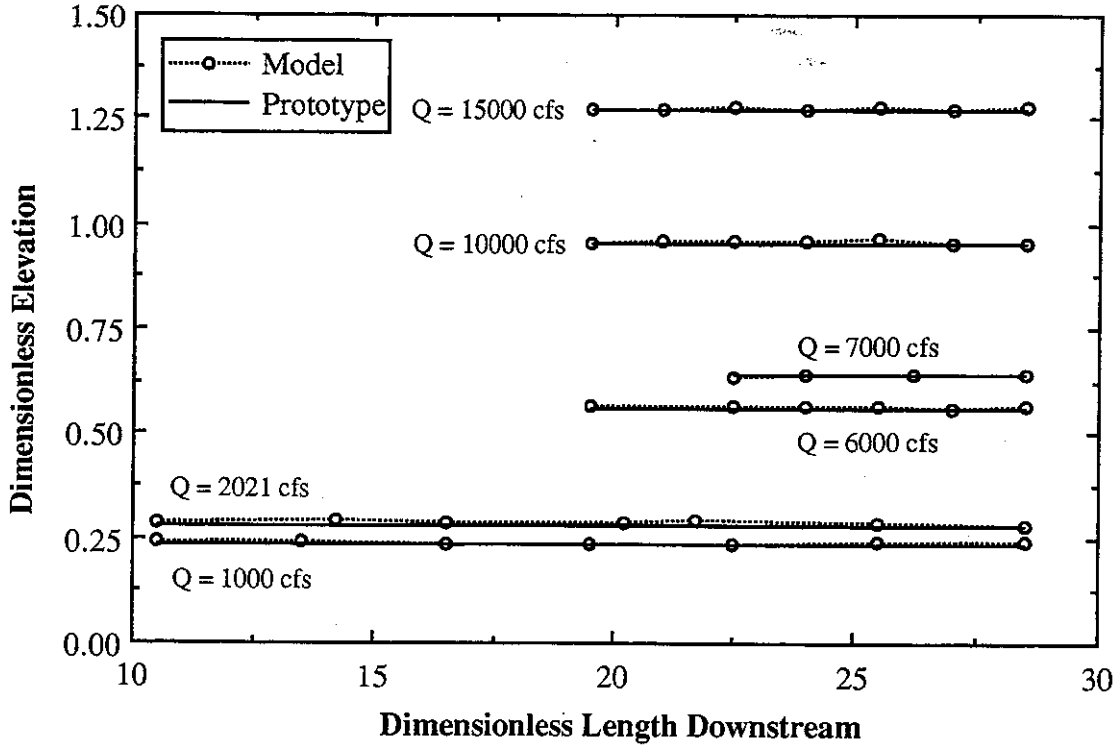

Figure 4.5: Model and prototype dimensionless tailwater elevations.

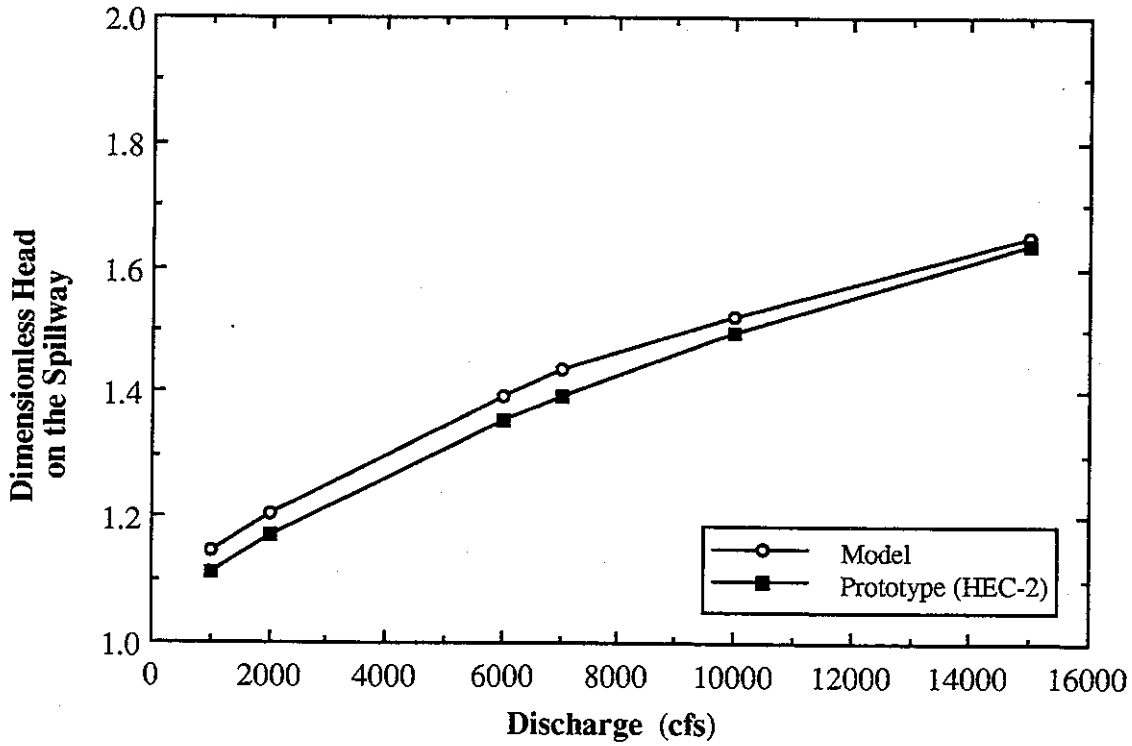

Figure 4.6: Model and prototype dimensionless spillway heads.

4.2 Riprap Failure

For the next part of the study, an attempt was made to develop the riprapped scour hole that was present in 1991 and is still present today. The model was setup using the original designs that were implemented from 1977-1978. Figure 1.5a is a schematic of this design. The scaled riprap (see figure 3.3) type 1 was placed to an elevation of 566.00 ft MSL. Then the scaled riprap type 2 was placed over top of the riprap type 2 to an elevation of 568.00 ft MSL. The first flow discharge studied for this arrangement was 1000 cfs. For subsequent experiments, the discharge was increased only slightly so that the threshold for the riprap scour could be assessed, and observations of the amount of scour for each discharge could be made. The major observations for each discharge are summarized in Appendix B.

A 1000 cfs discharge was not enough to move the riprap at all. At a discharge of 3000 cfs the rocks did start to move. This magnitude of flow was enough to make the rocks vibrate in place causing some of them to slowly roll away from the face of the spillway. At 4000 cfs, the "vibration" was becoming more obvious and there was a little more scour. At 5000 cfs the rocks were moving a little more. At this point, there was still not enough scour to reach riprap type 2, though. All the rock that was removed from below the spillway was mounding up behind the scour hole. A 7000 cfs discharge was enough to expose riprap type 2. It would seem though, the shape of the scour hole and flow structure were not at the right condition for the removal of riprap type 2 from the scour hole. At 9000 cfs the tailwater was starting to get quite high. There was not as much aeration as in the previous flows, but there was still some scour. From the side, this flow did not look as violent as some of the lower flows. The 9000 cfs flow had enough energy to start lifting the second layer of riprap out. At 10000 cfs the mound of scoured material was starting to become quite pronounced. The scour hole was growing more and more.

The scour hole developed by 10000 cfs was a good place to survey the hole, because the highest discharge that the Yorkville Dam had witnessed since the riprap placement was 9350 cfs. The comparison of this survey to the prototype survey, which is included in figure 4.7, showed that the scour hole in the model was still smaller than the measured scour hole in the prototype. This seemed to be odd at first, because the modeled riprap was smaller than the corresponding scaled down prototype riprap.

Shortly after the 10000 cfs scour hole was developed, the model was run at 5000 cfs as a demonstration for a class. It became apparent very quickly that the 5000 cfs flow rate was scouring an even larger hole. It had seemed that the exposure of the riprap type 2 and the lower tailwater elevation (i.e. the tailwater acts as a kind of cushion to the falling nappe) developed conditions for scour at a lower discharge. The shape of the scour hole at 5000 cfs seemed to be more vertical in nature. That is, the flow scoured deeper, but not farther downstream. The survey

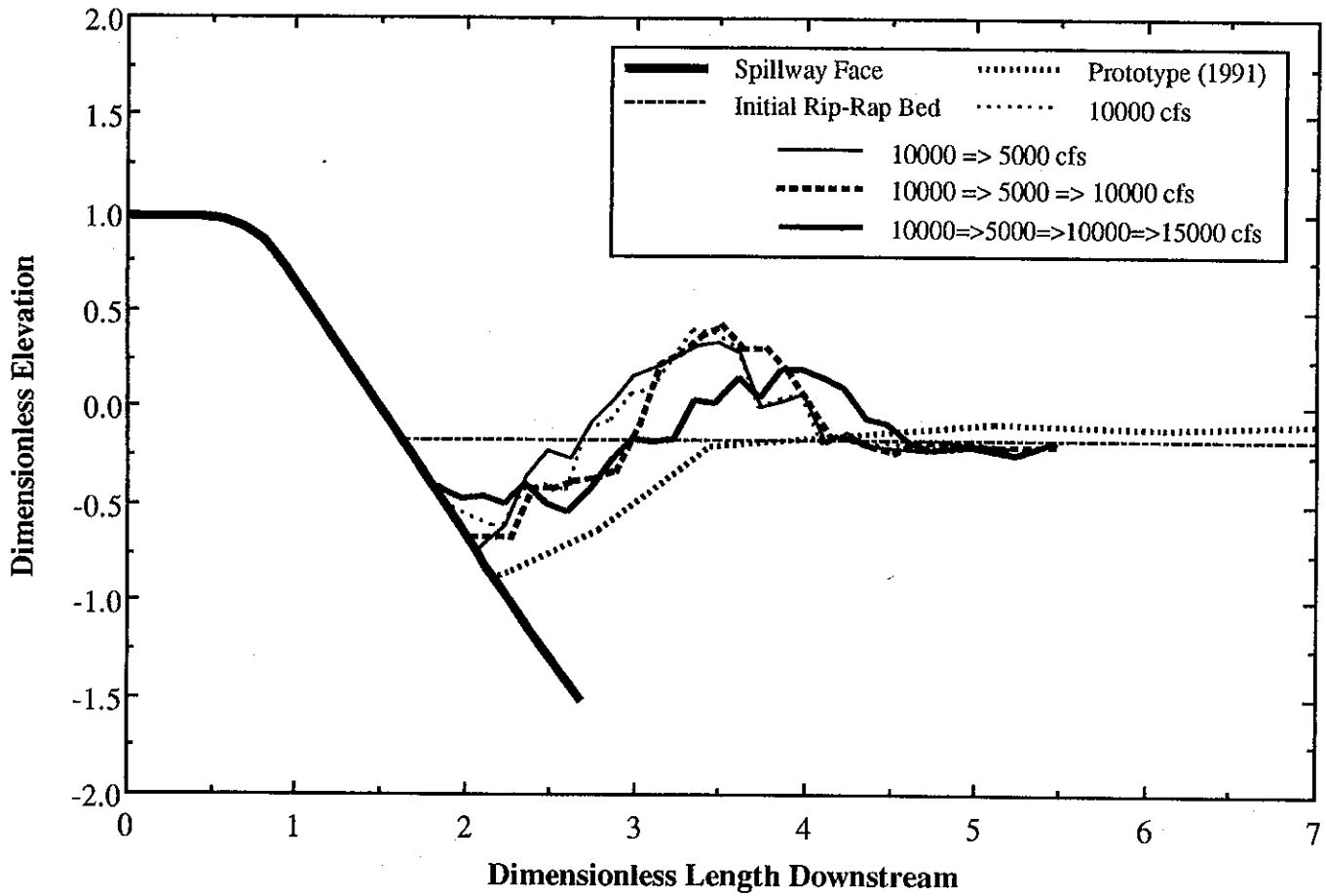

Figure 4.7: Experimental and prototype riprap scour holes.

after 5000 cfs is also included in figure 4.7.

Next, it was decided that a 10000 cfs flow might widen the scour hole. It was felt that the higher velocities could shear the mound of sediment built up behind the hole and move it downstream. The 10000 cfs discharge did exactly that. Comparison of the scour hole, after this chain of discharges, with the prototype scour hole still showed the scour hole was a little smaller, though (figure 4.7). After this comparison it was concluded that it would be impossible to try all the different flow combinations that could have caused the scour (i.e. the change in discharges and tailwater elevations) However, it was clear that periodic variations in discharge do have a widening effect. It would seem that the lower discharges in the prototype scoured the hole deeper, and then some time later a larger discharge might have widened the hole. These two events could have occurred any number of times, until the hole reached its present day size. This suggests that the scour hole in the prototype may not have met an equilibrium, yet. It could still scour to a greater extent while going through the above mentioned process.

Included as figure 4.8 is a picture of the riprap scour at 7000 cfs. Figure 4.9 presents the scour hole that was generated at 10000 cfs the second time (1000-10000 cfs, 5000 cfs, 10000 cfs). Figure 4.10 is the scour hole generated at 15000 cfs. Notice the large mound behind the scour holes for the 7000 cfs and 10000 cfs scour holes. Also, notice how this mound is pushed downstream and the scour hole is widened for the 15000 cfs scour hole.

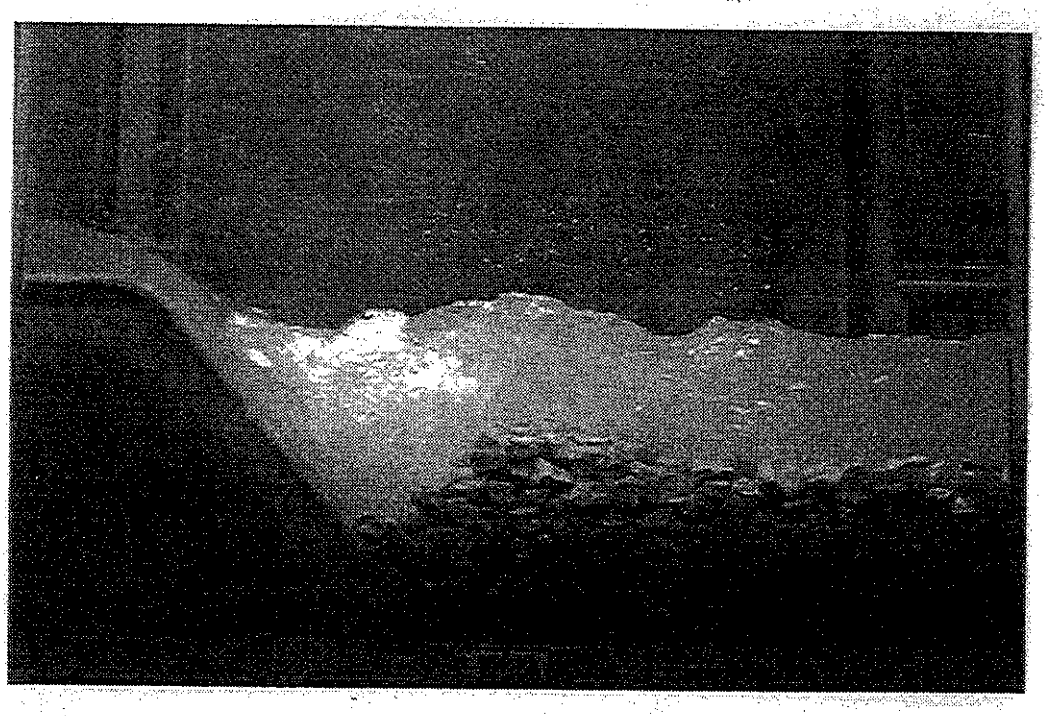

Figure 4.8: Riprap scour at Q = 7,000 cfs.

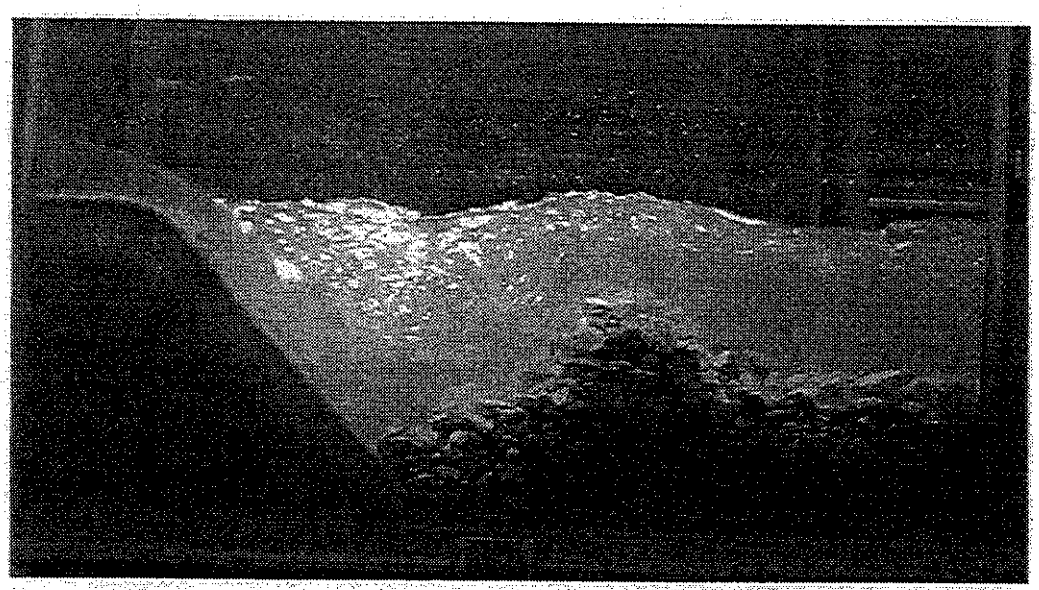

Figure 4.9: Riprap scour at Q = 10,000 cfs.

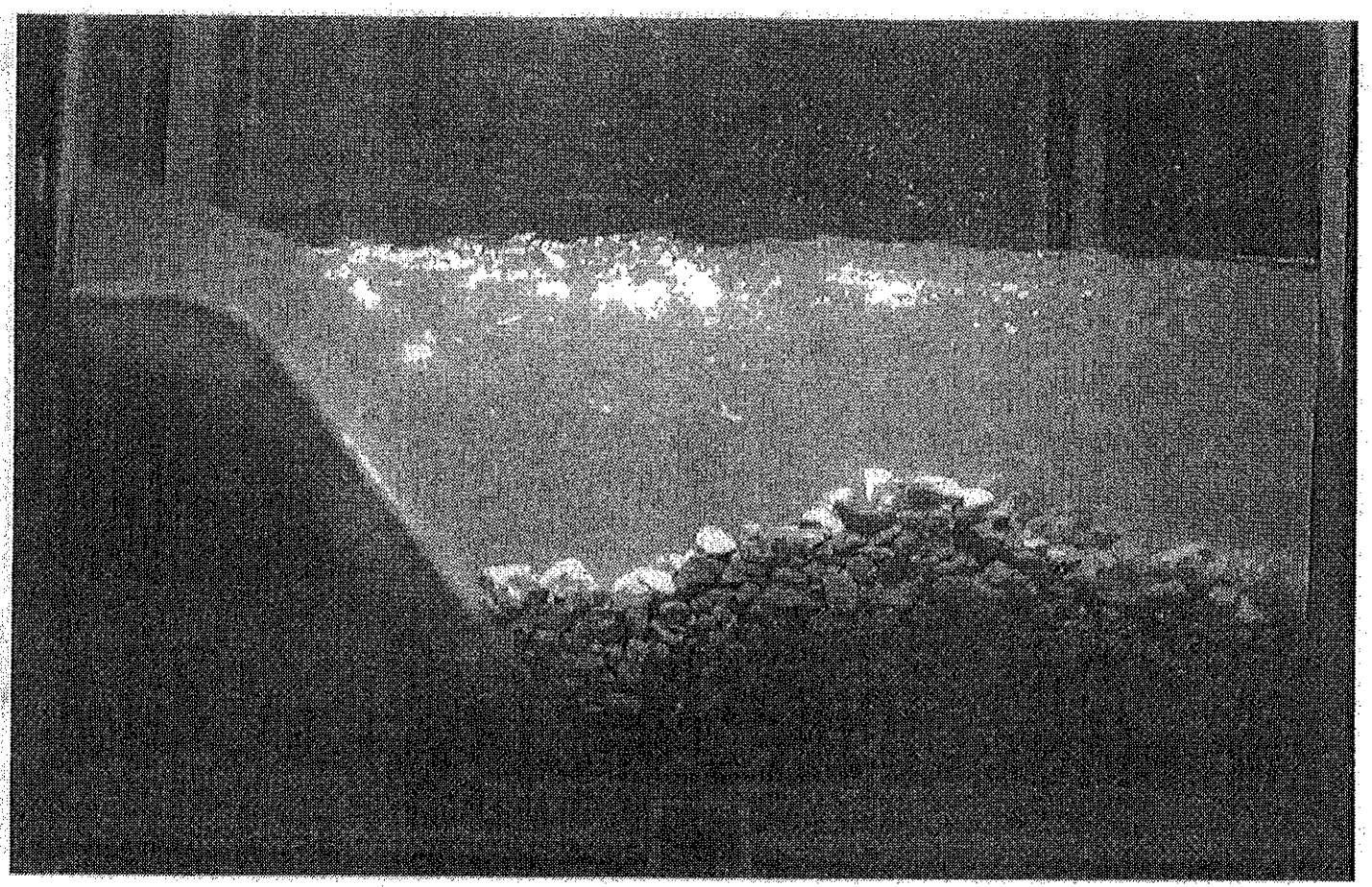

Figure 4.10: Riprap scour hole at Q = 15,000 cfs.

5. Roller Characteristics

5.1 "Boil Barrier"

The development of a submerged jump inside of a scour hole creates the same conditions, (i.e. a roller) that have been discussed in the literature review but its overall shape seems to be different. Figure 5.1 contains a schematic of the submerged jump/roller for the scoured bed condition at the Yorkville Spillway. The plunging flow rides along the face of the scour hole, and once it has reached the top of the hole on the downstream side, it has a strong vertical component. This vertical component eventually intersects the surface of the water. Subsequently, a form of a boil develops. The boil, which occurs at a short distance downstream from the spillway, rises the water above the normal flow depth. This elevated flow acts as a barrier to anything that may be on the water surface. The rolling action of the flow underneath the surface, coupled with this barrier, enables the flow structure to capture objects such as a boat, a tree branch, other objects in the flow, or a person.

The boil is present for all discharges, but tends to become less noticeable at the higher discharges. An increase in discharge, which in turn generates more scour, pushes the face of the scour hole farther downstream. This in turn pushes the "boil barrier" downstream, too. The water now has a longer path to follow, and does not elevate as high as it did for the smaller more compact scour holes. It appears that the boil develops at the end of the roller. It seems that it marks the transition between a downstream directed surface velocity and an upstream directed surface velocity. The water surface between the boil and the spillway is directed back towards the spillway, and the water surface beyond the boil is directed downstream.

From a visit to Yorkville Dam, it is clear that this flow pattern occurs not only in the laboratory, but also in the field. During a first visit to the dam, an automobile tire remained stuck inside the previously discussed barrier. It was impacted by the falling nappe and tumbled, but it could not escape over the top of the "boil barrier". A later visit to the dam, this time with a camera, captured this phenomenon (figure 5.2). It would seem that observation of this flow structure below a dam could be a good indication of a scour hole. It would also suggest that there may be a severe public safety problem (i.e. "hydraulic") at that structure.

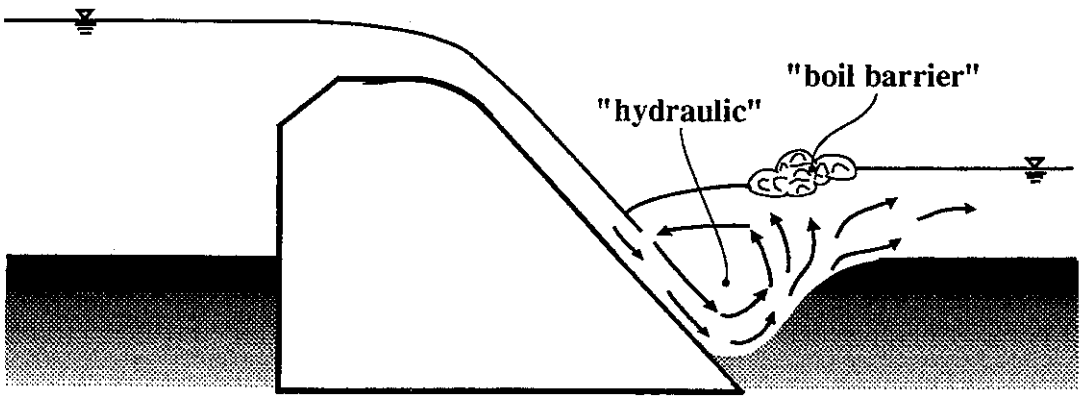

Figure 5.1: Submerged jump/roller for the scoured out condition at Yorkville Spillway.

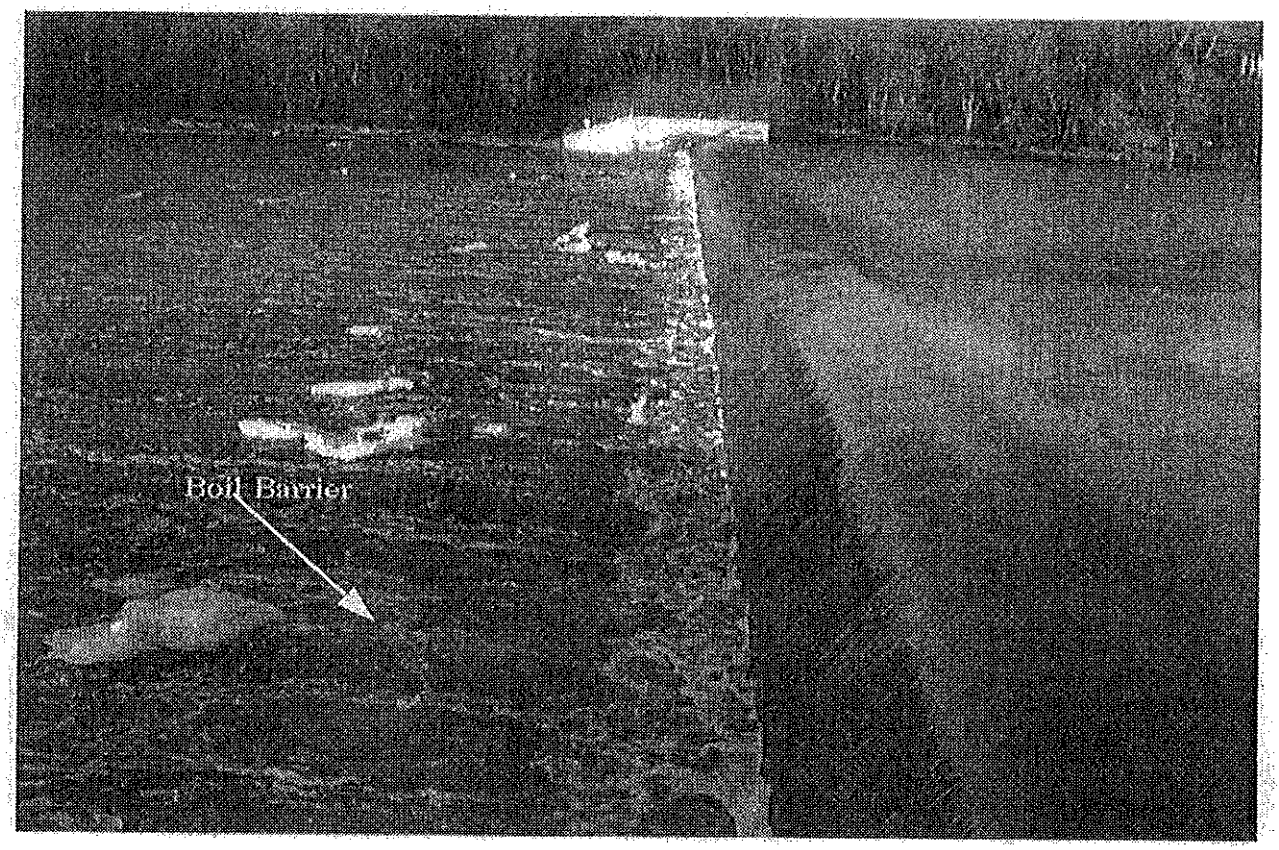

Figure 5.2: Flow characteristics at Yorkville Spillway.

5.2 Submerged Jump in Sediment Scour Holes

As seen in section 4.1.1, even at 1000 cfs a scour hole did develop below the spillway. This discharge is representative of a summer time flow. People have drowned at the structure when flows were even less than this (see table 1.1), so it is known that the prototype can generate the dangerous roller even at this low of a flow discharge. In the model, an approximately scaled boat (a piece of plywood cut into a shape of a boat that would be 9 ft long with a maximum 3 ft wide section in the prototype) was introduced over the spillway to assess the capture capabilities of the flow structure. For all flows during the sediment scour calibration, experiments A and B and 1-4, the boat was captured at the toe of the spillway and consequently inside the boil. At 1000 cfs, the boat just fit between the boil and the spillway. The falling nappe would impact the boat and cause it to wobble back and forth. The boil barrier kept the boat from wobbling too far. The impact of the boat with the barrier caused the boat to move back towards the spillway, only to be impacted again by the falling nappe. The roller was well defined below the surface by the motion of entrained air bubbles and the motion of the coarser sediment that remained in the scour hole.

At the next highest flow (6000 cfs), there was a much larger scour hole and roller. The boat would frequently become completely submersed (even to the bottom of the channel), rotate around in a chaotic manner, recirculate back to the falling nappe, and begin the whole process again. The roller was also clearly defined by the motion of the sediment and entrained air at 6000 cfs (see figure 4.1). The boat exhibited the same characteristics at the 10000 cfs discharge, too. When the boat was introduced at 15000 cfs the flow was less turbulent in appearance (compare figure 4.1 to figure 4.2) than the 6000 cfs and 1000 cfs flows, but it still flipped the boat around with the same amount of severity.

It should be noted that the boat was able to escape a few times. The escape often occurred after the boat had already been tossed around for a while. It seems that the flow at the very bottom of the scour hole does not recirculate and is directed downstream (see figure 5.1). When the boat was lucky enough to ride one of these streamlines, it was able to escape. Research on the submerged jump for flat beds showed this same tendency (see chapter 2, specifically figures 2.1a and 2.2). The actual depth of the downstream directed streamlines was not assessed in this research, but it is obvious that they exist.

5.3 Submerged Jump Under Riprapped Conditions Without Scour?

The introduction of the boat for the lowest discharge, 1000 cfs, under the 1977-1978 riprap design, demonstrated an unexpected observation. While the riprap had not scoured at all for this discharge, it was apparent that the flow had formed a roller. Entrained bubbles were clearly

rotating in a circulating pattern below the water surface. Once the boat traversed over the spillway it was captured in the same manner as before. The turbulence that was generated for this flat riprapped bed was not as strong as the turbulence that was generated for the scoured out bed at this same discharge, but it was still intense enough to impact the motion of the boat. The boat remained next to the spillway until it was removed by hand.

To explain why the flow generated this pattern, one must first consider figure 5.3. In figure 5.3, the simulated tailwater depths are plotted for a bed elevation of 569.00 ft MSL. Plotted along with the expected tailwater depths is the curve describing the calculated conjugate depth for a flat bed. This was computed with Belanger's hydraulic jump equation. By definition, when the actual tailwater depth is lower than the calculated conjugate depth, the jump is considered to be swept out (Case A, figure 1.2). When the actual tailwater depth equals the calculated conjugate depth, the toe of the hydraulic jump should reside right at the toe of the spillway (Case B, figure 1.2). It then follows that a tailwater depth greater than the calculated conjugate depth would result in a submerged hydraulic jump (Case C, figure 1.2). The states that the hydraulic jump will undertake are subdivided in figure 5.3.

With this in mind, one might recall that the riprapped design placed the bed at an elevation of 568.00 ft MSL. Figure 5.4 contains the same plot as figure 5.3, but for a bed elevation of 568.00 ft MSL. From this plot, one can see that all discharges will create a submerged jump when the bed is at this elevation. This clearly shows why the submerged jump developed below the spillway even for the 1000 cfs discharge. These results imply that even before the riprap had moved from below the spillway, the Yorkville Dam was a public safety problem.

One might recall from the literature search, that hydraulic design in those times might have considered designing for a submerged jump. It is now clear that the design of an overflow structure, which is frequented often by the public, should strongly consider the existence of the submerged jump. The design should allow the submerged jump to occur only at infrequent events (i.e. very large discharges when nobody would be present), or not at all (i.e. with a modified spillway design which this study is predicated on).

5.4 Submerged Jump Under Scoured Riprap Conditions

It was discussed in section 4.2 that the riprap had already started to scour at a discharge of 3000 cfs. At this flow, the boils were becoming very pronounced. The same conditions were starting to develop that occurred for the bed sediment scour. At 3000 cfs the roller was strong enough to capsize the boat and continue to turn it around. The impact of the nappe pushed the boat down into the roller, and the boat turned along with the submerged vortex while the boil hindered

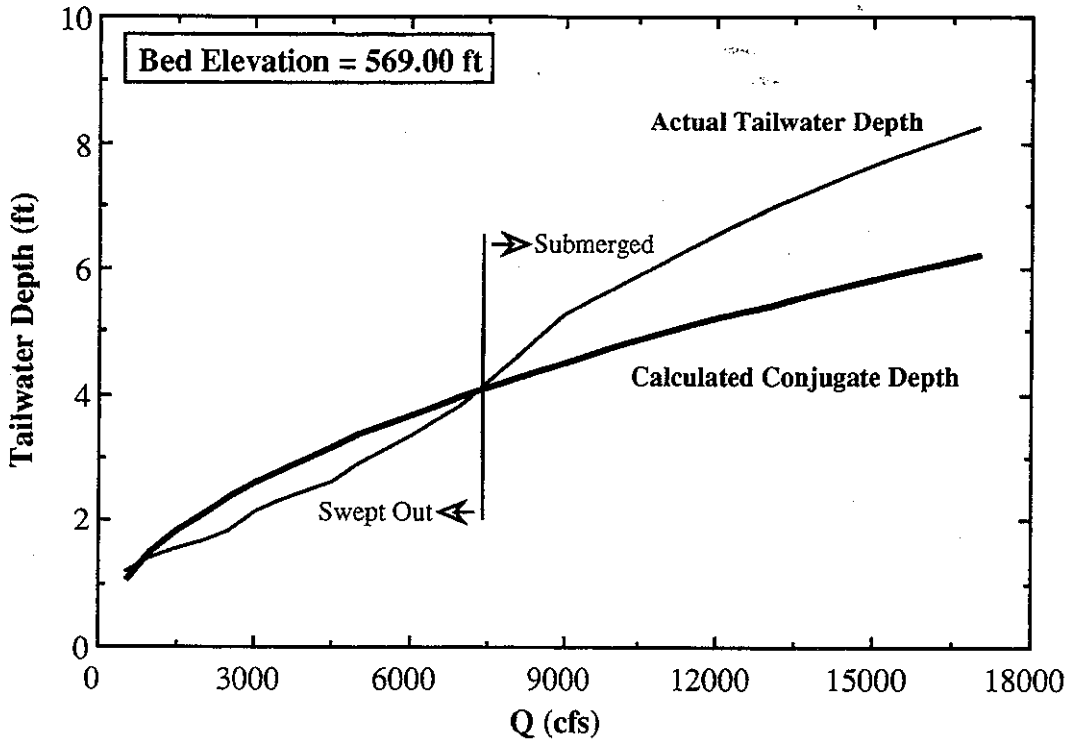

Figure 5.3: Hydraulic jump states for the bed at 569.00 ft MSL.

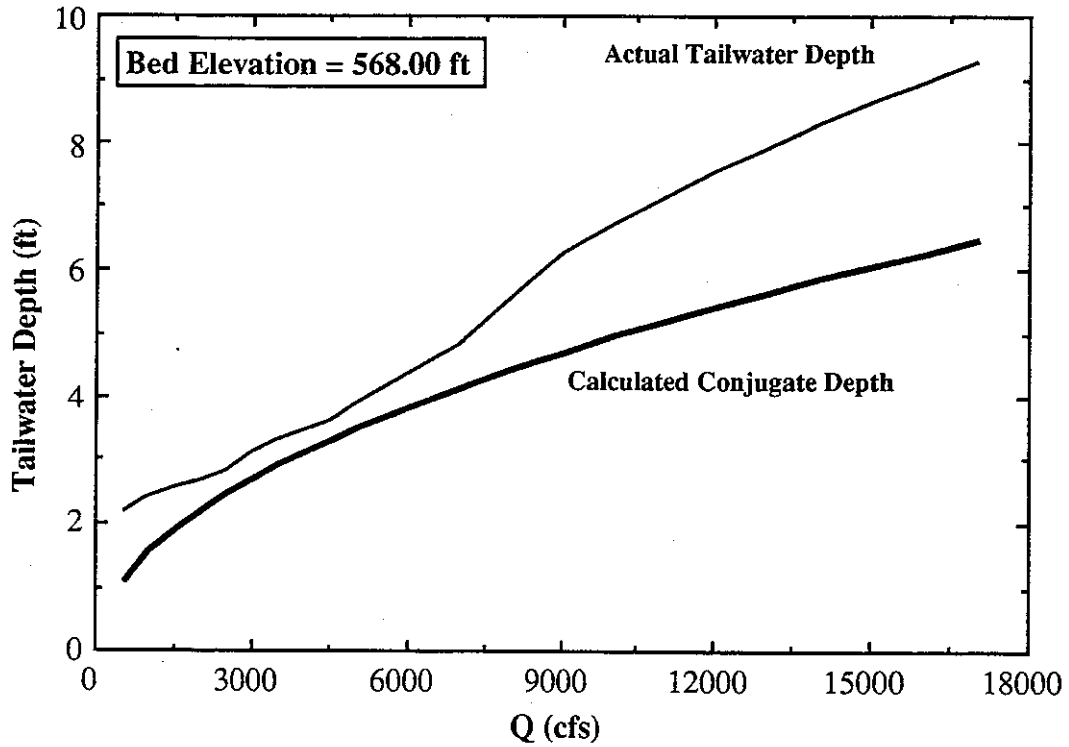

Figure 5.4: Submerged jump for all discharges when bed is at 568.00 ft MSL.

any escape attempts. Whenever the boat was pushed too far from the spillway the barrier, along with the upstream directed surface velocities, pulled it back towards the spillway.

At the higher discharges the boat was moved around more violently. The boat often impacted the spillway and even the bed. It was clear that the impact of the boat with the riprap also helped the scouring process. In the prototype there could have been any number of things that would have been swept around in the roller (i.e. tree branches) helping to promote the scouring process. An increase in discharge increased the amount of energy that needed to be dissipated. Therefore the roller needed to rotate faster and stronger. This increased the severity of the rolling process.

After the scour hole was developed with the chain of discharges (1000-10000 cfs, 5000 cfs, 10000 cfs, 15000 cfs; up to experiment 14; see Appendix B) it had a similar size and shape to the prototype scour hole (see figure 4.8). For the next few experiments (experiment 15-17), the rolling process was studied at lower, more frequent discharges inside this larger scour hole. The first discharge that was observed was a 1000 cfs discharge. The flow plunged down the spillway face into the pool generated by the scour hole, and formed a roller. The discharge was not high enough to spread the roller throughout the whole scour hole. It only took up a portion of it. Figure 5.5 contains a picture taken during this experiment. The introduction of the boat into this flow pattern had the same affect as previously. The low discharge did not cause as much violence as some of the higher discharges, but it did retain the boat. The forces that are generated below the surface were not quantified, but it can be presumed that they are above manageable levels.

For a 3000 cfs discharge the roller became more spread out inside the scour hole (see figure 5.6). At 7000 cfs, the roller had reached the full length of the scour hole (see figure 5.7). As a matter of fact, it was scouring the hole even larger. Just as other researchers had observed for the submerged jump over a flat bed, the length of the roller increased with an increase in discharge. With the increase in discharge, and an increase in the roller length, the boil moved downstream so that it was situated at the end of the roller.

5.5 Conclusions

From the above observations, a few things can be concluded about the submerged jump below a spillway with a scoured out bed. First of all, it is a very dangerous phenomenon. The forces the water generates when it is circulating in the roller are deadly. This is indicative of the numerous deaths that have occurred at the Yorkville spillway. This study's aim was not to quantify the forces (it is very difficult to make any flow measurements inside the scour hole because of the excessive amount of air entrainment). It is not necessary though, because it is clear that these forces are strong enough to cause a public safety problem.

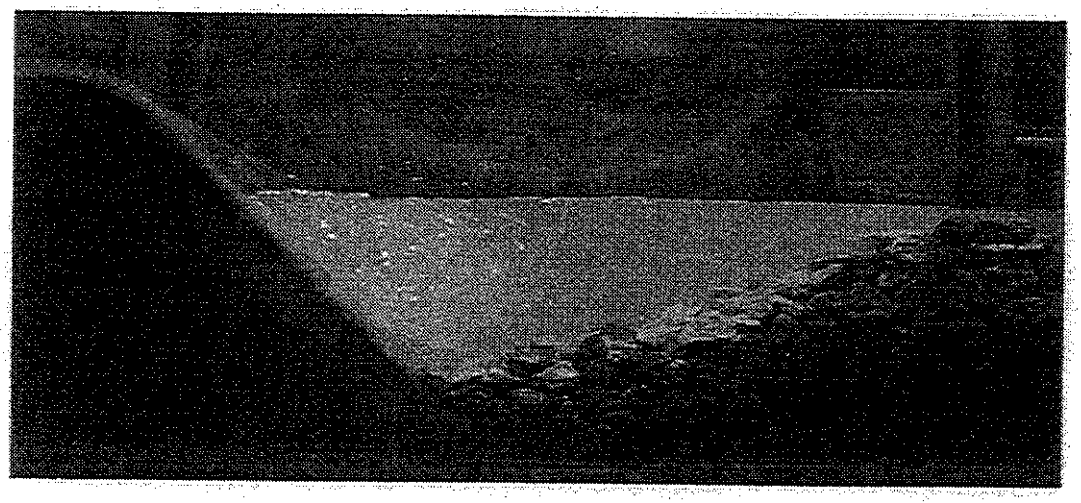

Figure 5.5: Submerged jump at Q = 1,000 cfs.

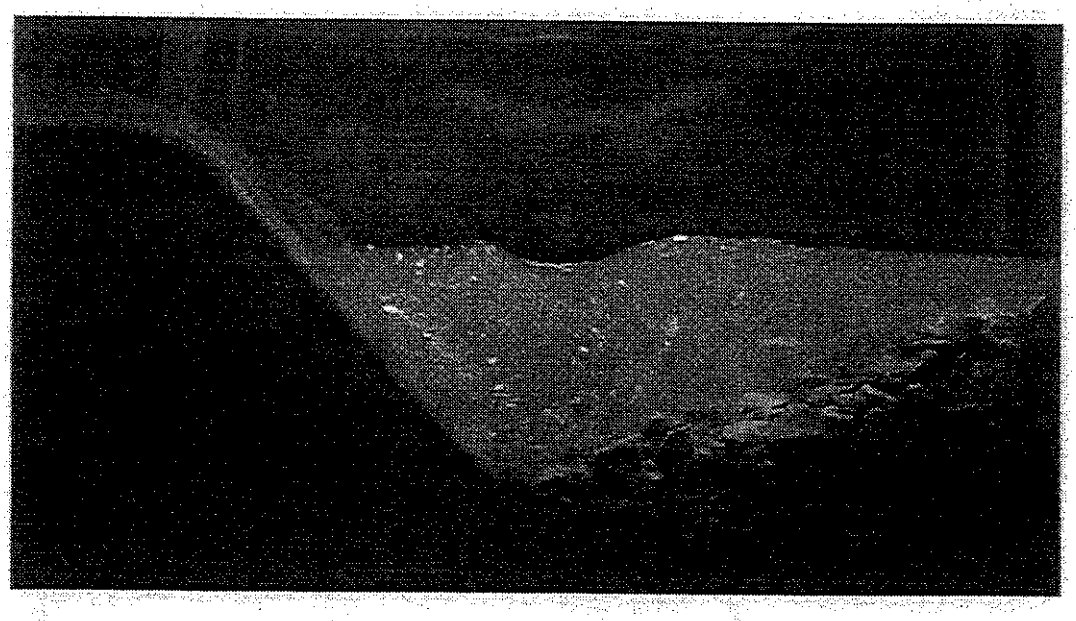

Figure 5.6: Submerged jump at Q = 3,000 cfs.

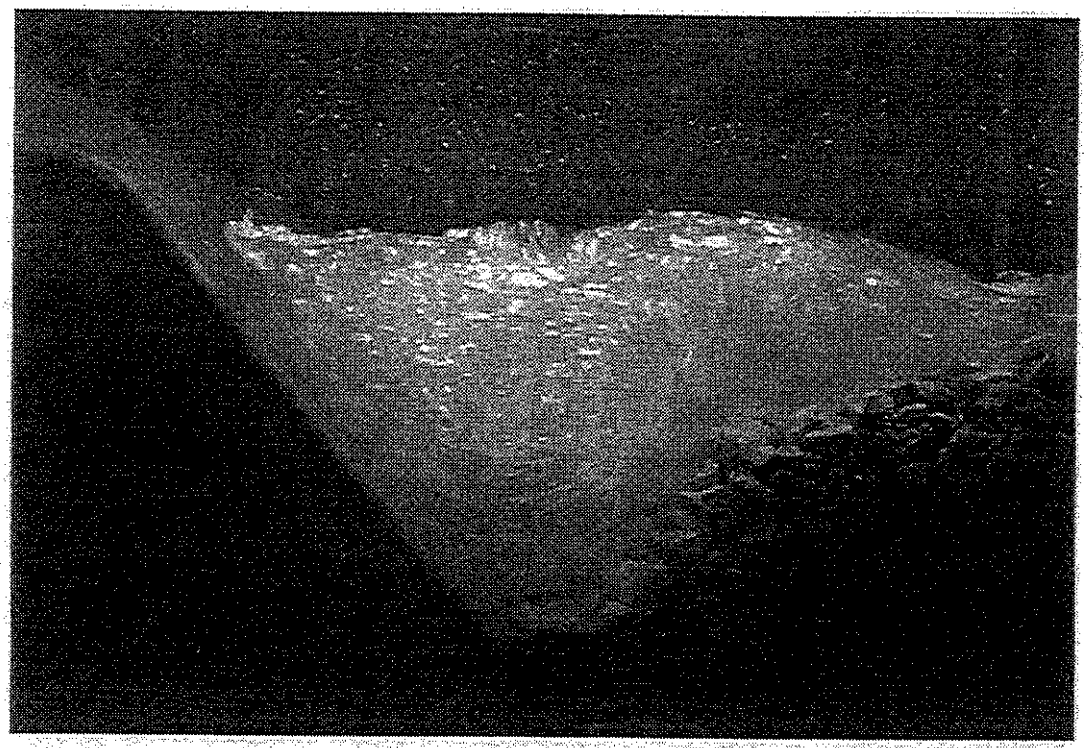

Figure 5.7: Submerged jump at Q = 7,000 cfs.

The size of the scour hole that can be developed by this process is definitely very case specific. It clearly depends on the hydraulics of the structure and the bed sediment characteristics at the toe of the spillway. Once a scour hole is developed, the dimensions of the roller that develops inside of it seems to be dependent on discharge. The length of the roller will take up a portion of the scour hole at lower flows and take up an even higher portion when the discharge is increased. The maximum size this roller can develop into is constrained by the dimensions of the scour hole. When the discharge becomes large enough that the roller takes up the whole scour hole, the flow can either scour even more or be constrained by the scour hole dimensions.

6. Alternatives/Solutions

6.1 Introduction

It has been shown that the development of the submerged jump below the Yorkville Spillway has become a serious deterrent to public safety. An ultimate solution to this problem would either limit the existence of the submerged jump or eliminate it completely. Hydraulically, the best solution to this problem would incorporate a design that maximizes energy dissipation and controls the energy dissipation in a safe manner. The design would need to minimize risk for ordinary water discharges. It would also need to be resilient enough so that large discharges do not create a situation that could become dangerous at low discharges (i.e. excessive amounts of scour).

The tested alternatives for the Yorkville Spillway draw on some of the designs discussed in the literature review, as well as traditional energy dissipation designs for an overflow structure. The five alternatives that were tested in this study include: 1) a grouted stilling basin, 2) a 10:1 sloping boulder face, 3) a 10:1 sloping smooth face, 4) a four-step spillway, and 5) a six-step spillway. The design and performance of each of the alternatives will be summarized and discussed in the following sections. A short, tabular description for each experiment can be found in Appendix B.

6.2 Grouted Pad (Stilling Basin)

Historically, a properly designed stilling basin has been the primary energy dissipation control technique for high energy flows at overflow structures. The objective of a stilling basin is to provide controlled energy dissipation when the flow goes through the energy transition of the hydraulic jump. Since an overflow structure will operate under a vast range of discharges, the design will try to minimize any risk that might be associated with the hydraulic jump. This includes controlling the excessive amount of scour that could be created as well as the frequency of dangerous flow conditions such as the formation of a roller.

Figure 6.1 depicts the stilling basin design that was tested. The grouted pad was created by using the riprap type 2 as aggregate and then capping each layer with grout. The pad was built on top of the original riprap type 1. The length of the pad was approximately three times the height of the dam (i.e. 18.5 ft). Initial test runs indicated that a patch of riprap was necessary beyond the pad, so the riprap type 2 was placed 13.5 ft from the end of the pad. The existing sediment was then placed beyond the riprap.

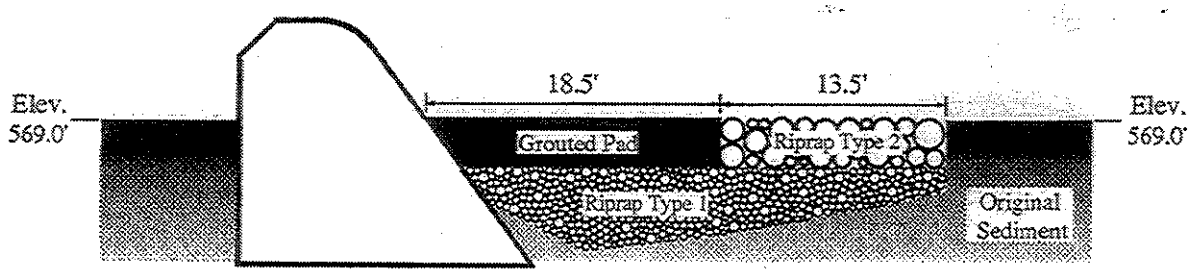

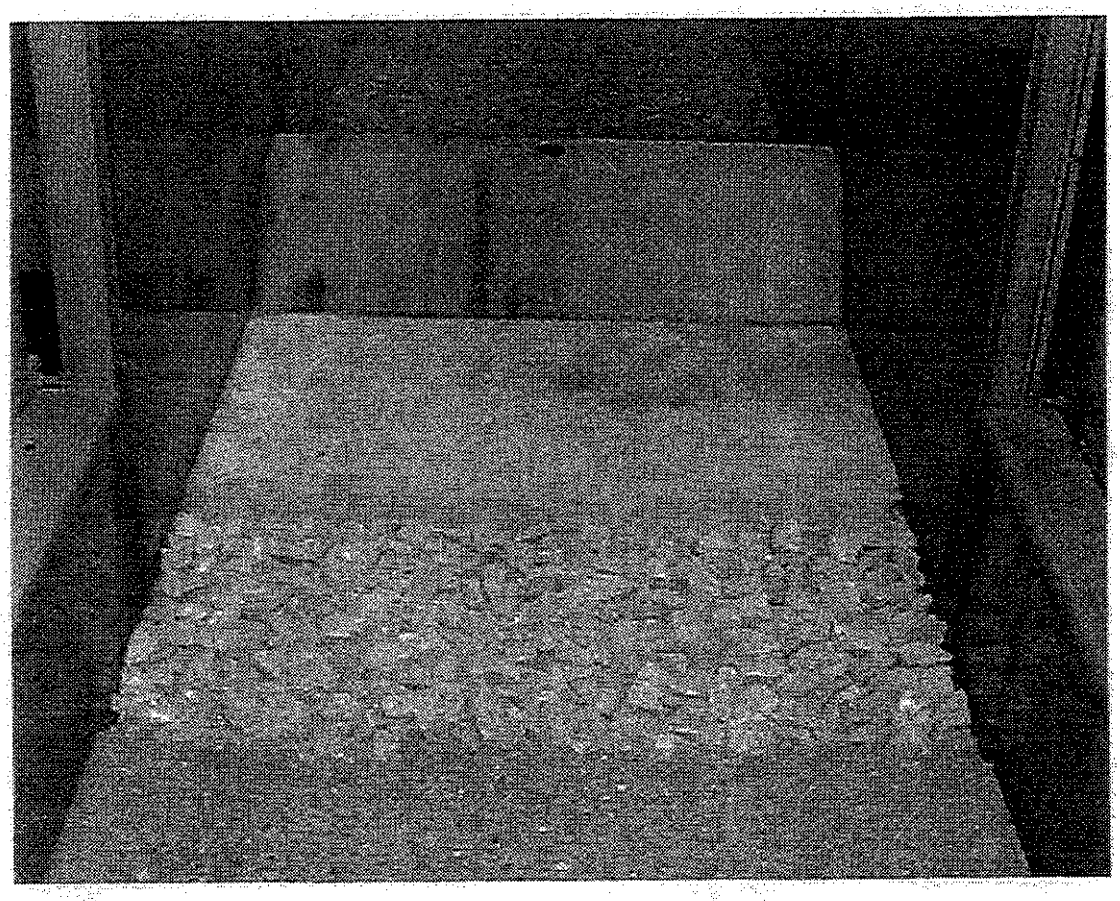

Figure 6.1: Grouted Pad (Stilling Basin) Alternative

As discussed in section 5.3, the elevation of the grouted pad must be determined for the range of discharges that it will operate under. The results of figure 5.3 suggested that the grouted pad should be placed at an elevation of 569.00 ft MSL. This would limit the submergence of the jump to discharges greater than approximately 7300 cfs. Since 7300 cfs corresponds to a 2 or 3 year return period (see table 3.2), it is clear that discharges of this magnitude or higher will not occur often.

6.2.1 Grouted Pad Performance

The grouted pad performed well as a stilling basin. A hydraulic jump developed within the protected portion of the downstream bed and satisfactorily dissipated the energy head. There was a limited amount of scour beyond the riprap at the higher flows (i.e. 10000 cfs and 15000 cfs) but that was expected at such large discharges.

At the lowest discharge observed, 1000 cfs, the jump was well within the grouted pad. There was not a lot of air entrainment for this low discharge, but that does not necessarily mean that would be the case in the prototype (i.e. because of scale effects). When the boat was introduced over the spillway, it did get caught. The capture of the boat, and the characteristics of its motions once it was captured, were similar to those observed for the scoured out submerged jump. The falling nappe impacted the boat and it tended to wobble back and forth.

To explain why the boat was retained for a jump that is considered swept out, one must look at the turbulent structures on the surface of the jump. On the surface of the hydraulic jump, there are eddies that are actually upstream directed. In the model, these eddies were strong enough to capture the boat. It is unclear whether these upstream directed forces are as strong as the submerged jump forces, but it was clear that these flow structures could cause a problem. The capture capability of this flow would definitely need to be considered when considering this alternative, because the strength of the eddies only increases for higher discharges.

For a 1500 cfs discharge and a 2000 cfs discharge the jump was becoming more violent. At 2000 cfs there was a significant amount of air entrainment. When the boat was captured next to the spillway, the turbulence that the hydraulic jump generated moved the boat around rather erratically. The 3000 cfs and 5000 cfs discharges demonstrated the same characteristics. The boat moved around more violently once it was captured, and occasionally it flipped over. On occasion, the chaotic turbulence pushed the boat a moderate distance from the spillway, but it was then quickly swept back towards the falling nappe by the upstream directed surface eddies. Figure 6.2 is a picture of the hydraulic jump at 3000 cfs.

A 7300 cfs discharge marks the optimum jump, whereas all discharges lower than that were considered swept out (according to figure 5.3). At this discharge, the jump seemed to entrain less

Figure 6.2: Grouted Pad at Q = 3000 cfs.

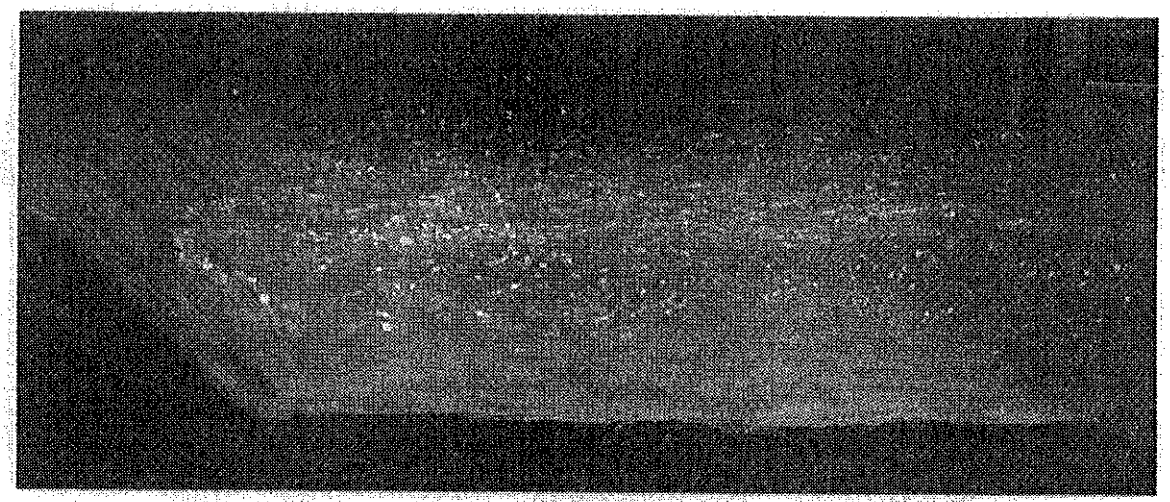

Figure 6.3: Grouted Pad at Q = 10,000 cfs.

air than the previous flows. The surface also seemed to look less violent than for some of the lower flows. It was clear though, that once the boat was placed in the flow that this discharge developed some violent turbulent characteristics. The boat was easily swept around. It often crashed into the spillway and the grouted pad. The boat turned over quite often and continued to roll for short time periods.

At 10000 cfs and 15000 cfs the jump was clearly submerged. There was much less air entrainment which made the surface look less violent (see figure 6.3). Since the jump was completely submerged, a roller developed. The roller easily captured the boat and tossed it around. The length of the roller for the 10000 cfs discharge spread beyond the length of the grouted pad and onto the riprap. It was clear that the tailwater still contained a moderate amount of energy because there was some local sediment scour beyond the riprap. Some of the finer material was moved downstream leaving the coarser sand and gravel. However, the scour was not extreme. It would correspond to a maximum of 1 ft of scour in the prototype.

At 15000 cfs the roller was even longer and there was a little more scour. The maximum amount of scour would correspond to 1.5 ft. For the 15000 cfs discharge the riprap, was beginning to vibrate in place. It did not, however, move downstream. This clearly shows that a riprap smaller than the riprap type 2 could potentially scour at the higher discharges.

6.3 10:1 Sloping Boulder Face

Another alternative tested for the modification of Yorkville Spillway consisted of placing large, unscourable, boulders at a 10:1 slope down the face of the spillway. This design is similar to the design Davis and George (1985) tested. It appears this design has also been implemented by the Wisconsin DNR in many locations. The Wisconsin designs place two-ton riprap at a slope of 6:1 along the face of the spillway (Bill Rice-personal communication, 1996).

Figure 6.4 depicts the design tested in this study. The boulders were scaled down from a two-ton boulder size in the prototype. This roughly corresponds to prototype boulders with an equivalent diameter of 5.6 ft. An impact block was placed on the face of the spillway at an elevation of 573.00 ft. The block directed the flow downstream and limited the amount of splashing the rocks created when the flow impacted them. The boulders were placed on top of the 1976 riprap type 1 design. The face of the boulders was placed at a 10:1 slope starting from the impact block and ending at the downstream bed elevation of 569.00 ft. For 9 ft beyond the boulders, a much smaller riprap was placed. The extra bed protection was thought necessary so the riprap could absorb some of the residual turbulent energy. The uniform riprap scales to a 2.25 in (5.71 cm) diameter riprap in the prototype. The existing sediment gradation was then placed beyond the riprap pad.

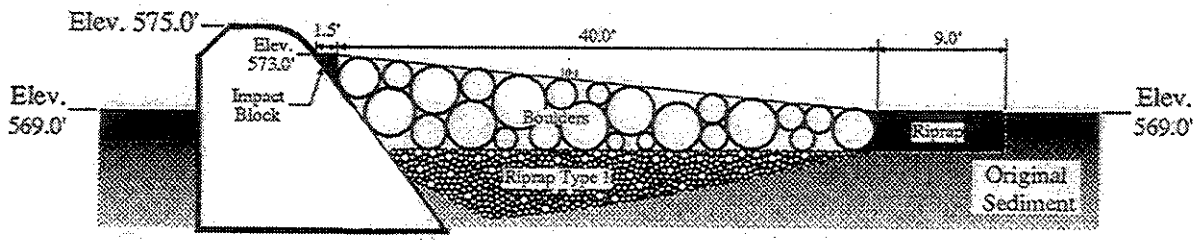

Figure 6.4: 10:1 Sloping Boulder Alternative

6.3.1 10:1 Sloping Boulder Face Performance

A discharge of 1000 cfs was not enough to submerse all of the rocks. The flow came off the impact block as a sheet of water. When the flow impacted the rocks, there was some splashing and air entrainment. Near the spillway, the flow was primarily inside the pores of the boulders. Farther down the slope the flow went along the face of the rock.

At a 2000 cfs flow there was a moderate amount of splashing on the rocks. There was a lot of air entrainment, as pointed out by the large amount of bubbles. Almost all of the rocks were submersed. A 3000 cfs discharge showed the same characteristics with only a few boulders left emergent. It was also noticed that air entrainment increased with the higher discharge.

For the 6000 cfs discharge, the rocks were completely submersed and the flow was predominately on the surface of the rocks. For this discharge, the falling nappe slid down the face of the spillway, over the impact block and then a short distance down the boulder face before it evolved into a form of a swept out hydraulic jump. Beyond the jump there was still a decent amount of turbulence left over. The surface remained agitated until the end of the slope. The riprap beyond the boulders had started to move, but only a minimal amount.

For the 10000 cfs discharge the flow skimmed along the face of the rocks for a longer distance than the 6000 cfs discharge, until it started a swept out jump (see figure 6.5). Beyond the jump there was still a lot of residual energy and the flow did not become completely two dimensional until after the riprap pad. The riprap started to move a little more, but not to any large extent.

The flow skimmed beyond the impact block for the 15000 cfs discharge. A short distance down the rock face the flow developed into a standing wave. Behind the standing wave the surface was quite undular and remained undular down the rest of the slope. There was still a moderate amount of turbulent energy left at the end of the face because the riprap had scoured a little more. The sediment beyond the riprap, on the other hand, was not showing signs of scour other than the expected bed load for such a high discharge. The riprap was scoured in pockets which correlated well with the closest boulder. It appeared the scour was very dependent on the boulder placement just upstream. The boulders did not show any signs of movement for any of the discharges.

At the lowest flows the boat could not continue through the rocks because there was not enough flow to move it along. At the higher discharges the boat moved through the hydraulic jumps and standing waves that occurred on the sloping face and continued downstream without experiencing any problems.

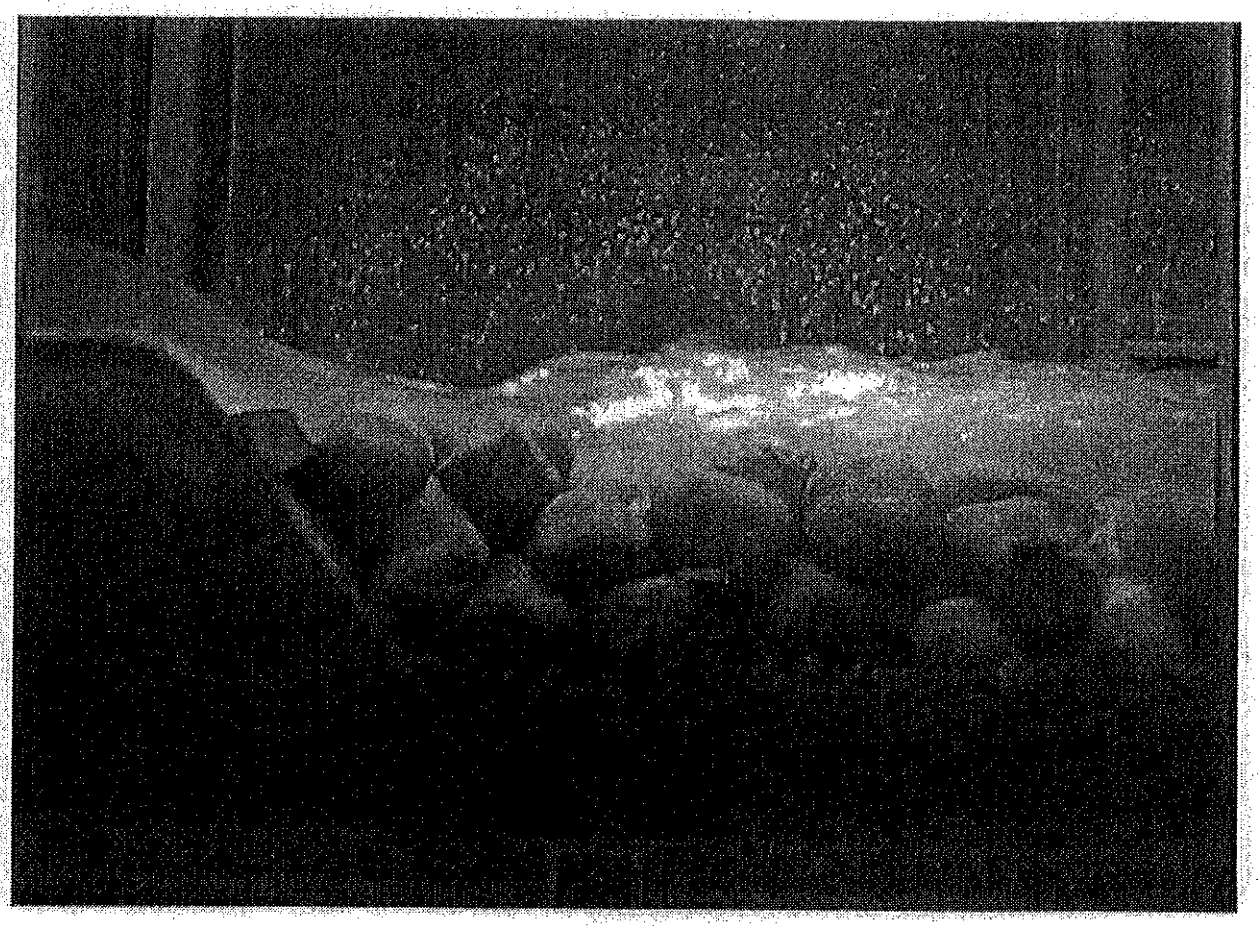

Figure 6.5: 10:1 Sloping boulder alternative at Q = 10000 cfs.

6.4 10:1 Sloping Smooth Face

The observations of the flow characteristics down the 10:1 sloping cobbles suggested that observations of flow down a smooth 10:1 sloping face would be useful. Figure 6.6 depicts the design of the 10:1 sloping smooth face. The impact block portion of the design and the sloping face had the same dimensions as the 10:1 sloping cobbles, but it was smooth. In the model the sloping face was cast into a concrete block. In the prototype, an alternative, cheaper material could be used to develop the 10:1 slope. For 9 ft beyond the sloping face, the riprap type 2 was placed for extra bed stability. Beyond the 9 ft of riprap the present day sediment was placed.

6.4.1 10:1 Sloping Smooth Face Performance

For a 1000 cfs discharge, the flow calmly moved along the face of the slope as a supercritical sheet. About 5 ft from the end of the slope the tailwater met the supercritical sheet and a small jump occurred. There was a moderate amount of aeration and a minimal amount of turbulence. The strength of the jump was barely large enough to capture the boat when it was placed from downstream. Once the object was captured it often floated next to the structure for a while and then moved downstream. When the boat was placed upstream and allowed to float down the face it was not captured.

The supercritical sheet generated by a 2000 cfs had enough energy to push the tailwater beyond the end of the slope. A surface wave occurred at the intersection of the riprap and the end of the slope. Behind the surface wave a small hydraulic jump dissipated the energy. Because the jump was pushed so far downstream, there was some sediment scour beyond the riprap. The jump was not able to capture the boat because the standing wave pushed it beyond the jump.

At 3000 cfs the flow was able to capture the boat, but it often escaped after a short amount of time. The supercritical sheet of water, with a Froude number of 4.14, evolved into a hydraulic jump right at the end of the sloping portion. The tailwater was just high enough so that the standing wave did not occur. The jump generated a good amount of aeration.

The 6000 cfs discharge also generated a large amount of aeration. The jump moved up the slope about 5 ft from the end. An odd turbulent structure that occurred only on one of the walls of the channel caused a pocket of sediment scour downstream. Otherwise, only a small amount of sediment was transported downstream. The riprap was wobbling a little bit, but none of the rocks moved downstream. The turbulence in the jump was able to capture the boat and tended to move it around quite handily. However, it often escaped after a short amount of time.

At a 10000 cfs discharge, there was an even greater amount of aeration. The supercritical sheet of water, with a Froude number of 2.74, developed a hydraulic jump about half way down the

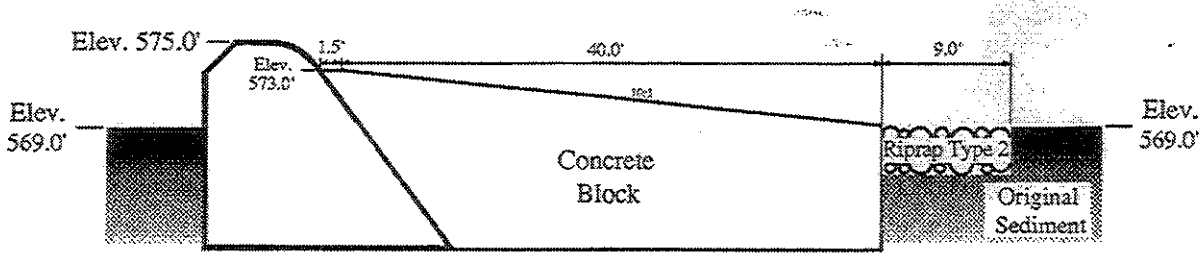

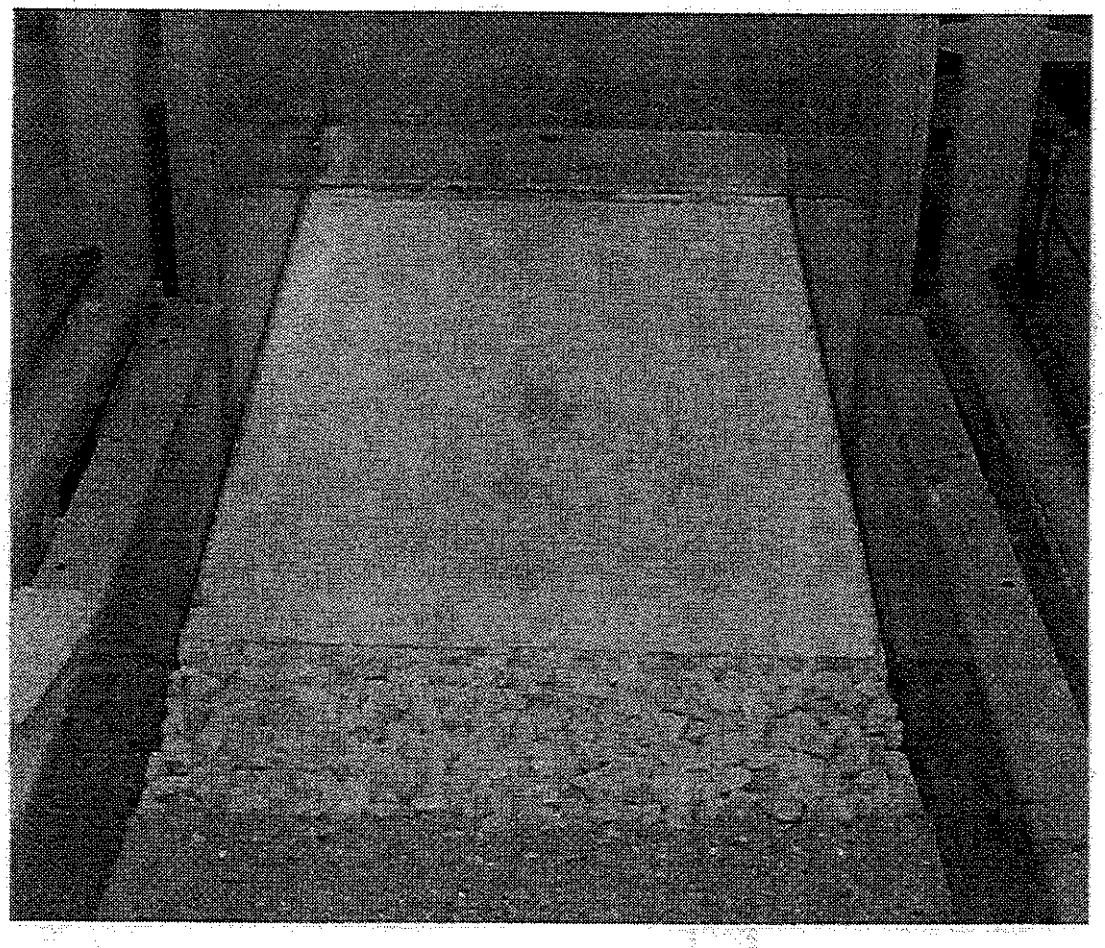

Figure 6.6: 10:1 Sloping Smooth Face Alternative

slope (see figure 6.7). The flow did not cause any extra sediment scour and the riprap remained stable.

A 17000 cfs discharge caused the hydraulic jump to occur shortly after the flow started down the slope. There was still a good amount of aeration at such a large discharge. The tailwater seemed uncharacteristically calm down stream (i.e. compared to some of the other alternatives). This suggests that the jump attained efficient dissipation.

6.5 Four-Step Spillway

Knowledge gained from the literature search suggested that maximum dissipation at a low stepped overflow structure will occur for the nappe flow regime. The primary dissipation mechanism for the nappe flow regime involves the partial or full development of hydraulic jumps on each step. Thus, longer steps give better sequential dissipation. It would seem that there are two ways the steps could be designed. One would be with a constant l/h ratio (where l = step length and h = step height) and the other would consist of differing l/h ratios along the stepped structure (i.e. Dodge, 1989). For the differing l/h ratio, there would be an infinite amount of possibilities. It would be unclear how each step contributes to the overall dissipation. There is also a possibility that the nonuniform step configuration could deplete the dissipation potential of the next step. For example, if the l/h ratio is larger in the preceeding step the water might only partially impact the next step or miss it completely.

Since nonuniform step arrangements might not utilize the dissipation potential of each step, it was decided a uniform stepped structure should be designed. Stephenson (1991) suggested a l/h ratio of 5 to achieve efficient dissipation. Beyond a ratio of 5, the size, and therefore, cost of the structure becomes excessive (Stephenson, 1991).

Figure 6.8 contains the design and a picture of the constructed four stepped structure. The top of the steps were placed at an elevation of 573.50 ft MSL. Above 573.5 ft MSL the spillway starts to form the ogee shape. Below this elevation, the spillway is straight. It would seem the straight portion would be the easiest portion of the spillway to fasten any type of structure. It was also noticed that placing the steps after the nappe had started to flow downwards would aid in energy dissipation.

Since the bed resides at an elevation of 569.00 ft MSL, there was 4.5 feet of step height to work with. For a four-step structure this set the step height at 1.125 feet. To achieve the l/h ratio of 5, this set the step length at 5.625 feet. The riprap type 1 from the 1977-78 design was built up to an elevation just below 569.00 ft MSL. A thin layer of masonry sand was placed on top of the riprap and then the rigid concrete cast steps where placed on top of that. This set the bottom of the steps at an elevation of 569.00 ft MSL. Beyond the stepped structure, riprap type 2 was placed.

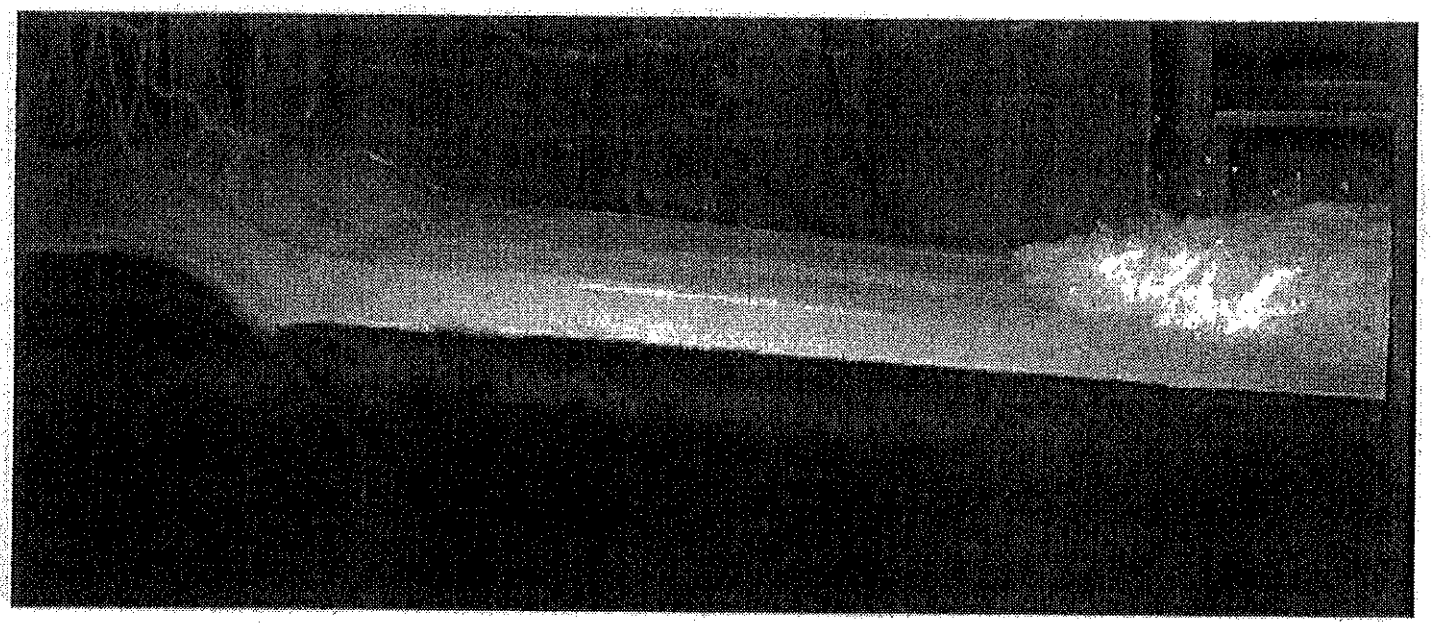

Figure 6.7: 10:1 sloping smooth face at Q = 10000 cfs.

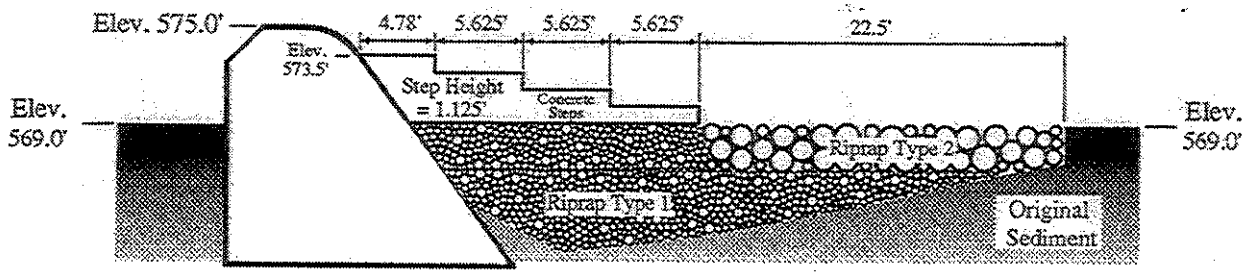

Figure 6.8: Four-Step Spillway Alternative

The length of the riprap type 2 was four times the step length of the structure (22.5 ft). The existing sediment gradation was placed beyond the riprap.

One might notice from inspection of figure 6.8 that the length of the stepped structure and riprap is still not as long as the 1977-78 riprap addition. It should also be pointed out that an actual constructed design in the prototype would not necessarily need to implement rigid steps. The steps could be made out of grouted bags or some other material that might not need an elaborate foundation (e.g. Davis and George, 1985). This would not change the hydraulics of the structure as long as the step design retained the same dimensions and had similar roughness characteristics.

6.5.1 Four-Step Spillway Performance

At the lowest flow tested, 1000 cfs, the stepped structure is aesthetically pleasing. The flow traverses over the face of each step and then falls to the next. When the falling nappe impacts the next step, it goes through a fully developed hydraulic jump. Figure 6.9 is a picture of the stepped structure model at this discharge. Pockets of air develop behind the falling nappe, just as depicted in figure 2.3a. The air pockets become larger farther down the steps, perhaps signifying an increase in the rate of energy dissipation. There is very little residual energy left over at the end of the structure. The little amount of excess energy creates weak surface disturbances and a small amount of bubbles. Since the flow depth was so shallow and the boat would not pass over the steps, a smaller piece of wood was introduced into the flow. Even for this lightweight object, the flow did not show any capturing characteristics.

For a 2000 cfs discharge, a portion of the flow energy was dissipated on each step with the development of a hydraulic jump. The residual energy was then dissipated with a well aerated hydraulic jump beyond the toe of the last step (see figure 6.10). An air pocket was not noticed behind the nappe of the first step down. The next step down had periodic air pockets, while the third step down had a defined air pocket across the whole spanwise length of the step. The last step down was submersed by the tailwater, so no air pocket was observed. The residual jump that occurs at the bottom of the step structure takes up about 20% of the riprap length. The jump showed no capture characteristics. It was observed that even if the surface of the jump contained some upstream directed eddies, the downstream directed inertia of the flow pushed any object beyond the residual jump. This occurred for this low discharge as well as for the higher discharges.

A 3000 cfs discharge developed an air pocket on the third step down, but not on either of the first two. The flow clearly impacted the face of each step, where a hydraulic jump appeared. The jump on each proceeding step became larger than the previous one, until the remaining energy was

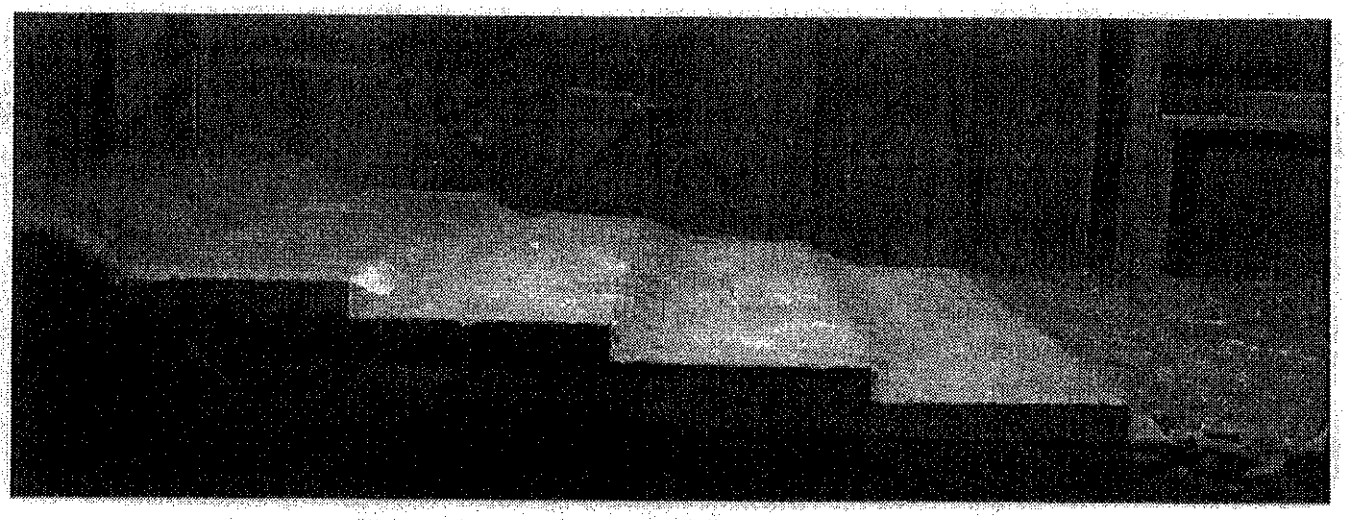

Figure 6.9: Four-Step Spillway at Q = 1000 cfs.

Figure 6.10: Four-Step Spillway at Q = 2000 cfs.

dissipated in a residual jump. The residual jump occurred approximately 3.75 feet from the end of the steps. The well aerated residual jump did not show any capture characteristics.

Similar characteristics were also observed for a 4000 cfs and a 4500 cfs discharge. There was an air pocket only on the third step down (periodic air pocket at 4500 cfs). Dissipation occurred on each step with a partially developed or fully developed hydraulic jump. The remaining energy was dissipated with a sizable residual jump. This residual jump was also highly aerated. Figure 6.11 depicts the model at a 4500 cfs discharge.

The flow corresponding to a 6000 cfs discharge marked the first observation of clearly skimming flow. There was no noticeable hydraulic jumps on the face of any of the steps. Therefore, energy dissipation on each step was achieved through momentum transfer from the skimming stream of flow to the recirculating vortices in each step cavity (see figure 2.4). The remaining energy at the bottom of the steps evolved into an oscillating hydraulic jump. The jump went from a distinct flow structure to two separate jumps that broke the riprap length into thirds. Neither of the states of the hydraulic jump captured the boat.

The 8000 cfs discharge skimmed down the face of the steps and developed into a turbulent hydraulic jump. The toe of the jump started at the end of the last step. There seemed to be minimal dissipation on the steps, but the jump after the steps dissipated the residual energy quite efficiently. Behind the major jump was another small jump. Neither jump stretched beyond the riprap length.

A 10000 cfs discharge developed a different flow structure than any of the previous discharges. The flow skims down the face of the steps, but once it meets the tailwater it develops into a surface wave (see figure 6.12). The surface wave starts after the third step down and peaks about the end of the last step. Behind the wave, there was a moderate hydraulic jump. There was much less air entrainment than the 8000 cfs discharge. The boat was able to pass over the surface wave and beyond the small hydraulic jump with ease.

For the 15000 cfs discharge, the surface wave becomes larger and moves farther up the steps. The wave begins at the end of the first step down and peaks at the middle of the last step. There was not any air entrainment observed for the surface wave. A small jump occurs behind the wave which dissipates the flows excess energy. The small jump entrained a minimal amount of air. At this large discharge, some of the smaller riprap particles were starting to wobble, but none of them moved from their resting place. The sediment behind the riprap had scoured a small amount leaving mostly coarser material.

Figure 6.11: Four-Step Spillway at Q = 4500 cfs.

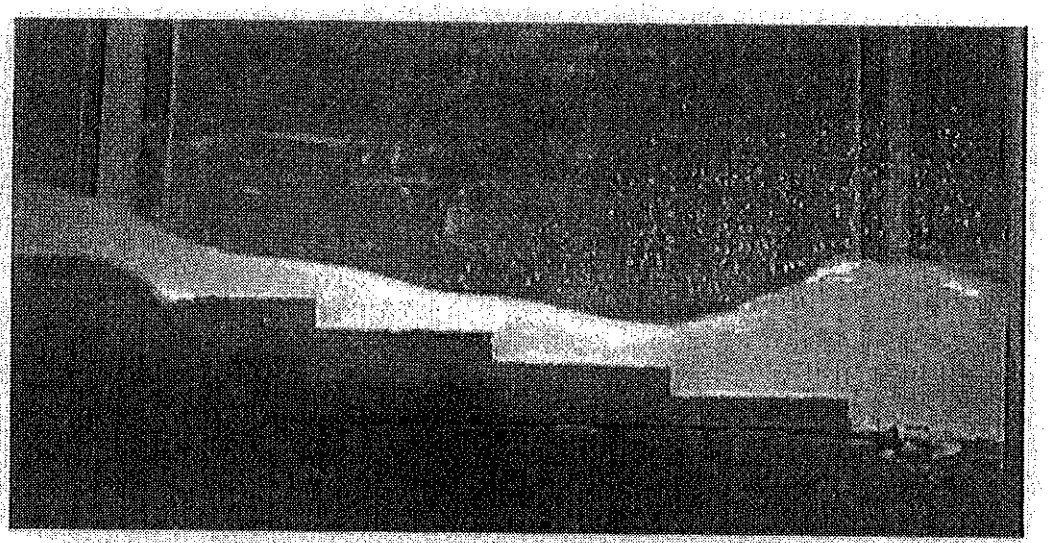

Figure 6.12: Four-Step Spillway at Q = 10000 cfs.

6.6 Six-Step Spillway

The good performance of the four-step spillway suggested that an increase in the number of steps could add even more dissipation. Drawing on the recommended design of Dodge (1989), a six-step structure was constructed to the top of the spillway and then tested. Figure 6.13 contains the design and a picture of the six-step structure. Since the elevation difference between the top of the spillway and the bed is 6 feet, each step was 1 foot tall. To keep the l/h ratio of 5, the step length was set at 5 feet. The rigid stepped structure was cast out of concrete and placed on top of the 1977-78 riprap type 1 design. Riprap type 2 was placed beyond the end of the steps at a length of four times the step length (20 feet). The existing sediment gradation was then placed beyond the riprap.

6.6.1 Six-Step Spillway Performance

Observations of the flow at a discharge of 1000 cfs showed that there was some extra dissipation over the four-step structure. The flow kind of fell over each step, evolved into a small hydraulic jump and then fell over the next step. The residual energy remaining at the second to last step was dissipated before the flow reached the last step down. Therefore there was no noticeable residual energy remaining. There were air pockets behind the falling nappe of each step down. The smaller piece of wood was introduced into the flow and no capture characteristics were noticed.

For a 2000 cfs discharge, there appeared to be hydraulic jumps on the face of every step except for the first. There was an air pocket behind parts of the fourth step down and across the whole length of the fifth step down, but not on the second or third step downs. There was a few bubbles caught behind the nappe of the first step down. There was a moderate residual jump about 2 feet from the end of the steps. This jump promoted good air entrainment, but was not strong enough to capture the boat.

A 3000 cfs discharge developed a small amount of bed load transport beyond the riprap. The sediment started to become armored. The flow developed hydraulic jumps on all of the steps except the first. There was air pockets behind the fifth step down and part of the fourth, but not on any of the others. The remaining energy at the end of the steps evolved into a low Froude number hydraulic jump. The jump was not able to capture the boat.

The 5000 cfs discharge developed periodic air pockets inside of the fifth step down, only. Figure 6.14 is a picture of the six-step structure for a 5000 cfs discharge. The flow smoothly skimmed across the first step down. After the second step down, the flow impacted a portion of the next step face and developed a small, partial hydraulic jump. When the flow went over the

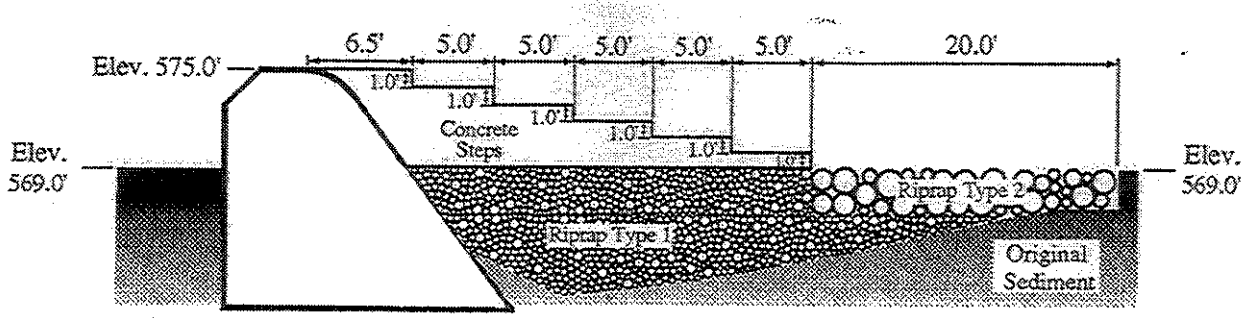

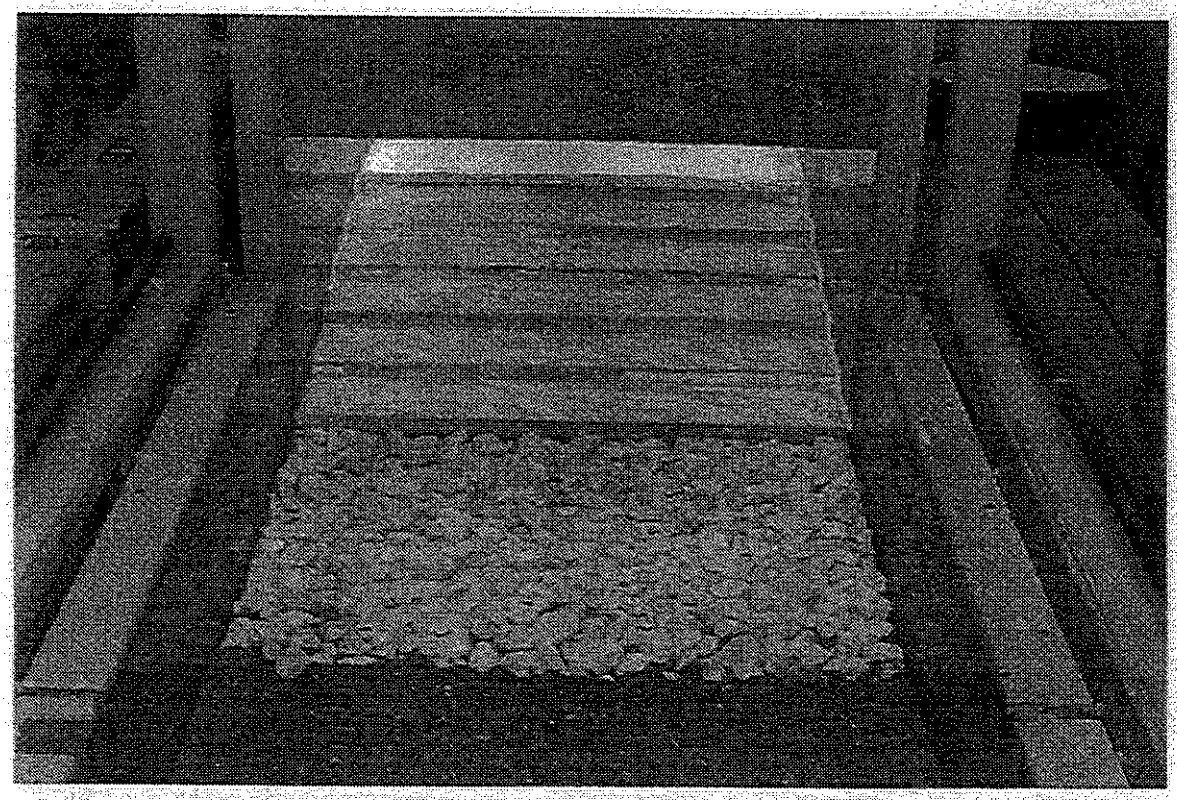

Figure 6.13: Six-Step Spillway Alternative

Figure 6.14: Six-Step Spillway at Q = 5000 cfs.

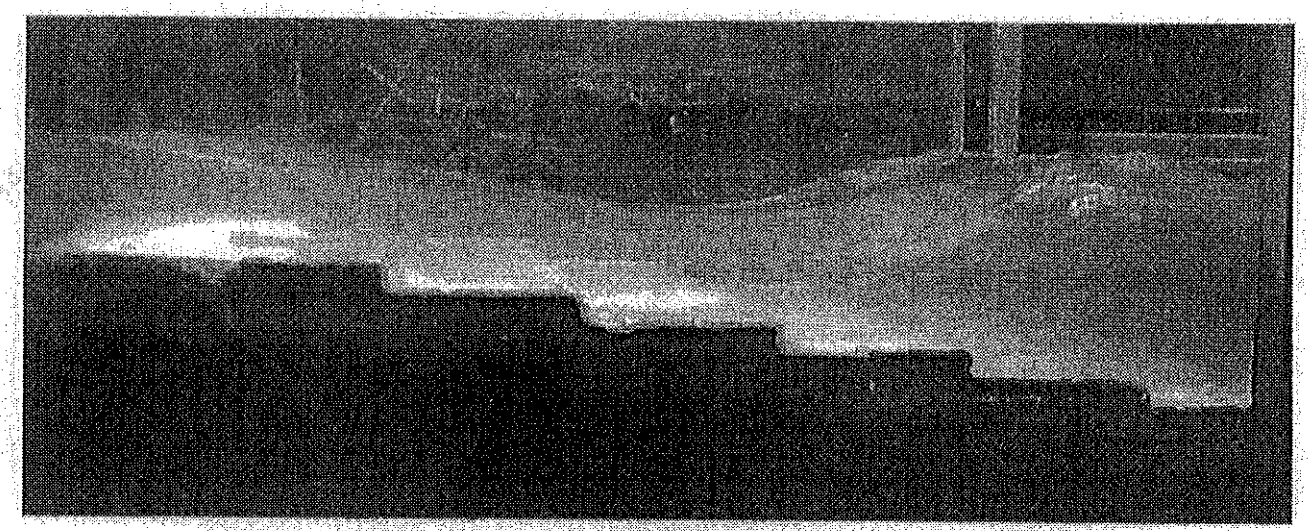

Figure 6.15: Six-Step Spillway at Q = 17000 cfs.

third step down it clearly impacted the step face and developed into a larger, partial hydraulic jump. The development of the hydraulic jumps increased for the fourth and fifth step down. The remaining energy at the bottom of the stepped structure was dissipated with another low Froude number jump. The residual jump at this discharge was not able to capture the boat, either.

The flow skimmed over the first three steps for an 8000 cfs discharge. There was a small hydraulic jump on the fourth step (step face after the fourth step down). The tailwater was so high that the residual jump moved onto the face of the fifth step. The residual jump dissipated the remaining energy quite efficiently. It also entrained a lot of air. When the boat was placed in the flow from upstream, it easily slid down the face of the steps and through the residual hydraulic jump. When the boat was placed from downstream, it sometimes became wedged between the hydraulic jump and the step face. Often, the turbulence first caught the boat. Then the sheet of flow down the face of the steps pushed the boat beyond the jump. It was noticed that more of the finer sediment beyond the riprap moved downstream, thus armoring the bed even more.

For a 10000 cfs discharge there was no noticeable hydraulic jumps on any of the steps. When the flow met the tailwater at the end of the fourth step, it oscillated between a standing wave and a hydraulic jump. There was a smaller hydraulic jump behind each of the two states, which dissipated any of the remaining energy. When the boat was placed upstream of the spillway, it quickly floated down the face of the steps, impacted the hydraulic jump(s), which drastically slowed the velocity of the boat down, and then proceeded downstream. When the boat was placed into the flow from downstream, the second hydraulic jump showed some capture capabilities, but only for a short period of time. Eventually the boat was released downstream.

Very near the 100 year discharge (i.e. 17000 cfs), the flow develops into a surface wave at the end of the second step (see figure 6.15). Behind the surface wave, a small hydraulic jump creates the small energy transition from the pool water to the high tailwater. The riprap was stable and the sediment only scoured a small amount.

6.7 Transition Between the Nappe and Skimming Flow Regimes

As mentioned in the literature review, Rajaratnam (1990) described that the transition between the nappe flow regime and skimming flow regime occurs when the ratio of critical depth with step height equals 0.8. Discharges above that ratio are skimming flows while discharges below 0.8 are considered nappe flows. On the other hand, Chanson (1994) defined that the onset of skimming flow occurs when the air pocket behind the falling nappe disappears. He then used some experimental data to develop equation 2.2. Equation 2.2 defines that the transition flow for a constant step geometry (i.e. constant h/l) is a function of the ratio of critical depth to step height.

Mondardo and Fabiani (1995) then took Chanson's relationship one step farther and developed equation 2.3.

Table 6.1 presents the predicted discharges as well as the discharges in which the transitions were observed for the four step and six step configurations. From table 6.1 one can see that none

	Transition Discharges	
Research	Four Steps (cfs)	Six Steps (cfs)
Rajaratnam (1990)	2565	2150
Chanson (1994)	3400	2850
Mondardo and Fabiani (1995)	4000	3355
Observed (approximate)	4500	5000

Table 6.1: Computed and observed discharges for the transition between the nappe and skimming flow regimes on the stepped structures.

of the equations predict the transition discharge well but that Mondardo and Fabiani's equation predicts the transition discharges most closely.

It should be noted that the above relationships were derived without considering the tailwater depth. In this study, one has seen that the model was operated with a tailwater rating curve. Presumably, the tailwater changes the discharge characteristics of the steps just as the tailwater changes the discharge relationships for a spillway. It is clear that more observations would need to be conducted to come up with better relationships describing the transition.

6.8 Tailwater and Pool Water Measurements

Tailwater elevations were taken along the first 170 feet of the reach downstream of each alternative. The measured elevations compared quite favorably with the simulated/expected elevations that occur in the prototype. There were no noticeable tailwater affects for this section of the reach for all of the alternatives tested.

The measured dimensionless heads for four of the alternatives (i.e. grouted stilling basin, 10:1 sloping smooth face, and both of the stepped spillways) are plotted in Figure 6.16. The measured heads for these alternatives compare quite well to the original spillway measurements. The crest change for the six-step spillway did, however, have an affect on the pool water rating curve. The crest change for this alternative can not pass discharges as efficient as the modified ogee crest.

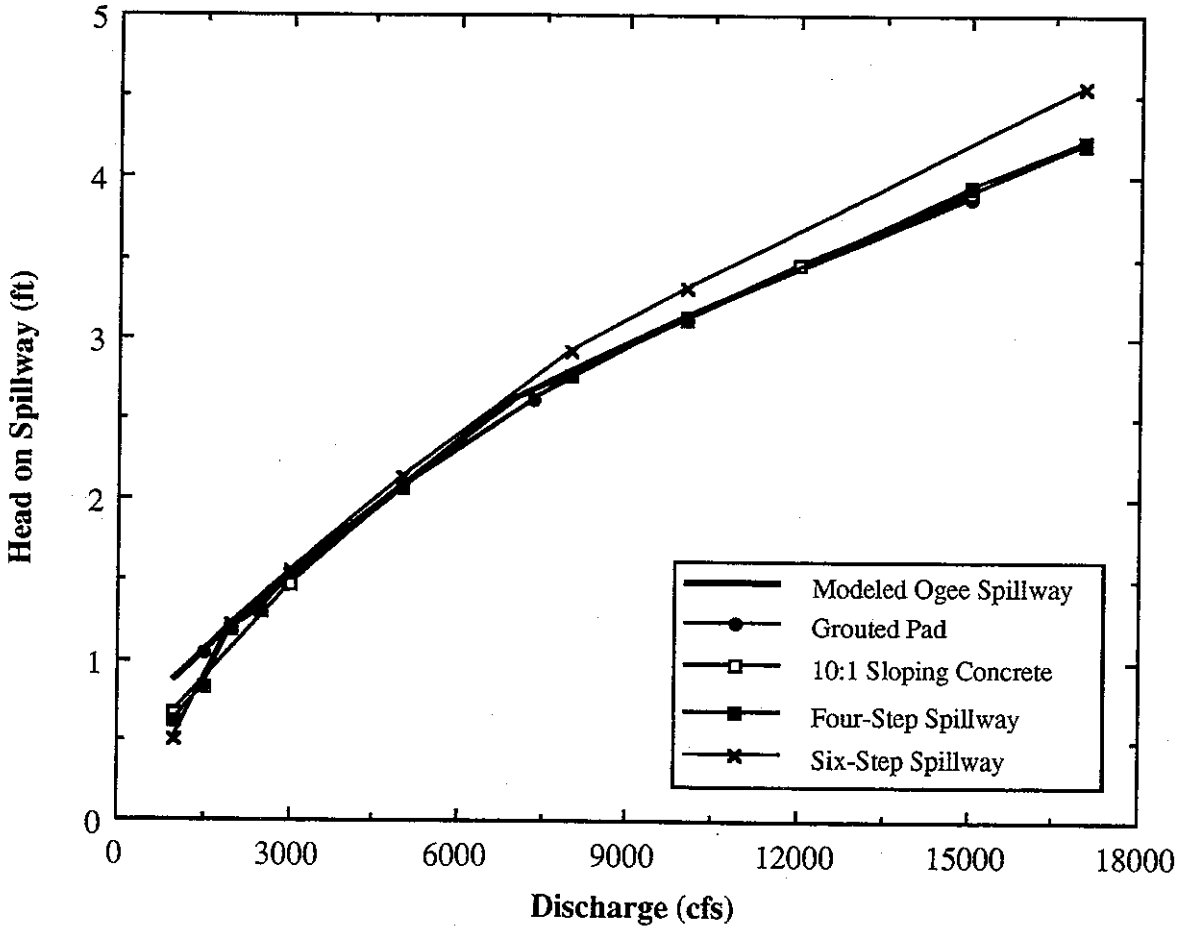

Figure 6.16: Measured pool water rating curves.

Thus the pool water rose in elevation. The rise in pool water supplied the necessary head to pass the given discharge. This rise in head would be minimal in the prototype, though. The maximum rise in head over the existing rating curve would be 3.84 in (9.75 cm) for a 17000 cfs discharge. At a 10000 cfs discharge the head change would be 2.38 in (6.04 cm).

It should be noted that the pool water rating curves for the 10:1 smooth slope, and the two stepped structures deviated from the existing modified ogee crest for the smallest discharges studied (i.e. < 2000 cfs). This was unexpected because it suggests that the alternatives became more efficient than the ogee crest at these low discharges. At first, it was thought the deviation could be attributed to measurement error. This was dismissed when repeated measurements for the four-step structure reproduced the same phenomenon. The deviation was then attributed to wall effects, but this did not make sense, either. If it was wall effects then the relationships for the alternatives would not have deviated from the existing modeled spillway measurements because the walls would have affected the spillway also. It seems a reasonable conclusion can not be drawn to explain this deviation. Nevertheless, the decrease in pool water elevation was only for the smallest discharges and therefore would not have any adverse affects in the prototype.

7. Summary and Conclusions

7.1 Model Calibration and Scour Hole Development

A 1:9 Froude scale sectional model of the Yorkville Spillway was constructed and calibrated. Sediment samples were obtained, and scaled using appropriate sediment transport criteria. It was found that the existing sediment was clearly susceptible to the scouring action of the falling nappe and turbulent structure that developed below the spillway. While modeling the existing sediment downstream of the spillway, the 1976 scour hole was reproduced with relatively good results.

Then the IDOT Division of Water Resources 1977-78 riprap design to eliminate the effects of the roller was modeled. It was noticed that flows as low as 4000 cfs started to scour the riprap away from the face of the spillway. It was clear that the largest discharge encountered at the Yorkville Spillway, approximately 10000 cfs, created a large scour hole that was similar in size to the 1991 surveyed scour hole. Once the scour hole was developed and came to an equilibrium for the 10000 cfs discharge, it was found that a lower, moderate discharge of 5000 cfs had enough energy to begin the scouring process again. Subsequent experiments at higher discharges then widened the scour hole.

Observations of the flow in the vicinity of the scour holes showed its devastating capturing capabilities as well as its violent characteristics. When the boat was introduced near the spillway, whether upstream or downstream, it was clear that the rolling action of the submerged jump clearly acted as a "drowning machine". It was also noticed that the flow near the downstream face of the scour hole, and therefore at the end of the roller, had a strong vertical component. When that vertical component reached the water surface, it created a "boil barrier". This rise in the water surface acted as a barrier to any objects that became captured next to the spillway.

Observations of lower flows inside a much larger scour hole showed that the roller length increases with an increase in discharge. This is in agreement with observations of the submerged jump for flat bed conditions. The roller took up only a portion of the hole at lower discharges and then a larger portion of the scour hole at larger discharges. Once the discharge became large enough, and the roller spanned the whole length of the scour hole, the flow had two options. If the flow had enough energy to scour the hole larger (i.e. moderate discharge with moderate tailwater depth) than it started with the scouring process, again. However, if the flow did not have enough energy to scour a larger hole (i.e. large discharge but high tailwater) then the length of the roller was constrained by the length of the scour hole.

7.2 Alternatives/Solutions

After the model was calibrated and the scouring process was observed, five alternative designs for the spillway were constructed and tested. The ultimate objective of these designs were to eliminate the existence of the roller or any other public safety nuisance. This would in effect render the Yorkville Spillway drown proof (at least from a hydraulic point of view).

The first of the five alternatives tested was the traditional stilling basin. The stilling basin performed excellent hydraulically with good dissipation and a minimum amount of scour, but it did show some dangerous characteristics. While the excessive amount of turbulence created in the normal hydraulic jump would probably act as a deterrent to anyone who might consider approaching the spillway, this excessive turbulence did show some capturing capabilities. Upstream directed eddies on the surface of the jump where strong enough to capture the boat when placed upstream or downstream. Since this spillway is very accessible to the public and there is a good chance that somebody may approach the spillway either accidentally or purposely, it does not seem safe to implement this solution.

Next a 10:1 boulder slope alternative was tested. While this alternative showed excellent dissipative qualities, it is unclear how feasible and safe the structure might be. It was noticed that the section of the slope closest to the top of the spillway was not submersed at the lower discharges. This perhaps, would attract people out to the rocks and therefore onto the spillway where they could possibly become harmed. It must also be considered that the two-ton riprap scales to an equivalent diameter of 5.6 ft in the prototype. Since riprap of this size is not available throughout most parts of Illinois it is unclear how feasible this solution would be. In parts of the country where riprap of this size is omnipresent (e.g. Wisconsin), this setup could be considered.

Observations of the 10:1 boulder slope suggested that it would be beneficial to observe flow over a 10:1 smooth sloping face. It was found that the flow down the face of the slope was aesthetically pleasing, but that there was low head loss. Most of the energy dissipation occurred when the supercritical stream met the subcritical tailwater through the existence of one large hydraulic jump. The concentrated turbulent dissipation of this structure showed some capture capabilities, though. For this reason and the fact that it would be difficult to construct this solution cost effectively, this alternative did not seem feasible, either.

The last two alternatives tested were stepped spillways. The four-step structure, which was set below the ogee curvature on the face of the spillway, showed good dissipative qualities along with an aesthetically pleasing appearance. For flows lower than 3000 cfs a hydraulic jump appeared on the face of most of the steps and dissipated most of the energy effectively. For flows between 3000 and 4500 cfs partial hydraulic jumps on each step partially dissipated the flow. The remaining flow was dissipated safely with a residual hydraulic jump at the toe of the step overlay.

For flows greater than 4500 cfs , the flow moved over the steps in the skimming flow regime. For this flow regime most of the energy was dissipated at the toe of the spillway with a residual jump. Discharges greater than 9000 cfs created a surface wave on top of the steps and then usually a jump behind that.

It was observed that the four-step structure had absolutely no capture characteristics for any of the discharges. Introduction of the boat, or the smaller wooden object, upstream and downstream showed that none of the flows had enough power to capture either object. Even if there was a large residual jump that contained some upstream directed surface eddies, the motion of the flow down the face of the steps pushed the object beyond the jump.

The performance of the six-step structure was very similar to the four step structure. Discharges below 5000 cfs were in the nappe flow regime. At the lower flows it appeared that the extra steps gave some extra dissipation. This was because there was more steps to create hydraulic jumps. At the higher skimming flows there was a minimal amount of dissipation on the steps (as was seen in the four-step structure). Most of the energy was dissipated at the end of the structure with a residual jump. For all of the lower discharges the flow did not posses any capturing characteristics. At an infrequent flow of 10000 cfs some capture was noticed when the boat was placed from downstream, but it was only for a short amount of time.

Construction of this step configuration to the top of the spillway would be difficult and require extra consideration. Another consideration for the crest change is the fact that the discharge coefficient of the spillway will change and consequently raise the pool water head slightly.

Observations and comparisons of the two stepped structures (i.e. four-step and six-step) suggest that the four-step arrangement is more cost effective and a more feasible solution than the six-step arrangement.

References

Chanson, H. (1994a), Hydraulic Design of Stepped Cascades, Channels, Weirs and Spillways, first edition, Elsevier Science Ltd., New York, 261 p.

Chanson, H. (1994b), "Comparison of Energy Dissipation Between Nappe and Skimming Flow Regimes on Stepped Chutes," *Journal of Hydraulic Research*, Vol. 32, No. 2, pp 213-218.

Chanson, H. (1995), Reply to "Discussion of Comparison of Energy Dissipation Between Nappe and Skimming Flow Regimes on Stepped Chutes," *Journal of Hydraulic Research*, Vol. 33, No. 1, pp 114-143.

Chamani, M. R. and Rajaratnam, N. (1994), "Jet Flow on Stepped Spillways," *Journal of Hydraulic Engineering*, ASCE, Vol. 120, No. 2, pp 254-259.

Christodoulou, G. C. (1993), "Energy Dissipation on Stepped Spillways," *Journal of Hydraulic Engineering*, ASCE, Vol. 119, No. 5, pp 644-650.

Davis, J. E. and George, J. F. (1985), "Model Tests of Little Falls Dam Potomac River, Maryland," U.S. Army Engineer Waterways Experiment Station, Corps of Engineers, Vicksburg, Mississippi, 82 p.

Dodge, R. A. (1989), "Model Study of Roosevelt Diversion Weir," Bureau of Reclamation R-89-17, Denver Office, Hydraulics Branch, 40 p.

Fan, J. J. (1993), Submerged Hydraulic Jumps at Overflow Structures, Master's Thesis, University of Toronto, 152 p.

Frizell, K. H. (1992), "Hydraulics of Stepped Spillways For RCC Dams and Dam Rehabilitations," *Proceedings of the ASCE Specialty Conf.*, RCC3, San Diego, CA, pp 423-439.

Frizell, K. H., Smith, Douglas H. and Ruff, J. F. (1994), "Stepped Overlays for Use in Protecting Overtopped Embankment Dams," *Proceedings of the Annual Conf. of the Association of State Dam Safety Officials*, Boston, MA, Sep. 11-14, pp 299-308.

Govinda Rao, N. S. and Rajaratnam, N. (1963), "The Submerged Hydraulic Jump," *Journal of the Hydraulic Division,* ASCE, Vol. 89, No. HY1, pp 139-162.

Hauser, G. E., Shane, R. M. and Brock, W. G. (1991), "Innovative Reregulation Weirs for Dam Releases," *Proc. 1991 Nat. Conf. on Hydr. Eng.*, ASCE, Jul. 29-Aug 2, pp 178-183.

Hotchkiss, R. and Comstock, M. (1992), Discussion of "Drownproofing of Low Overflow Structures," *Journal of Hydraulic Engineering*, ASCE, Vol. 118, No. 11, pp 1586-1588.

IDOT (1995), Strategic Planning Study for Flood Control - Fox River, Draft Report, Illinois Department of Transportation, Division of Water Resources, Springfield, IL.

Long, D., Steffler, P.M. and Rajaratnam, N. (1990), "LDA Study of Flow Structure in Submerged Hydraulic Jump," *Journal of Hydraulic Research*, Vol. 28, No. 4, pp 437-460.

Leutheusser, H. J. (1988), "Dam Safety, Yes. But What about Safety at Dams?" Hydraulic Engineering, *Proceedings of the 1988 National Conference HY Div.*, ASCE, Colorado Springs, CO, August 8-12, pp 1091-1096.

Leutheusser, H. J. and Birk, W. M. (1991), "Drownproofing of Low Overflow Structures," *Journal of Hydraulic Engineering*, ASCE, Vol. 117, No. 2, pp 205-213.

Leutheusser, H. J. (1992), Closure to "Discussion of Drownproofing of Low Overflow Structures," *Journal of Hydraulic Engineering*, ASCE, Vol. 118, No. 11, pp 1589.

Peyras, L., Royet, P. and Degoutte, G. (1992), "Flow and Energy Dissipation Over Stepped Gabion Weirs," *Journal of Hydraulic Engineering*, ASCE, Vol. 118, No. 5, pp 707-717.

Pugh, C. (1989), "Tieton Diversion Dam Proposed Modification for Boater Safety," U.S. Bureau of Reclamation Water Resources Research Laboratory, Denver, CO, PAP-563.

Mondardo, Jr., M. and Fabiani, A. L. T. (1995), Discussion of "Comparison of Energy Dissipation Between Nappe and Skimming Flow Regimes on Stepped Chutes," *Journal of Hydraulic Research*, Vol. 33, No. 1, pp 119-121.

Narasimhan, S. and Bhargava, V. P. (1976), "Pressure Fluctuations in Submerged Jump," *Journal of the Hydraulics Division*, ASCE, Vol. 102, No. HY3, pp 339-350.

Parker, G., Garcia, M., Johannesson, H. and Okabe, K. (1988), Model Study of the Minnesota River Near Wilmarth Power Plant, Minnesota, St. Anthony Falls Hydraulic Laboratory, University of Minnesota, Project Report No. 284.

Rajaratnam, N. (1965), "Submerged Hydraulic Jump," *Journal of the Hydraulic Division,* ASCE, Vol. 91, No. HY4, pp 71-96.

Rajaratnam, N. (1990), "Skimming Flow in Stepped Spillways," *Journal of Hydraulic Engineering*, ASCE, Vol. 116, No. 4, pp 587-591.

Sorenson, R. M. (1985), "Stepped Spillway Hydraulic Model Investigation," *Journal of Hydraulic Engineering*, ASCE, Vol. 111, No. 12, pp 1461-1472.

Stephenson, D. (1991), "Energy Dissipation Down Stepped Spillways," Water Power & Dam Construction, Vol. 43, No. 8, September, pp 27-30.

Appendix A

A.1 Model Friction Velocity Determination

The sediment scaling, as described in section 3.2, requires model and prototype friction velocities. This section includes a full explanation for those computations.

First, the prototype friction velocity u_{*p}, was determined. In a shallow wide open-channel flow with a hydraulically rough boundary, where the bed roughness length is greater than the height of the viscous sublayer, the mean flow velocity profile is fairly well described by:

$$\frac{\bar{u}}{u_{*p}} = \frac{1}{\kappa}\ln\left(\frac{z}{k_s}\right) + 8.5 \qquad (A.1)$$

where $\bar{u}$ is the streamwise velocity at a distance z above the bed, $\kappa = 0.4$ is Von Karman's constant, and k_s is the bed roughness length = $2D_{50}$, where D_{50} is the bed particle size for which 50% of the material is finer.

A depth averaged velocity can be obtained by integrating the velocity over the water depth as given by the following equation:

$$U = \frac{1}{H}\int_{k_s}^{H} \bar{u}\,dz \qquad (A.2)$$

where H is the water depth and U is the depth-averaged velocity. Substituting (A.2) into (A.1) yields:

$$\frac{U}{u_{*p}} = \frac{1}{H}\int_{k_s}^{H}\left[\frac{1}{\kappa}\ln\left(\frac{z}{k_s}\right) + 8.5\right] dz \qquad (A.3)$$

Performing the integration in (A.3), results in :

$$\frac{U}{u_{*p}} = \frac{1}{\kappa}\ln\left(\frac{H}{k_s}\right) + 6 = \frac{1}{\kappa}\ln\left(11\frac{H}{k_s}\right) \qquad (A.4)$$

which is known as Keulegan's resistance law.

For the application of equation (A.4) a depth-averaged velocity along with the corresponding water depth are needed. Since no flow measurements at Yorkville Dam were available, the closest

gaging station was used to back calculate an average flow along the Yorkville reach. The gaging station was at Dayton, Illinois. By applying the Log-Pearson Type III distribution with no skew to 26 years of annual maximum discharges at Dayton, the return periods for the Dayton reach were determined (see figure A.1). Next, these return periods were compared to the return periods generated by the Corps of Engineers at Yorkville, by taking the ratio of the two (see figure A.2).

From the annual averaged Dayton measurements, an average annual discharge was obtained for the 26 years. Then, figure A.2 was used to obtain an approximation for the Dayton/Yorkville flow ratio (this of course assumes that the annual maxima comparisons behave in the same manner as the ratio of annual average flows). The Dayton annual average flow was calculated to be 2352 cfs and from figure A.2 this corresponds to a Dayton/Yorville ratio of 1.16. With this ratio, an average flow of 2021 cfs for the Yorkville reach was estimated.

Next, the tailwater height that corresponds to 2021 cfs was read from the tailwater rating curve that the Corps of Engineers simulated at Yorkville (figure 3.6b). Assuming a rectangular channel cross section and a channel width of 530 feet (width of the spillway) the average flow velocity was estimated as:

$$U = \frac{Q}{A} = 0.694 \text{ m/sec.} \tag{A.5}$$

Using this average velocity, the water depth, a roughness length of 2.69 cm (the prototype D_{50} was computed from the USGS samples and is given in Section 3.2 as 13.43 mm), the prototype friction velocity was estimated to be 0.0520 m/sec with the help of A.4. The model friction velocity was then obtained using Froude similarity. From equation 3.6, the friction velocity can be scaled as:

$$u_{*r} = L_r^{1/2} = 3 \tag{A.6}$$

This resulted in a model friction velocity, u_{*m}, of 0.0173 m/sec.

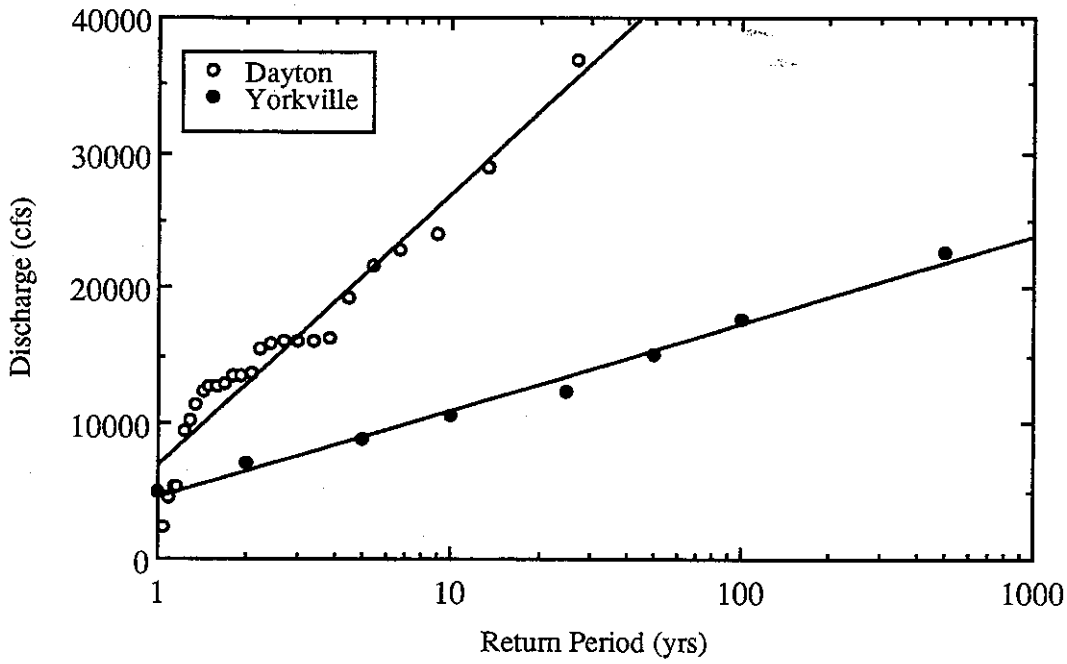

Figure A.1: Annual exceedance for Dayton and Yorkville.

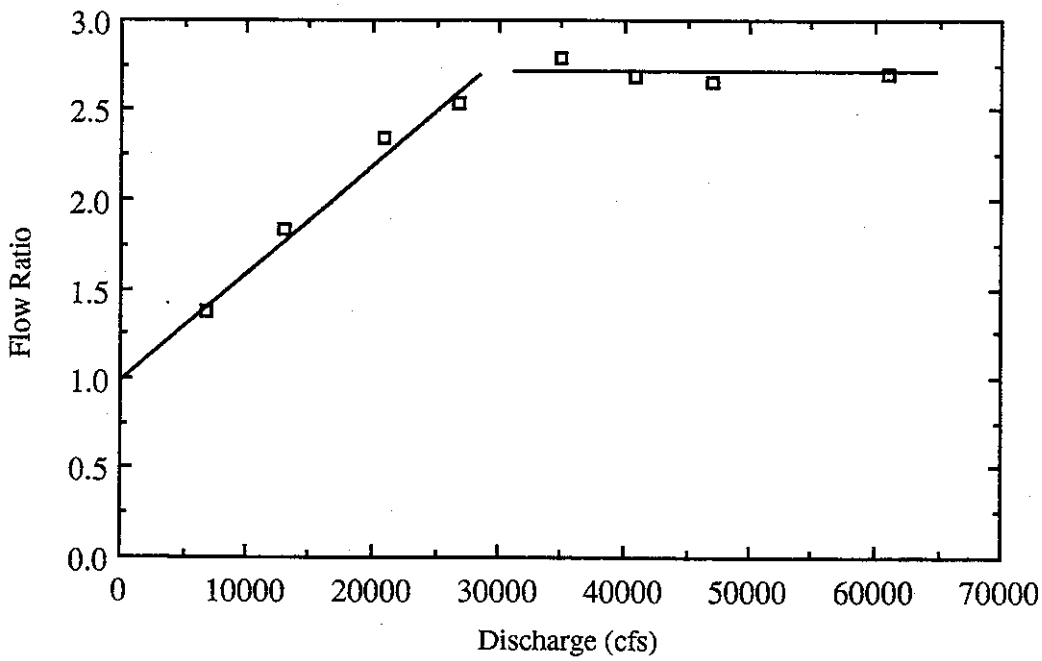

Figure A.2: Dayton/Yorkville exceedance ratio.

Appendix B

Note: All experiments summarized herein were recorded with a standard camcorder and have been transferred to unedited VHS tapes.

Experiment #	Prototype Flow Rate (cfs)	Date	Objective	Observations
Sediment Scour Holes				
a	2021	10/2/95	familiarize with model/generate & survey scour hole	moderate scour hole/sorting of sand/delta
b	7000	10/6/95	familiarize with model/generate & survey scour hole	moderate scour hole/sorting of sand/delta
1	1000	10/25/95	generate & survey scour hole & proceed to next flow	moderate scour hole/sorting of sand/beforms
2	6000	10/27/95	generate & survey scour hole & proceed to next flow	moderate scour hole/sorting of sand/beforms
3	10000	10/30/95	generate & survey scour hole & proceed to next flow	second delta forms on top of first/scour to bottom
4	15000	11/1/95	generate & survey scour hole	large scour/beforms beyond delta
Rip-Rap Failure				
5	1000	11/29/95	start from original rip-rap setup/document flow/scour??	no rock movement/roller??/boat can't escape
6	3000	12/1/95	document flow/check for scour??/attempt to use ADV	vibration then movement of rocks/roller/small scour
7	4000	12/4/96	document flow/check for scour	more vibration & movement/odd shaped jump
8	5000	12/6/95	document flow/check for scour	rock slowly rolls/not enough scour to reach 2nd rip-rap
9	7000	12/6/95	document flow/check for scour	patches of exposed 2nd layer but no scour of that layer
10	9000	12/5/95	document flow/check for scour	rocks move little @ time/large hole/no bedload dwnstrm
11	10000	12/6/95	document flow/check for scour	scour reaches 2nd layer/large turbulent roller/mounding
12	5000	12/8/95	see affects of the plunging @ 5000 for a 10,000 cfs hole	scoured even more/low tailwater = less cushion effect
13	10000	12/14/95	check if mounding moves downstream & have larger hole	little mounding movement/more scour-mostly 2nd layer
14	15000	12/15/95	generate & document scour hole after this flow	plunging-low effect/hole larger-mound moves/armoring
15	1000	12/28/95	check flow characteristics for insitu scour hole-ADV also	no ADV-bubbles/roller only portion of scour hole
16	3000	12/28/95	check flow characteristics for insitu scour hole	large roller/a lot of bubbles/odd surface shape (boil??)
17	7000	12/28/95	check flow characteristics for insitu scour hole	air entrainment/deeper scour but hole has smaller length

Experiment #	Prototype Flow Rate (cfs)	Date	Objective	Observations
			Solution #1 - Grouted Pad	
18	1000	1/3/96	check swept-out flow structure/if any scouring	no scour/jump all on pad/surface rollers capture boat
19	3000	1/4/96	check swept-out flow structure/if any scouring	small local scour after pad/turbulent jump/air entrainment
20	5000	1/4/96	check swept-out flow structure/if any scouring	huge air entrainment/length of jump=length of pad/armoring
21	7300	1/4/96	check flow structure/how much scour	more turbulent jump/less air entrainment/armoring in scour hole
22	1500	1/8/96	check swept-out flow structure/focus on low flows	turbulence becomes dangerous?/boat flips around quite handily
23	2000	1/8/96	check swept-out flow structure/focus on low flows	probably too dangerous/boat moves a lot/air entrainment increases
24	10000	1/9/96	check submerged flow structure/how much scour	jump length > then pad length/small air entrainment/less turbulent
25	15000	1/9/96	check submerged flow structure/how much scour	minimal air entrainment/much larger hole/2nd layer of rock exposed
			Riprap Addition Beyond Pad	
26	3000	1/12/96	check for scour/make ADV msrmnts. to size rock	no riprap movement or any scour after the riprap
27	5000	1/12/96	check for scour/make ADV msrmnts. to size rock	no riprap movement/some bedload transport (only fine sediment)
28	7300	1/12/96	check for scour/make ADV msrmnts. to size rock	no riprap movement/more bedload transport/armoring
29	10000	1/15/96	check for scour/make ADV msrmnts. to size rock	no riprap movement/minimal scour (max = 1 3/8")/armoring
30	15000	1/15/96	check for scour/make ADV msrmnts. to size rock	riprap wobbling a little/some more scour/more armoring
			Solution #2 - 10:1 Sloping Cobbles	
31	1000	1/22/96	observe dissipation and flow structure	some rocks aren't completely submerged/some bubbles
32	3000	1/22/96	observe dissipation and flow structure	water shoots in all directions when it impacts rocks/small rapids
33	10000	1/22/96	view dissipation & flow strctr./ADV for riprap sizing	bedload transport in open channel flow portions/large jump on rocks
34	15000	1/22/96	view dissipation & flow strctr./ADV for riprap sizing	good jump/good air entrainment

Solution #2 (Continued)

Experiment #	Prototype Flow Rate (cfs)	Date	Objective	Observations
35	1000	1/26/96	view dissipation & flow structure/check for scour	flow over block is pleasing/decent air entrainment for this flow
36	2000	1/26/96	view dissipation & flow structure/check for scour	turbulence after block/air entrnmnt/threshold of rock submergence
37	3000	1/26/96	view dissipation & flow structure/check for scour	good air entrnmnt/no sed mvment/small rapids/block = nappe flow
38	6000	1/26/96	view dissipation & flow structure/check for scour	block=skimming flow/jump swept down slope/some rip & sed mvmnt
39	10000	1/26/96	view dissipation & flow structure/check for scour	riprap wobbling (less than 6000cfs??)/washed down jump/low air
40	15000	1/26/96	view dissipation & flow structure/check for scour	undular surface/riprap scour in pockets/not much sed movement

Solution #3 - Four-Step Spillway

41	4000	1/31/96	setup for demonstration	infiltration of water scours some of the foundation
42	6000	2/5/96	view dissipation & flow structure/check for scour	nappe flow/good dissipation on 3rd step/oscillating jump on riprap
43	8000	2/5/96	view dissipation & flow structure/check for scour	nappe flow??/sediment has armored/jump @ end of last step
44	10000	2/5/96	view dissipation & flow structure/check for scour	skimming flow/ski jump @ flow & tailwater impact/armored sediment
45	15000	2/5/96	view dissipation & flow structure/check for scour	ski jump with no air entrnmnt/small jump behind/scour in pockets
46	1000	2/6/96	view dissipation & flow structure/check for scour	aesthetically pleasing/pockets of air/good dissipation/small jump
47	2000	2/6/96	view dissipation & flow structure/check for scour	streaking pattern on steps/air pocket on some steps/small, safe jump
48	3000	2/9/96	view dissipation & flow structure/check for scour	air pocket on 3rd step (4th??)/jumps on all steps/nappe flow/safe jump
49	4500	2/9/96	view dissipation & flow structure/check for scour	jumps on 3rd & 4th steps/air pocket on 4th/good final jump/entrnmnt
50	8000	2/9/96	check for nappe flow or skimming flow	main jump @ 1/2 of last step/good air entrainment
51	17000	2/9/96	view dissipation & flow structure/check for scour	undular surface/no air entrainment/no extra scour

Solution #4 -10:1 Smooth Face

Experiment #	Prototype Flow Rate (cfs)	Date	Objective	Observations
52	1000	2/16/96	view dissipation & flow structure/check for scour	supercritcal streaking flow/small jump @ end of slope/catches objects
53	2000	2/16/96	view dissipation & flow structure/check for scour	jump beyond slope/causes odd shape/good aeration/some scour
54	3000	2/16/96	view dissipation & flow structure/check for scour	jump @ bottom of spillway/does not capture/good aeration/armoring
55	6000	2/16/96	view dissipation & flow structure/check for scour	good aeration/jump at end of slope/some riprap wobbling/capture
56	10000	2/16/96	view dissipation & flow structure/check for scour	huge aeration/calm tailwater dwnstrm/stable riprap/jump far up face
57	17000	2/16/96	view dissipation & flow structure/check for scour	undular surface/riprap scour in pockets/not much sed movement

Solution #5 - Six-Step Spillway

58	1000	4/15/96	view dissipation & flow structure/check for scour	excellent dissipation/air pockets all steps/low residual energy
59	2000	4/15/96	view dissipation & flow structure/check for scour	air pockets on some steps/good dissipation/residual jump/no capture
60	3000	4/15/96	view dissipation & flow structure/check for scour	some air pockets/farely good dissipation/low Froude # jump
61	5000	4/16/96	view dissipation & flow structure/check for scour	some air pockets/1st step skimming/rest have jumps/some bedload
62	8000	4/16/96	view dissipation & flow structure/check for scour	1st three steps skimming/4th partial jump/large residual jump
63	10000	4/16/96	view dissipation & flow structure/check for scour	all skimming flow/oscillating surface wave:residual jump/aeration
64	17000	4/16/96	view dissipation & flow structure/check for scour	large surface wave/behind small jump/stable riprap/low scour

Appendix C

The U.S. Customary units of measurement used in this report can be converted to metric (SI) units as follows:

Multiply	By	To Obtain
inches	2.54	centimeters
feet	0.3048	meters
cubic feet per second	0.028317	cubic meters per second
tons (short)	907.1847	kilograms
pounds	0.453592	kilograms